Development of new characterization methodologies and modelling of transport properties on plastic materials : application to homologous series of tracers.

Martinez-Lopez, Brais

Publication date:
2014

Document Version
Publisher's PDF, also known as Version of record

Collège Doctoral du Languedoc-Roussillon

THÈSE

Pour obtenir le grade de

Docteur

INRA SCIENCE & IMPACT

Délivré par l'**Université de Montpellier II**

Préparée au sein de l'école doctorale:

Sciences des Procédés - Sciences des Aliments

Et de l'unité de recherche:

Ingénierie des Agro-polymères et des Technologies Émergentes

Spécialité: **Génie des Procédés**

Présentée par **Brais Martínez López**

Development of new characterization methodologies and modelling of transport properties on plastic materials : application to homologous series of tracers.

Soutenue le 17 Septembre 2014 devant le jury composé de

M. Ferruccio Doghieri	Università di Bologna	Rapporteur
Mme Mª de Fátima Poças	Universidade de Porto	Rapporteur
Mme Catherine Faur	Institut Européen des Membranes	Présidente du Jury
Mme Catherine Joly	Université Claude Bernard Lyon	Examinateur
M. Miguel Mauricio Iglesias	Danmarks Tekniske Universitet	Examinateur
M. Stéphane Peyron	Université de Montpellier II	Co-directeur de thèse
Mme Nathalie Gontard	Université de Montpellier II	Directrice de thèse

UNIVERSITÉ MONTPELLIER 2
SCIENCES ET TECHNIQUES

"I hate it when people quote me on the internet, claiming I said things that I never actually said"

Leonardo DaVinci

Table of contents

Dissemination of knowledge issued from this work:

Publication I: Predictive and experimental determination of diffusivity of tracers through polymeric matrices applied to food packaging: a critical review.

Brais Martínez López, Stéphane Peyron, Valérie Guillard, Nathalie Gontard.

To be submitted to *Critical reviews in food science and nutrition*

Publication II: Determination of mass transfer properties in food/packaging systems by local measuring with Raman micro-spectroscopy.

Brais Martínez López, Pascale Chalier, Valerie Guillard, Nathalie Gontard, Stephane Peyron

In press. *Journal of Applied Polymer Science* **2014**, *131*, 40958.

Publication III: Practical identifiability analysis for the characterization of mass transport properties in migration tests.

Brais Martínez López, Stéphane Peyron, Nathalie Gontard, Miguel Mauricio-Iglesias.

To be submitted to *Industrial Engineering and Chemistry Research.*

Publication IV: Setting up a mechanical model of molecules diffusion in polymers in the rubbery state.

Brais Martínez López, Patrice Huguet, Nathalie Gontard, Stéphane Peyron

To be submitted to *Macromolecules.*

Publication V: Updating the model parameters for worst case prediction of additives migration from polystyrene in contact with food, application to food safety evaluation.

Brais Martínez López, Stéphane Peyron, Nathalie Gontard

In preparation

Chapter I : Introduction

Packaging has several roles during the process that converts food from raw materials into a product available to consumers. It is at the same time a wrap that protects a product, a barrier designed to preserve the product properties until its expiration date and a message to consumers based on marketing strategies. Packaging can also be regarded as a combination of a material, such as plastic or cardboard, and other substances such as plasticizers, antioxidants, colourants, resins and stabilizers among others, that may be considered as additives.

Packaging are the most common Food Contact Materials (FCM), and as such, they must comply with legislation which states that (Regulation 1935/2004 of the European Parliament and Council, 27 November 2004) "any material or article intended to come into contact directly or indirectly with food must be sufficiently inert to preclude substances from being transferred into food in quantities large enough to endanger human health or to bring about an unacceptable change in the composition of the food or a deterioration in its organoleptic properties". Since no material can be rigorously considered as inert, packaging materials are expected to interact with food in two main ways (i) by the uptake of substances such as oil and aroma compounds from the food, which is called scalping and (ii) by releasing substances into the food in a process called migration. Both interactions must be well asses in order to offer safe and quality food.

Recent regulation 10/2011 provides general recommendations about the utilisation of plastic materials for food contact. This translates the requirements of Regulation 1935 to plastics and includes a substance authorisation list, a limit for the amount of substances that are allowed to be transferred during standardised migration test, as well as specific migration limits for each substance based on its previous toxicity evaluation. A migration test consists on putting into contact a sample representative of the packaging with the food product or with a food simulant under certain conditions. The use of food simulant instead of the actual food product is an strategy that greatly simplifies the migration tests. However and in order to avoid these time consuming tests, the regulation allows as an alternative way for safety assessment of materials the application of "generally recognised diffusion models based on scientific evidence that are constructed such as to overestimate real migration".

Today, the general approach on packaging conception is a sequence of steps that includes: (*i*) study of the food properties (product nature, shape, volume, oxidation sensitivity, water sensitivity...), (*ii*) analysis of the needs in terms of barrier properties

of the packaging film (water permeability, O_2/CO_2 selectivity, thermal resistance...), (*iii*) selection of material composition and packaging dimensioning in function of the barrier needs, and (*iv*) control of the contact compliance by migration test or numerical simulation. This means that the compliance with legislation is carried out after the actual conception of the package, in most cases by the packaging filler (usually a small or medium company) who has poor or no knowledge on technical specifications and formulation of materials from different suppliers involved in the package conception, with the consequent waste of time and money. SFPD (acronym for Safe Food Pack Design) is a French *Association Nationale de la Recherche* project that aims to develop a risk-based approach to address permeation and migration issues during all stages of package conception, which will result on the delivery of safe-by-design instead of safe-as stated packaged food products.

This project comprises 11 academic and industrial partners and is divided in 8 tasks, spanning different goals, each one dealing with 1) Deformulation of food packaging materials, 2) application of FMECA principles (Failure Mode, Effects and Criticality Analysis) to the safe design of food packaging, 3) Inference of expert rules when decisions are supported by migration calculations, 4) Scaling of diffusion coefficients and their activation energies, 5) Feeding large database of partition coefficients, 6) Gathering permeation properties of gas through packaging materials, 7) Engines and interfaces for the Safe Food Pack Design framework and 8) Case studies applications and dissemination. This dissertation has been carried out within the framework of the task 4 of SFPD. The goal of this task was to characterize diffusivity of model molecules in polymers used by packaging industry. This data would be used to build a diffusivity and activation energy database that. The use of this diffusivity data to predict migration levels in commercial packaging would result in the aforementioned safe-by-design food products.

Thesis organization

The creation of the diffusivity and activation energy database requires the previous development of a methodology that allows a fast characterisation of diffusivity. This way, the methodology, the database and the ties between molecular geometry and diffusion behaviour that can be derived from the diffusivity data are the main goals of this dissertation.

As represented in the following scheme, the coefficient that, along with the operating conditions (temperature, geometry of the system) allows the prediction of migration levels, is actually the global mass transfer coefficient. This global mass transfer coefficient, known as apparent diffusivity or simply D_{App} is the sum of the resistances to mass transfer, represented by the diffusion coefficient also known as diffusivity or D, and the mass transfer coefficient or k. Under certain conditions, when for example,

the film sample is immersed in a stirred solution D_{App} and D may have similar orders of magnitude. In this case, they are both often simply called *diffusivity*, leading to misconception of their actual physical meaning. D_{App} may, the same way as the migration levels, be determined experimentally or by means of predictive modelling. For an experimental determination, the partition coefficient KPL or the concentration of the migrant at equilibrium C_∞ will be needed. A determination based on predictive modelling might be carried on by the use of semi-empirical correlations based on diffusivity data present in literature, or deterministic models that yield diffusivity from physico-chemical characteristics of the system. Having said this, the characterisation of the individual coefficients D and k is, as of today, only possible by the means of experimentation.

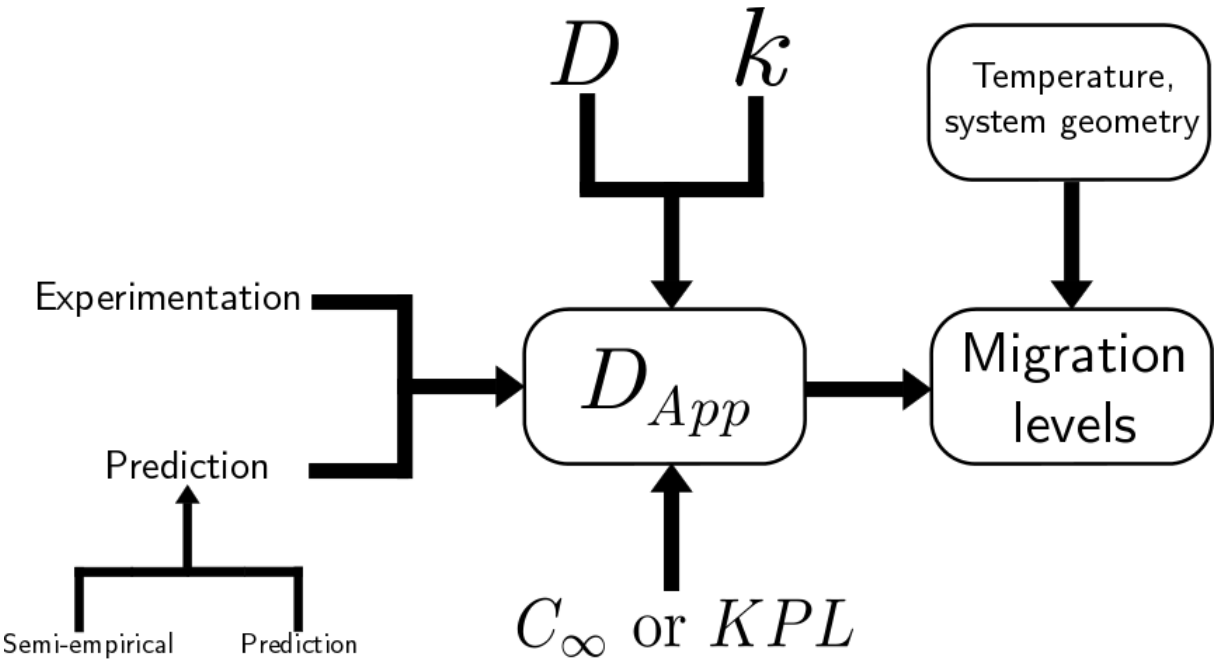

On this basis, this dissertation consists of six chapters including this introduction, which provides background information, the context and overall goals of this research. Chapters II to V are structured in publications in preparation, submitted or accepted in peer-reviewed journals

Chapter II (Publication I) provides a state-of-the-art overview of the methodologies to determine the diffusion coefficient in food/packaging systems by either experimentation or predictive modelling available in literature. The section dedicated to predictive modelling covers both semi-empirical and deterministic models.

Chapter III summarises the experimental methods, numerical schemes and statistical treatment of data developed for the determination of transport properties. It presents the applicability of the vibrational spectroscopy tool Raman microspectroscopy to determine the diffusion coefficient and the solubility limit in a high barrier polymer in

glassy state (Publication II). In order to clearly determine the limits to the application of such methods, an identifiability analysis to determine the conditions for the determination of both diffusivity and mass transfer coefficient by different methodologies (Publication III). More specifically, Publication II shows the application to a system where D_{App} and D have the same physical meaning; differently from Publication III, where the system under investigation was chosen in order to study the influence of k in D_{app} .

Chapter IV (Publication IV) applies the diffusivity characterisation methodology developed in Publication II to two families of homologous molecules in order to relate molecular geometry to diffusion behaviour. Particularly, it tries to lay the foundations of a predictive model of diffusivity by relating it to molecular compressibility, describing the molecules as springs-beads systems.

Chapter V (Publication V) gives new guidelines for a correct application of an empirical equation widely used in industry to overestimate apparent diffusivity, in order to predict worse-scenario migration levels.

Chapter VI provides a synthesis of the main results obtained during this work. A general discussion with the main conclusions is presented with recommendations and perspectives for future work in this field.

The diagram will be shown before each chapter, highlighting how its subject fits into the main goal of this dissertation.

Symbol list

This is the list of variables used in the text. Since the original notation of the equations has been respected, some symbols are used more than once. In order to facilitate the lecture, have been classified according to their context.

General scope

Bi	Biot number.
c	dimensionless concentration.
C	concentration ($kg \cdot m^3$).
C_0	initial concentration ($kg \cdot m^3$).
C_∞	concentration at equilibrium ($kg \cdot m^3$).
Fo	Fourier number.
J	matter flux ($kg \cdot m^2 \cdot s^{-1}$).
k_B	Boltzmann constant.
M	molecular weight.
$SSQR$	sum of squared residuals.
t	time (s).
T_g	glass transition temperature (^oC).
V_m	molecular volume.
x	distance (m).
X	dimensionless space.

Macroscopic and microscopic modelling

a, b, c and d	polymer-specific parameters (Welle equation).
A	proportionality factor.
A_p*	polymer specific conductance type parameter (Piringer equation).
B	minimum hole size.
D_0	self-diffusion coefficient (macroscopic diffusion models)
	pre-exponential factor (Arrhenius equation).

f_V	average free volume per molecule.
K_{ij}	free volume parameters for the solvent.
R_H	hydrodynamic radius.
v_f	average free volume of the system.
v_g	volume at the glass transition temperature.
α	difference between thermal expansion coefficients.
β	shape parameter (Weibull equation).
$\varkappa$	screening hydrodynamic interactions.
ξ	ratio of the molar volume of the jumping unit (model of Vrentas and Duda), friction coefficient (Rouse model).
τ	system time constant (Weibull equation)
	polymer specific activation energy type parameter (Piringer equation).
ϕ	polymer volume fraction.
χ	rod/sphere shape factors (obstruction models).
	polymer/solvent interaction factor (model of Vrentas and Duda).
ω_i	weight fraction of component i.

Practical identifiability analysis

S_a	sensitiviy matrix.
SC_i	scale factor.
S_{nd}	non-dimensionalised sensitivity matrix.
S_{norm}	normalised sensitivity matrix.
$\|S_{nd}\|$	Euclidean norm of Snd.
γ	collinearity index.
θ	predictor variable.
ρ_m	determinant measure.

Springs-beads model.

A_{min}	minimum area that can be projected by the molecule.
F	frequency of the stretching vibration.
F_V	vertical compound of the traction/compression force.
F_H	horizontal compound of the traction/compression force.
F_T	resultant of the traction/compression force.
k^{ph}	elasticity constant of the phenyl-phenyl bond
k^{-}	elasticity constant of the C-C single bond between the phenyl group and the C=C double bond.
$k^{=}$	elasticity constant of the double bond between two single bonds.
k_{eqH}	elasticity constant of the horizontal compound.
k_{eqV}	elasticity constant of the vertical compound.
k_{eq}	elasticity constant of the equivalent spring.
L_{Seq}	length of the equivalent spring.
μ	reduced mass.

Chapter II : State of the art

This chapter provides a state-of-the-art overview of the methodologies to determine the diffusion coefficient in food/packaging systems by either experimentation or predictive modelling available in literature. The section dedicated to predictive modelling covers both semi-empirical and deterministic kinds of models. This chapter fits in the main goal of this dissertation as shown in the following diagram:

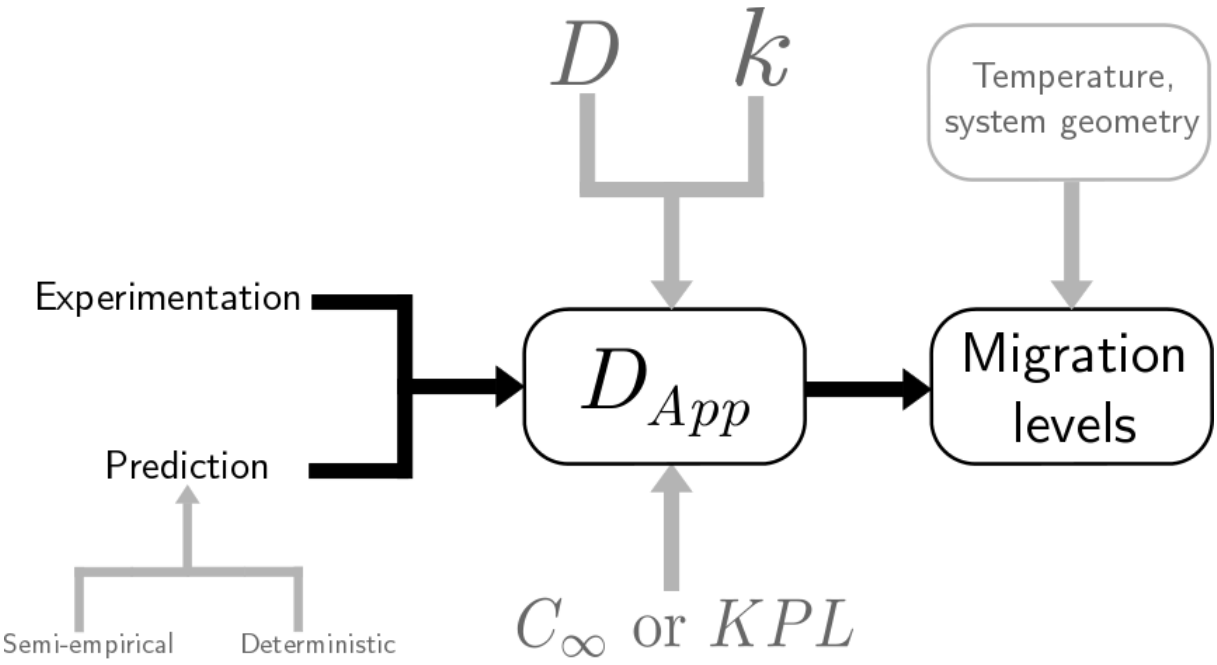

Publication I: Predictive and experimental determination of diffusivity of tracers through polymeric matrices applied to food packaging: a critical review.

Brais Martínez López, Stéphane Peyron, Valérie Guillard, Nathalie Gontard.

Abstract

During packaging fabrication, certain substances are added to the polymers to make processing easier or to confer special properties to the final product. Migration is a contamination process produced by the release of these substances into the foodstuff, that can be physically formalized according to mass transfer laws. European directive 10/2011 allows the determination of migration levels by mathematical modelling. These models need of transport properties (diffusion coefficient, mass transfer coefficient, partition coefficient) as input variables to accurately predict specific migration levels of these substances. A bibliographical review has been carried out in an effort to compile existing ways to characterize the diffusion coefficient by means of experimentation or mathematical modelling. After the introduction, there is a part entirely dedicated to definitions used in the text and other one explaining the vision of mass transfer according to macroscopic phenomenological laws, and models developed after them. Then, the experimental section summarizes the main points on top of which a diffusivity characterisation methodology should stand; and classifies the existing methodologies in literature according to the analytical technique chosen to monitor kinetics (chromatography, NMR, UV, Vibrational spectroscopy). Finally, a section compiling the efforts carried out to predict diffusivity at microscopic scale is followed by the main conclusions and perspectives. Strengths and weaknesses of each approach are discussed in terms of their applicability to safety assessment of food packaging. Generally speaking, literature shows that despite the development of modelling in the last years, an accurate diffusivity characterisation may still rely on experimentation.

Keywords: mass transfer, diffusivity, experimental, modelling, mobility, packaging.

To be submitted to *Critical reviews in food science and nutrition*

1 Introduction

Food contact materials (FCMs) must comply with European regulation 1935/2004, which can be summed up in two main requirements. Packaging materials shall not transfer their constituents to food in quantities that could (1) endanger the human health and (2) bring about deterioration in organoleptic characteristics. To ensure the safety of consumers, European regulation 10/2011 translates the requirements of regulation 1935/2004 to plastic materials and lays down the procedure for their compliance. In addition to the requirement of inertia for plastic FCMs, regulation 10/2011 provides guidelines on the testing procedure for migration assessment. An important aspect of the regulation is that it allows the use of "generally recognized diffusion models based on experimental data [...] under certain conditions" to determine overestimated migration levels and to prevent expensive and time-consuming experiments. In this way, the existing models used to describe migration are based on the macroscopic Fickian diffusion equation, which involves at least two key parameters: (1) the diffusion coefficient, or diffusivity (D), and (2) the partition coefficient (KPL). Little attention has been paid though to the assessment of the KPL, and a commonly accepted approach is the use of a KPL value of 1 if the migrant is soluble in the food or 1000 otherwise. In contrast to KPL, D must be determined for each polymer–migrant couple because it depends on physical characteristics of both (molecular mass, molecular volume, polarity of the diffusing molecule, and glassy or rubbery state of the polymer matrix). The experimental determination of D consists on two steps: (1) monitoring the diffusion of a molecule through a polymer resulting from the imposition of a concentration gradient and (2) identification of diffusivity from the experimental data by comparison with a mathematical model with a dedicated optimization algorithm. The greatest constraint in the determination of diffusivity is the need to reach equilibrium or to know the KPL between the polymer and the medium in contact with it. Because KPL data is scarce, and because of the time required to reach equilibrium, which is specially exaggerated in the case of high-barrier polymers; the experimental determination of D is often a time-consuming task. In addition to experimentation, D might be determined via predictive modelling; but as of today, these models are often too complicated for a direct application; either requiring extensive experimental input or great computing power.

This review tries to compile the experimental methodologies and predictive modelling strategies to characterize diffusivity, present in literature as of today. It targets only polymers used in packaging industry (mostly polyolefins, PET and polystyrene) and migrants with a molecular weight of up to 1200 $g \cdot mol^{-1}$. The goal of this work is to give a vision of a practical application to food/packaging systems, of both experimental and predictive diffusivity characterization strategies. Including this introduct-

ory section, this review is divided in six sections. Section 2 gives brief definitions of the main concepts used in the text, such as the differences behind the microscopic and the macroscopic description of diffusion. Section 3 explains the laws of diffusion from a phenomenological or macroscopic point of view, as it has been classically understood on the food packaging domain. As well, this section cites the most important models that allow the prediction of the macroscopic or fickian diffusion coefficient. Section 4 is entirely dedicated to the experimental ways to characterize diffusivity. It covers the main points from which a diffusivity characterization methodology may be built, mainly media into contact and analytical technique needed to monitor the transfer; and classifies the methodologies available in literature according to the latter (chromatography, NMR, UV, vibrational spectroscopy). Section 5 provides a classification, made according to the division of the matter; of the existing strategies to describe diffusion at a microscopic scale. The review ends with section 6, where a synthesis and future perspectives are given.

Basic definitions of mass transfer in food packaging systems.

For the sake of clearness, this section gives the definitions most used in the text:

Transport: conductive or convective motion of a chemical species through a single phase. Concretely, conductive transport is a consequence of the Brownian motion or random walk of the chemical species.

Diffusion (macroscopic/phenomenological approach): conductive transport of a chemical species through a single phase as a consequence of a concentration gradient.

Diffusion (microscopic/self-diffusion approach): diffusion of a chemical species in the absence of a concentration gradient. It is argued whether the concentration gradient used for the macroscopic definition is a consequence of both the random walk of the diffusing species, combined with the probability of the diffusing species to move towards the region of the system where it is not present yet.

Diffusivity or diffusion coefficient (macroscopic/phenomenological approach): ratio between the mass flux and the concentration gradient at a specific section.

Diffusivity (microscopic/self-diffusion approach): measuring of the mean square displacement of the centre of masses of a chemical species.

Transfer: conductive or convective transport of a chemical species between two phases.

Diffusing species: whatever chemical species that diffuses. On this work, the terms tracer, surrogate or migrant will be used in a generic way for this concept. However,

the term migrant should be exclusively used for molecules with technological value used in commercial packaging.

Migration: contamination process caused by the transfer of migrants from commercial packaging into food by combination of conductive and convective transport phenomena.

2 Mass transport in polymers from a phenomenological point of view.

In the study of migration, mass transfer is always, considered from a macroscopic point of view. This means that the matter, in this case the packaging is a continuum, and that all its physical properties have well-defined values at any given point of the system (Gubbins and Moore 2010). Although this is not correct, it is a good approximation when dealing with system lengths on the order of the µm and time scales of days or even months. The macroscopic point of view is by far the most widely used because of the general recognition of Adolf Fick's laws (Fick 1855) as the best way to describe mass transport. Mass transport defines the motion of a chemical species in an immobile phase, while mass transfer involves at least two immobile phases and transport of the mobile species between them. Fick's law has the following form (equation 1):

$$J = -D\,\frac{dC}{dx} \quad (1)$$

Where J is the matter flux, D the diffusion coefficient, C the concentration, x the distance and $\frac{dC}{dx}$ the gradient of concentration along the x axis. This law postulates that the flux goes from regions of high concentration to regions of low concentration and is valid only under the assumption of steady state. With Fick's first law and the mass conservation equation in the absence of chemical reactions, Fick's second law can be derived, as in equation 2

$$\frac{\partial C}{\partial t} = D\frac{\partial^2 C}{\partial x^2} \quad (2)$$

Fick's second law describes how diffusion causes the concentration change with time. Fick's first and second law can be solved for many types of geometries (plane sheets, cylinders, spheres) by choosing the correct boundary and initial conditions, and give equations that yield concentration profiles in space, time or both. Analytical, as well as numerical solutions to this differential equation have been carefully listed and dis-

cussed by Crank 1980 for specific, simplified geometries (e.g. sphere, cylinder, plane sheet) and initial and boundary conditions. They are essential in the study of mass transfer in food/packaging systems. According to Fick's postulates, the diffusion coefficient is the ratio between the mass flux and the concentration gradient at a specific section, and it is a kinetic parameter representative of the diffusion speed of the diffusing substance.

There are other ways than Fick's laws to describe mass transport that use different concepts to describe the concentration variation through time, but there are not as widely used as Fick's laws. A solution was proposed by Weibull 1951 in the form of a probability density function useful for representing processes such as the time to completion or the time to failure. This density function can be integrated into a kinetic model, as given in equation 3

$$\frac{C(t) - C_\infty}{C_0 - C_\infty} = e^{-\left(\frac{t}{\tau}\right)^\beta} (3)$$

Where $C(t)$ is the concentration changing with time t , C_∞ is the concentration at equilibrium and C_0 is the initial concentration. Besides of this variables, the model is fed by the parameters τ and β. τ is the system time constant or scale parameter, and varies in function of the process rate, being the time required to accomplish a one log cycle (63.8 %) of the process. β is the shape parameter and is related to the initial rate of the process quantifying the patter of curvature observed. The scale parameter quantifies the rate of mass transfer and is temperature-dependent according to an Arrhenius expression. The shape parameter is apparently nor migrant nor temperature-dependent and ranges between 0.5 and 1, according to the importance of the resistance to the transfer at the interface. A comparison between this model and solutions of Fick's law can be found at Poças et al. 2012. Authors conclude that this model is expected to have a practical application in describing transfer from packaging systems, and specially from paper packaging systems, since their concentration profiles present a characteristic sigmoidal shape that is well fitted by this equation.

It can be stated that an accurate prediction of migration levels is well subjected to an accurate knowledge of the diffusivity of the molecule in the packaging, so it is possible to correctly simulate the mass transport. Hence the importance of a good determination by either experimentation or predictive modelling.

2.1 Prediction of the phenomenological diffusion coefficient

The phenomenological diffusion coefficient, diffusivity or simply D of what it has been defined as tracers, surrogates or migrants, through a polymeric matrix, is a parameter that has been traditionally obtained experimentally. Differently from other physical parameters, D cannot be directly measured. It must be identified from a set of experimental data using a mathematical model (analytical or numerical solution of Fick's second law dedicated to the representation of the set-up/system under study) and an optimisation algorithm. The diffusion coefficient (identified D value or optimized D value) is the value that permits to obtain the best fit of the experimental data by the model. In an attempt to avoid time consuming experiments, a number of efforts have been made to predict it by means of mathematical modelling. These models, as well as Fick's laws consider the system from a macroscopic point of view, and can be divided in four types: based on obstruction effects, based on hydrodynamic theories, based on the free volume theory and empirical or semi-empirical. All of them yield phenomenological diffusivity values with the same physical meaning than the one defined by Fick. The three first types of models listed above (obstruction effects, hydrodynamic theories and free volume theory) share common characteristics that make them different from the fourth: they have been originally developed to model the diffusion of a molecule of solvent in dilute or semi-dilute polymeric solutions. First, the diffusion behaviour of the solvent in the absence of polymer chains is studied (what, according to the definitions of section 12) and then it is compared with the diffusion behaviour in the polymer solution. Since the case of a tracer in a polymeric matrix is equivalent to the case of the solvent on a highly concentrated polymer solution, some of these models are applicable to food/packaging systems, but the majority deviate from experimentally measured diffusivity along with the concentration of polymeric chains in the solution increases. These models usually link the ratio between the diffusion coefficient and the self-diffusion coefficient of the solvent to certain structural parameters of the system related to the interactions between them, always considering that these properties have the same value on every point of the system. Due to the difficulty to gain information on the self-diffusivity of the tracer and the sometimes extensive experimental input, most of these models are not applicable to the case of tracer diffusion in the current state of knowledge on tracer/polymer systems. They are thus just cited here but not fully detailed. For exhaustive explanation, including full description of the equations, the reader can refer to Masaro and Zhu 1999.

The last type of models is the semi-empirical or empirical correlations. The principle is always the same: to find relationships between diffusivity data of tracers in polymeric matrices used in packaging industry and evident properties of the tracer and/or

polymer (molecular weight, the temperature or structural parameters found in literature). It is worth noticed that all these models, even the most theoretical ones, need, first, a set of experimental data to determine the correlation/missing parameters.

2.1.1 Models based on obstruction effects

Diffusion models based on obstruction theories assume that the polymer chains in solution or within a network create fixed pores or openings within which the solute can diffuse. The polymer chains themselves, usually conceived as spheres act as obstructions to diffusion increasing the diffusion path length and hence tortuosity, but interactions between molecules are never taken into account (Figure 1a). This obstruction concept was first introduced by Maxwell 1873 and Fricke 1924 separately. Assumptions of the obstruction model are that the size, shape, location and number of pores or openings within the polymer gel remain more or less fixed on the time scale of diffusion. All the obstruction effect models predict diffusivity of small molecules in dilute or semi-dilute polymer solutions. Hence, the diffusivity is always expressed in the form of $D=f(D_o,\phi)$ where D_o is the self-diffusion coefficient of the solvent and ϕ is the fraction of the considered volume occupied by the polymer. Other parameters, like the fraction of non-diffusing solvent or geometrical considerations of the polymer or the solute, are likely to appear depending on the original work. Some famous models based on this theory are Pickup and Blum 1989, Waggoner et al. 1993 (first equation based on the Maxwell and Fricke theories), Mackie and Meares 1955, Ogston et al. 1973, Amsden 1999 (based on the work by Ogston), Johansson and Loefroth 1991; Johansson et al. 1991a Johansson et al. 1991b (hard sphere theory). As an example, equation 4 gives the Maxwell-Frick equation, on which there are present the typical parameters used by models based on obstruction effects:

$$\frac{D(1-\phi)}{D_0} = \frac{1-\phi'}{1+\phi'/\chi} \quad (4)$$

where D is the diffusivity, D_0 is the diffusion coefficient of the pure solvent, ϕ is the polymer volume fraction, ϕ' is the volume fraction of polymer plus the fraction of solvent considered as immobile, and χ is the shape factor, ranging from 1.5 for rods to 2 for spheres. There is a simplified version of the equation that assumes $\phi=\phi'$. As said, to the best of the authors knowledge, there is no record of the use of these models for the prediction of diffusivity in packaging-like systems.

2.1.2 Hydrodynamic theories based models

The hydrodynamic theories take into account the frictions between polymer chains and between solute and polymer chains, which did not happen with the obstruction models (Figure 1b). This allows the description of more concentrated regimes, when the polymer chains overlap. Again, since most of them describe diffusion within polymer solutions, they will not be detailed but cited here: Langevin and Rondelez 1978 (sedimentation of spherical particles in polyethylene oxide), Cukier 1984 (diffusion of brownian spheres in semi-dillute polymer solutions), Phillies 1986, Phillies 1987, Phillies 1989 (self-diffusion of macromolecules). The Darken equation Darken 1948 can be classified into this category. It was originally developed for metal alloys systems, and it describes diffusion on the solid state of the two components of a binary solid solution within each other. An interdiffusion coefficient is then defined as a combination of self diffusion coefficients, times a thermodynamic factor got from fugacities and concentrations of the phases involved. It has been reported outdated (Okino 2013). Equation 5 is the one developed by Cukier, and can serve as an example for this section:

$$\frac{D}{D_0} = e^{-\kappa R_h} (5)$$

where $\varkappa$ represents the screening hydrodynamic interactions between the polymer and the solute in a semi-dilute polymer solution, and R_h is the hydrodynamic radius of

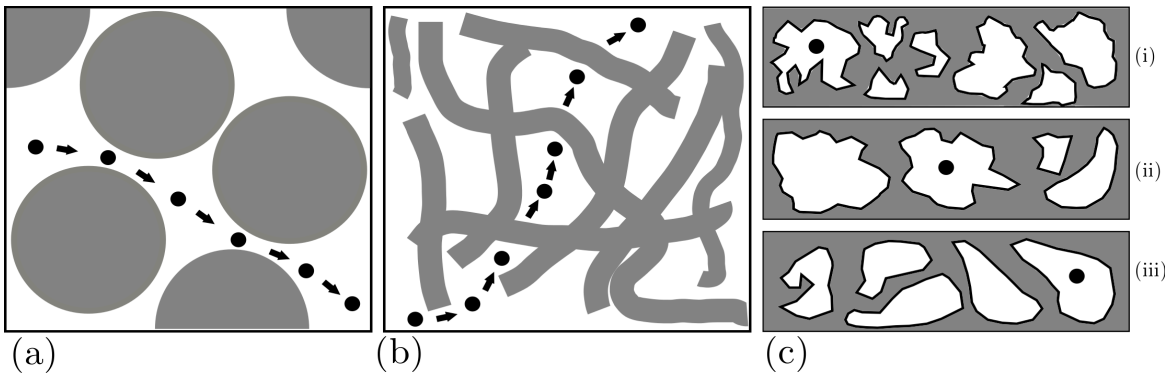

Figure 1: Diffusion path (arrows) of a solvent molecule (black dot), described according to the macroscopic conceptions of polymer/solvent systems: models based on obstruction effects (a) usually conceive polymer molecules as immobile spheres (big grey spheres) that do not interact between them, neither with the diffusing solvent. Hydrodynamic theories (b) describe polymer molecules (grey lines) as rods and take into account overlapping and interactions with the diffusing solvent, which allows the description of more concentrated regimes. According to the free volume theory (c) i, ii and iii, the tracer/solute can only diffuse when a contiguous hole at least its size is available. This means that not only the free and the accessible volumes are important, but also the distribution and the dynamics of these volumes, as well as the size of the diffusing molecule.

the diffusing sphere. As supposed, D and D_0 have the same meaning as in equation 4. As stated for the models based on obstruction effects, there is no record of the use of models based on hydrodynamic theories for diffusion of tracers in solid polymeric matrices.

2.1.3 Free volume theory based models

The term "free volume" has several definitions: it refers to the empty space between the molecules, the volume not occupied by the polymer, or the volume of a system at the temperature of study minus the volume of the same system at 0 K. Models based on the free volume theory describe diffusion as a consequence of the redistribution of the free volume within the polymeric matrix (Figure 1c). From a macroscopic point of view, the free volume remains the same in the whole system, as defined, for example by Williams et al. 1955 in equation 6

$$v_f = v_g[0.025 + \alpha(T - T_g)] \quad (6)$$

Where v_g is the volume at the glass-transition temperature T_g and α is the difference between the thermal expansion coefficients of the liquid and the glass. The best-known models relating diffusion to the free volume theory are two: Fujita's model and the model of Vrentas and Duda.

Fujita's model Fujita 1961 proposed the first diffusion model based on the free volume theory using a probability concept originally developed by Cohen and Turnbull 1959. In this model, given in equation 7 the diffusivity is closely linked to the probability of the molecule finding in its surrounding a hole large enough to permit displacement:

$$D = RTA\ e^{\left(-\frac{B}{f_V}\right)} \quad (7)$$

Where A is a proportionality factor and B the measure of the minimum hole size required for tracer displacement, which depends only on the particle size but not on the temperature or on the polymer concentration; f_V is the average free volume per molecule. This model, as well as the others based on obstruction and hydrodynamic concepts, was originally developed for the diffusion of small molecules in dilute and semi-dilute polymer solutions, but there are records showing that it describes successfully the case of the tracer diffusion through a polymeric matrix: Kulkarni and Stern 1983 (CO_2, CH_4, C_2H_4, and C_3H_8 in polyethylene); Stern et al. 1986 (Ar, SF_6, CF_4 and $C_2H_2F_2$ in polyethylene). The model of Vrentas and Duda spanning the articles Vrentas and Duda 1977a Vrentas and Duda 1977b Vrentas and Duda 1977c Vrentas

and Duda 1977d Vrentas and Vrentas 1994 Vrentas and Vrentas 1995 Vrentas et al. 1996 and Vrentas and Vrentas 1998, is perhaps the most known model based on the free volume theory applied to the determination of the phenomenological diffusivity of solvents in polymer solutions. To the best of the author's knowledge, there is no record for the use of this model for determining tracer diffusion through solid polymeric matrices. It must be noticed that the whole model requires no less than 13 parameters such as, temperature, polymer concentration, solvent size, activation energy and free volume contributions; some of which require exclusive experimental determination. Because of this, the model is often considered too complicated for a direct application, which has prevented its generalized use. Hong 1995 calculated the parameters and predicted diffusion behaviour for several polymer/solvent systems, like polycarbonate, polypropylene, polystyrene and poly(vinyl acetate) among many others, over wide ranges of concentration and temperature. The explicit form of the model, as found in Hong 1995, are given by equation 8 and 9:

$$D_0 = \frac{-(\omega_1 \hat{V}_1^* + \xi\omega_2 \hat{V}_2^*)}{\omega_1 \left(\frac{K_{11}}{\gamma}\right)(K_{21} - T_{g1} + T) + \omega_2 \left(\frac{K_{12}}{\gamma}\right)(K_{22} - T_{g2} + T)} A e^{-\frac{E}{RT}} \quad (8)$$

this is the expression for the solvent self-diffusion coefficient, which can be substituted in equation 9, to obtain the diffusion coefficient:

$$D = D_0 (1 - \phi_1)^2 (1 - 2\chi\phi_1) \quad (9)$$

where, A is a pre-exponential factor, E is an energetic parameter with a very similar definition to the activation energy of diffusion, γ is an overlap factor V_i* is a specific hole free volume of component i required for a diffusion jump, ω_i is the weight fraction of the component i, χ is a polymer-solvent interaction parameter, ξ is the ratio of the molar volume of the jumping unit of the solvent to that of the polymer, K_{11} and K_{21} are free volume parameters for the solvent, K_{12} and K_{22} are the free-volume parameters for the polymer and T_{gi} is the glass transition temperature of component i. This model suffered modifications throughout the years, but it is the perfect example of a model considered too complicated because of the extensive experimental input required. For a detailed description of the physical meaning of all parameters, it is advised to refer to the original publications.

2.2 Empirical or semi-empirical correlations

In addition to the theoretical approaches previously presented, a fourth class of models, consisting on semi-empirical or fully empirical has been developed. It is based on relationships between diffusivity obtained experimentally and certain characteristics of the system, commonly the molecular weight of the surrogate and temperature. Differently from the other models based on obstruction, hydrodynamics or free volume considerations, these correlations have been all extensively developed for the case of tracer diffusion through solid polymeric matrices, to face the problem of the lack of predictive modelling approach in the field of food packaging. These solutions while criticized for oversimplifying the system and sometimes low accuracy, yield diffusivity values without requiring high computing power or hard to retrieve parameters, and may include an overestimation factor to ensure worst case scenario estimation of migration levels into food. The most famous of these approximations, by far the most used in food packaging and recommended by the EU commision for the estimation of specific migration levels; is the commonly called Piringer equation or Piringer interaction model (equation 10, 11). It was originally presented by Baner et al. 1996 and has been justified by Piringer 2007 or Piringer and Baner 2008. To the best of the author's knowledge, the only demonstration found in peer-reviewed journals is Piringer 2008.This equation has been studied by other authors (Cruz et al. 2008; Welle 2012). Its goal is not to provide accurate values of D, but to overestimate them in order to provide a worst-case scenario when calculating specific migration levels.

$$D_p = e^{Ap - 0.1351M^{2/3} + 0.003M - \frac{10454}{T}} \quad (10)$$

where

$$Ap = Ap^* - \frac{\tau}{T} \quad (11)$$

D_p is the overestimated tracer diffusivity, M is the relative molecular mass of migrant (g·mol^{-1}), T is the temperature in K, $A_p{}^*$ is an upper bound polymer specific diffusion parameter, τ is a polymer specific activation energy parameter in K. It is supposed to work for $M < 4000$ g·mol^{-1}. Two of the parameters are not linked to the polymer: the molecular mass of the migrant M, and the absolute temperature T. The parameter A_p is polymer specific and supposedly describes the basic diffusion behaviour of the polymer matrix in relation to the migrants in soft/flexible polymers, such as LDPE. A_p values being high reflect a high diffusion behaviour and hence important migration levels through the polymer. A_p can vary with temperature whereas $A_p{}^*$ is a temperat-

ure independent term. Both are upper-bound values and have been derived statistically so that equation 10 generates worst-scenario values of the diffusion coefficient (Begley et al. 2005, Simoneau 2010).

The parameter τ together with the constant 10454 contribute to the diffusion activation energy, according to $E_A=(10454+\tau)\cdot R$. Upon analysing data from literature for a large series of migrants in many polymer matrices, it was concluded that $\tau=0$ for many polymers. Thus, setting $\tau=0$ as a first approximation for LDPE gives $E_A=86.92$ KJ·mol^{-1} which is in good agreement with the mean value of $E_A=87$ KJ·mol^{-1} found from literature data. For other important groups of plastics relevant to food packaging, like HDPE and PET, a higher activation energy is generally observed. A good mean value for these matrices is $E_A=100$ KJ·mol^{-1} corresponding to $\tau=1577$. The values of the parameters A_p^* and τ can be found at Simoneau 2010. The main drawback is that the values of the parameters A_p^* and τ on which it depends cannot be found without a fair amount of experimental diffusivity data for a specific polymer, molecular weight and temperature range. As well, since the original parameter values were proposed, new diffusivity data has been published, that might show systematic underestimation of diffusivity by the equation, specially for polymers other than polyolefins, like PS or PET. This is especially dangerous for its use with the security purposes it was originally conceived for. This second point has a positive consequence: with the new diffusivity data, new values for A_p^* and τ can be proposed to solve the issue.

Welle 2013 presents a small review of this kind of empirical equations, and another empirical approach, developed by gathering diffusivity data present in literature on PET. This approach replaces the molecular weight by molecular volume as the main descriptor of the diffusion behaviour. The model results in the simple equation

$$D_p = b\left(\frac{V}{c}\right)^{\frac{a-1/T}{d}} \quad (12)$$

where a and b are parameters got from relating activation energies and pre-exponential factors of the Arrhenius relationship; c and d are parameters got from relating molecular volume and activation energy. Those relations where substituted in the Arrhenius equation, giving equation 12 as result. All the four parameters are polymer specific and, in the original article, they are calculated for PET. However, since the deductions are pretty straightforward, they can be calculated for other polymer provided there is enough data of pre-exponential factors and activation energies in the literature. This equation was proven by the authors to give more realistic diffu-

sion coefficients than previous overestimating approaches, at least for PET. The last empirical correlation that will be presented in this text is a work by Vitrac et al. 2006 on polyolefins (LLDPE, LDPE, MDPE and PP). This model is based on CART (classification and regression tree). The approach consists on classifying a population of molecules attending to the values of chosen molecular descriptors and their diffusivities. In this study, the population consisted on 267 molecules ranging from 50 to 1200 $g{\cdot}mol^{-1}$, making a total of 657 diffusivity values. The molecular descriptors selected were the molecular weight, the Van der Waals volume, length/width shape factor and gyration radius; in order to consider the surrogate shape and rigidity as main characteristics controlling diffusion. Results show that a robust estimation of D, may not rely in just one molecular descriptor; and that the risk of getting a bad estimation increases the closer to the mean of the population the expected value of D is. This implies that for a correct estimation of diffusivity using this kind of approach, the tree must be built from a molecule population with disperse diffusivity. Authors conclude that trees may replace data collection in the future, and that they might be very useful for risk assessment and compliance to safety rules. As main advantages, they are not deterministic (no equation), they offer a good compromise between comprehensibility and accuracy without big computing power requirements at the cost of requiring large amounts of data.

2.3 Conclusion

As seen, with the current state of the art at the macroscopic scale, there are not models yielding a fully reliable prediction of phenomenological diffusivity, usually because of being too complicated for a direct application. As a consequence, robust estimation of diffusivity should rely almost completely on experimentation.

3 Experimental determination of diffusivity

As seen, although far from being completely accurate, prediction of diffusivity from empirical macroscopic models could be feasible in the near future if enough diffusivity data was available. This diffusivity data is gathered by experimentation and fitting according to the solutions of Fick's law. No simple method for measuring diffusion coefficient of low molecular weight molecules in polymer is universally accepted and the experimental setup depends on the system under investigation. Several factors are known to control diffusion of tracers in polymeric matrices; The most impacting of which are: the temperature, the chemical structure of the tracer, in terms of molecular weight, molar volume, functional groups and their repeating pattern; the polymer chain mobility, which is affected by the degree of cristallinity, degree of cross-linking,

extent of unsaturation and glass transition temperature; and in the case of commercial plastics, the eventual presence of additives, like plasticizers.

These factors distinctly affect the degree of swelling, and the blooming of the diffusing molecules at the surface of the film sample; and consequently, they influence the rate at which a tracer is sorbed and transported. Of course, the respective contribution of each of these factors varies for each potential combination of polymer and diffusing substance. Considering the research performed in the food packaging domain, a wide variety of values are available in the literature. An overview of the compiled data shows a widely recognized trend relating higher cristallinity degrees, higher molecular weights and lower temperatures with lower diffusion coefficients. Other phenomena, like the change from Fickian to case II transport when going from rubbery to glassy state have been reported (Sammon et al. 2000).

Depending on the system of study, it can be pointed out that diffusivity is characterized using different experimental strategies and analytical techniques. A generalized protocol to determine diffusivity of a tracer through a polymeric matrix does not exist. There are several ways to proceed, but all of them need of the same basic principle which consists on creating a concentration gradient of the diffusing molecule in order to generate a matter flow. The concentration variation is followed using an appropriate analytical technique. Diffusivity is deduced by comparison to a mathematical solution to Fick's laws that describes the concentration variations. More in detail; two media are used; the one is spiked with the diffusing molecule at a defined concentration and acts as a source, while the other is initially virgin. These media are put into contact at the desired temperature and mass transfer can be characterized either by monitoring diffusing substance losses in the source and/or gains in the virgin media. The value of diffusivity can be deducted from sorption/desorption or permeation experiments fitting the experimental concentration evolution to a theoretical one, generally obtained from the resolution of Fick's laws with the appropriate boundary conditions. This characterization way requires knowing the concentration of the diffusing substance in the polymer at equilibrium, a parameter retrieved from the partition coefficient, which may be difficult to determine if transport occurs at very low speed, and requires a very long experimenting time. The choice of the type of media, the analytical technique and the appropriate theoretical mathematical solution are the main points when developing a methodology to determinate diffusivity.

3.1 Media into contact

There are two main types of experimental methodologies according to the media put into contact: the solid-solid contact methods and the solid-liquid contact methods, each one with its own pros et contra.

3.1.1 solid-solid contact methods

Following the principle, in this case, two solid films are put into contact, the one containing a known concentration of the diffusing substance and other originally virgin. This method was initially developed by Moisan 1980, using very specific conditions. Due to the evolution of this method since back in the day, solid-solid contact methods are going to be classified in two types, provided that we are going to focus on the applications in polymers giving a preference to those that are representative of food industry: different nature polymers or same nature polymers. The choice of the same or different nature is given by the temperature at which the test will be performed. Below T_g both possibilities exist no matter what kind of polymers are used; above T_g for amorphous polymers or above T_f for semi-crystalline polymers, since the source must remain solid during the test to prevent mixing with the virgin and alter the transfer, polymers exhibiting different transition temperatures may be used.

Different nature polymers The Moisan test puts into contact two thick layers of different nature. The virgin layer is generally made out of the polymer subject of study, while the source must be made out of a material able to allow diffusion around

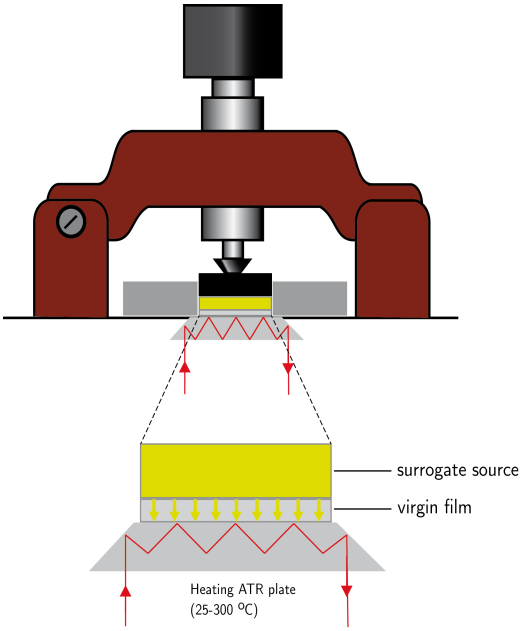

Figure 2: Schematic representation of monitoring diffusion on a solid-solid contact by a heating ATR-FTIR. The yellow square represents the migrant source, whereas the grey one represents the originally virgin film. The detector is placed directly under the virgin film, and measures the migrant gain on the originally virgin film.

1000 times faster than the virgin layer (Rosca et al. 2001) in order to allow a fast and non-limiting supply of diffusion molecule. Although other solutions might be possible, ultra low molecular weight polyethylene (also known as PE wax) is usually found in literature (Reynier et al. 1999). The concentration in the source must be high enough to be able to consider it infinite, so the concentration in the source-polymer interface remains constant. Reynier et al. 1999 set conditions of pressure and wax composition while Dole et al. 2006 proposed a concentration of diffusing molecule of around 1000 $mg \cdot kg^{-1}$. Intimate contact between both layers is mandatory to avoid air bubbles that would increase mass transfer resistance in an unacceptable way. The Moisan test aims to monitor the concentration profile of the diffusing substance in the virgin layer once the test is finished. It allows following sorption /desorption kinetics by measuring gains in the virgin film and/or losses in the source. Variations in the method are possible with, for example, a three-layer test Dole et al. 2006 which consists in superimposing three films, an inner virgin layer between two contaminated layers. It is used to measure low diffusion coefficients because the transfer surface and consequently the mass transfer flux are doubled (Dole et al. 2006). This is particularly adapted to high barrier polymers since equilibrium time is considerably reduced, making easier to determine the partition coefficient. In the case of volatile compounds special precaution regarding the losses by evaporation may be taken and the using of a closed Moisan cell is recommended.

Same nature polymers. The principle is exactly the same as in the Moisan test described above, but this time the materials put into contact have the same nature, eliminating the necessity of knowing the partition coefficient. There is a variation of the test that puts into contact several slices of the same polymer. One (or more) of them, containing a known concentration of tracer is placed in a known position, usually the middle, and acts as source. After contact time, slices are taken apart and their concentrations are measured. This test, called the Roe test (Ferrara et al. 2001) exhibits as main disadvantages the difficulty to obtain an intimate contact between the layers, more likely to get air bubbles in the interfaces, increasing the mass transfer resistance. On the other hand, such a test cannot be applied to completely amorphous polymers above their T_g since they turn into rubbery state, leading to the melt of the system, making impossible to take the slices apart for their analysis.

3.1.2 Solid-liquid contact methods

Liquid contact methods consist on immersing a layer of the polymer subject of study into a liquid. In case of determining migration levels and as recommended by the european regulation (EC 10/2011), food simulating liquids (FSL) are used. FSL may have different natures depending on the simulated food. The liquid (FSL or not) must not interact with the polymer but grant a good affinity for the migrant. There are

two cases: either the liquid is used as source and the polymer is originally virgin, which involves mass transfer from the liquid to the solid (sorption), or the polymer is spiked and the liquid is originally virgin (desorption). Theoretically, in a solid-liquid test, diffusion coefficients found by either sorption or desorption may be the same. However, in reality this means that swelling and/or blooming do not occur, and in the case of a desorption; that the tracer is originally well dispersed in the polymer so it does not have any plasticizing effect on the polymer. Sorption has been used to spike polymers used in other tests (Pennarun et al. 2004a) or as an actual method to determinate diffusion coefficients in the polymer (Sammon et al. 2000, Wind and Lenderink 1996); but mostly to quantify solvent/FSL intake in the polymer (Helmroth et al. 2003, Mauricio-Iglesias 2009, Reynier et al. 2002, Riquet et al. 1998), specially olive oil. Although one of the advantages of this method is that knowing the diffusion coefficient on the liquid is not necessary, it does knowing the order of magnitude of chemical affinity between the liquid and the polymer. If the chemical affinity is much higher for the liquid ($K_{P/F} << 1$), there is mainly a risk of underestimation but diffusivity can be still determined from short contact time experiments (equilibrium not reached). When the chemical affinity is much higher for the polymer ($K_{P/F} >> 1$) diff cannot be estimated without knowing the value of $K_{P/F}$ or the concentration in the liquid at equilibrium. Temperature is also a constraint in this case: T_{eb} of the liquid can never be surpassed in order to keep a solid-liquid contact.

Swelling The capacity to swell is a characteristic property of polymers caused by their macromolecular structure. It is caused by absorption of liquids or vapours from the environment. As it can be deduced, the effect can be more clearly quantified in a solid-liquid contact case. When swelling occurs, diffusing substances have their mobility increased in the polymeric matrix, making diffusion appear falsely faster. Effect of swelling in diffusion by liquid intake has been studied and quantified by Reynier et al. 2001a Reynier et al. 2002, Sammon et al. 2000). Reynier et al. get to an interesting conclusion by studying diffusion of homologous series of n-alkanes as well as other molecules often present in food packaging, which apparently contradicts the basics: since swelling has an influence on the geometry and distribution of the free volumes, it mainly affects polymer and not tracer mobility. This reduces the dependence of the diffusion coefficient on the tracer molecular weight.

Agitation and blooming Agitation plays an important role in determining overall migration kinetics. The whole process can be pictured as a set of resistances, as in equation 13:

$$\frac{1}{D_{app}} = \frac{1}{D} + \frac{1}{k\Delta x} \quad (13)$$

Where D_{app} is the global mass transfer coefficient (also known as apparent diffusivity), D is the diffusion coefficient in the polymer, k is the mass transfer coefficient between the polymer and the fluid and Δx is the film thickness. The greater the agitation in the fluid, the greater the value of this coefficient and the smaller the resistance to mass transfer, making diffusion appear falsely faster. If agitation is poor, solubility of the migrant in the fluid decreases and the tracer is more likely to crystallize in the surface of the polymer in a phenomenon called blooming. Blooming can also occur when the tracer is present in the polymer in concentrations above saturation solubility, leading to physical loss by crystallisation at the surface. The rate of loss of diffusing substance from polymers by blooming is controlled by the rate of the additive diffusion (Lazare and Billingham 2001). This phenomenon is well known for polyolefins, for which Calvert and Billingham 1979 proposed a model to predict the loss of additives by surface evaporation or blooming, based on the data on diffusion and solubility of stabilizers. Later on, this model was used by Lazare 2000 to create another model able to predict the amount of bloomed tracer as a function of time and temperature. Dong and Gijsman 2010 calculated the blooming rate of Irganox 1098 as a function of time and temperature from known diffusion coefficients and solubilities at different temperatures by using this model. In resume, the type of contact is chosen regarding the characteristics of the system, specially the attended value of the diffusivity and the T_g of the polymer. Solid contact methods allow tests at higher temperature than liquid contact methods, and also avoid swelling. Liquid contact tests assure no air bubbles in the contact interface but swelling and blooming are likely to occur. Besides, the temperature to which tests can be performed is lower than in solid-solid contact because it is limited by the evaporation temperature of a liquid, that may be lower than the fusion temperature of a solid.

3.2 Type of concentration profile.

There is another characteristic that comes determined from the selection of the contact type and will determine the analytical technique used to follow the concentration profile: the possibility of obtaining a local or a global concentration profile. A local concentration profile is a concentration gradient in the polymer thickness. It is obtained once per test, when it ends. It gives a concentration profile with enough points without taking too long and the exact coordinates where the measures are got are known. A global concentration profile is the concentration evolution on time. They take longer to obtain exploitable kinetics and require one measure to be representative of the whole sample (hence, it is called global measuring). They are commonly ap-

plied using liquid contact methods, although they are also possible with solid contact. A typical example is a desorption: a spiked polymer film is introduced into a liquid under agitation. Measures of the global concentration on the polymer and/or the liquid can be taken at certain time intervals until equilibrium is reached. Local concentration profiles should be chosen whenever possible.

3.3 Analytical techniques

Several analytical techniques (spectroscopic or chromatographic) can be used to monitor concentrations or concentration distributions during or after the test. They choice of one or another is made according to the answers to these questions:

I. The tracer is quantifiable by the technique i.e. the limit of detection (LOD) is low enough to allow quantification at low concentrations.

II. The technique is suitable for characterisation of local concentration profiles with accurate spatial resolution.

III. The technique is non-destructive.

IV. The technique allows a fast measure.

The goal is hence, to select the most sensitive, non-destructive fastest technique that provides local concentration profiles. Although the choice might seem complicated most of the time, the unique characteristics of the tracer will make impossible to choose a technique that fulfils all requirements. Global concentration profiles are achievable by using any available quantitative technique, provided that it is able to detect the tracer/s subject of study in reasonable minimal quantities. However there are possibilities to modify these techniques in order to get these global concentration profiles in a non-destructive way, or to get local concentration profiles. There are two ways to obtain a local concentration profile: to couple the analytic tool to a microscope; which allows performing the analysis in an exact spot of the sample, or to cut the sample into slices using a microtome and subsequently performing an analysis in each one of them. When using microspectroscopy, the result is an spectrum that is correlated to a visual image of the sample. In almost every case, the spot of interest is surrounded by a matrix that can also generate an spectrum. The goal is to isolate the small area of interest from the surrounding matrix, in order to obtain a spectrum that is representative of the AOI with minimal contributions from the surrounding region. This spatial isolation is achieved by using apertures placed before, after or both before and after the sample. These apertures play a major role in defining the spatial

resolution of the system, since they are a source of diffraction, which is an effect produced when an optical device is placed in the path of the light beam and the size of that device is smaller than the beam diameter. Apertures decrease the signal/noise ratio when they are closed to confine the beam to smaller areas, affecting resolution. The effects of various aperture schemes on resolution has been studied both theoretically and experimentally by Sommer and Katon 1991. This section treats the most relevant analytical techniques available in the literature, citing only works that lead to determination of diffusion coefficients. Compiled data are summarized in Table 1.

Chromatographic methods Two types of chromatography are commonly used in migration tests: HPLC and GC, depending on the physical state of the mobile phase. They are chosen in function of the volatility of the tracer to follow. Chromatographic methods offer an outstanding limit of detection, reaching concentrations of ppm or even ppb depending on the detector used, and thus allowing to work with high barrier polymers and with more than one tracer at the same time, provided that their retention times are different enough to distinguish them. On the other hand, besides being destructive, they require the development of an extraction protocol whose performance is not always easy to quantify. Other example, for styrene and ethylbenzene in polystyrene in molten state is Sakakibara et al. 1990. Already cited Reynier et al. 2001a calculated diffusion coefficients of a large panel of molecules representative of several shapes and functionalities in virgin PP at 40 and 70 °C and in swollen PP at 40 °C. Diffusion coefficients were extracted from a local concentration profile obtained by the Roe test. This paper is an example of utilisation of an extraction protocol to quantify concentrations in the solid phase. Chromatographic methods have also been used to measure diffusion coefficients on PET, measuring concentrations in the liquid phase of a solid-liquid contact at time intervals: Franz and Welle 2008 , Welle and Franz 2012 (toluene, chlorobenzene, phenylcyclohexane, benzophenone, methyl stearate; the second also adds methyl salycilate). Ewender and Welle 2013 performs a special migration test, in which migrants pass directly to a gaz phase and into the chromatogram. The extraction protocol on PET is only used to quantify initial concentrations. There are, however several examples of determination of diffusion coefficients by inverse gas chromatography, which consists on injecting the tracer in gas form directly in the stationary phase; a polymer in this case. This technique has been applied both above and below T_g : Benzene, toluene and ethylbenzene in polystyrene (Pawlisch et al. 1987, Pawlisch et al. 1988), toluene in polystyrene (Duda et al. 1994), styrene in polystyrene (Miltz 1986), chlorobenzene in cured epoxy resins (Jackson and Huglin 1995), ethyl acetate and 2-ethylhexyl acrylate in polyacrylate and ethanol in cellulose diacetate and poly(ether ketone). More examples are available in literature, but will not be cited because of the tracers having to be in gaseous state. A complete review on determination of model migrants by chromatography, in-

cluding general guidelines for mobile phase, detector and extraction protocol has been made by Sanches Silva et al. 2006.

Nuclear Magnetic Resonance spectroscopy NMR spectroscopy gives useful information about the structure and dynamics of systems involving polymers. Based on the absorption of electromagnetic radiation from NMR active nuclei, such as ^{1}H or ^{13}C. NMR allows the reconstruction of images or spectra. Examples of imaging by using classic ^{1}H -NMR are Grinsted et al. 1992 for methanol and hydroxy-deuterated methanol among others into poly(methyl methacrylate) rods and Wei et al. 1993 who studied diffusion of acetone in polycarbonate but did not extract any coefficient. NMR microscopic imaging is noninvasive and continuous. Solid-solid or solid-liquid contact methods described previously would work with this technique provided that the tracers are able to absorb electromagnetic radiation. Pulsed Field-Gradient Spin-Echo (PGSE) is a method to measure two-dimensional lateral mobility of the tracers. A pulse magnetic field gradient labels the tracers present in small spot of the sample by creating phase variations of their nuclear spins. The signal intensity will decay as the labelled tracers diffuse into the zone originally out of scope of the magnetic field. Plenty of examples can be found in the literature for determining diffusion coefficients, but studied systems are mostly gels or polymer solutions and will not be treated here. There is however, a review of the subject by Matsukawa et al. 1999. With this technique, self-diffusion coefficients can be obtained. This technique is applicable to a single piece of material, although surrogates labelled this way can be imagined diffusing into another material, solid or liquid.

Ultraviolet spectroscopy UV/Vis and fluorescence spectroscopy are methods based, respectively, on the absorption and emission spectroscopy in the ultraviolet-visible spectral region. UV/Vis is widely used for determination of transition metal ions and highly conjugated organic compounds, but there are not a lot of records for measuring diffusion coefficient of tracers. An example of a global concentration profile obtained by UV/Vis is Reynier et al. 2002, who followed migration of Uvitex OB from polypropylene into liquid fluid simulants. Besides this one, we find two different ways to obtaining local concentration profiles. The Roe method, used by Ferrara et al. 2001 to follow the diffusion of Irganox 1010 in a polypropylene homopolymer(of commercial name HomoQ) and more recently, Fang et al. 2013 homologous series of olygophenyls and diphenyl-alkanes in PLA, PP, PCL and PVA. The other is UV-microspectroscopy, used by already mentioned Reynier et al. 2002 (Uvitex and polypropylene) and Pennarun et al. 2004b to follow diffusion of 2,5-dimethoxy-acetophenone in PET. Two methods based on changes in fluorescence have been used to determine diffusion coefficients in polymeric matrices according to literature: steady state fluorescence and fluorescent recovery after photobleaching. Both are used

to obtain local concentration profiles. In the steady state fluorescence method, the changes in fluorescence intensity from probe molecules are monitored. These probe molecules are either attached to the host polymer matrix or dispersed in it. The diffusing molecules quench fluorescence as they diffuse into the polymeric matrix. Anandan et al. 2004a Anandan et al. 2004b studied the effect of concentration and viscosity in the diffusion of pyrene in silicone coatings and resins. It is conceivable to obtain a global or a local concentration profile by both solid-liquid or solid-solid contact.

Fluorescent recovery after photobleaching (FRAP) is a method for measuring two-dimensional lateral mobility of fluorescent particles. A small spot on the fluorescence surface is photobleached by a brief exposure, and the subsequent recovery of the fluorescence in the bleached spot is monitored until equilibrium. It is a relatively new technique. The principles were stated by Axelrod et al. 1976, and the first record for the use of this technique for the determination of diffusivity is Tseng et al. 2000 for rubrene in amorphous polystyrene, followed by Karbowiak et al. 2008 for fluorescein in edible films. Later on, Pinte et al. 2008 Pinte et al. 2010 applied the technique to a homologous series of halogen substituents of fluorescein in different types of polysytrene ranging from 800 to 1850000 $g{\cdot}mol^{-1}$ to both measure diffusion coefficients in polystyrene and relate migrant characteristics to the obtained values of diffusivity. A short review of the FRAP technique, not only applied to diffusion in polymers but with a special focus on heterogeneous materials can be found at Loren et al. 2009. Author concludes that although useful, errors on data analysis derived from the heterogeneous structure of materials should be the goal of further research. Similarities between this technique and PGSE are evident, but this time labelling is made by photobleaching and not by application of a magnetic field and thus, theoretically applicable to the same type of systems. FRAP has not been extensively used yet due to its relatively short time of life. Today, that its module can be easily implemented on commercial confocal laser scanning microscopes (Waharte et al. 2010), it is supposed to become an important alternative. It is important to emphasize that these methods are limited to molecules that produce fluorescence. Besides in the case of steady state fluorescence, the tracer must be able to quench fluorescence and, in the case of FRAP, to be photobleached. Particularly, regarding commercial additive migration in plastic packagings, its utilisation is limited to the molecules that prevent the polymer from ultra-violet radiation or anti-UV molecules like benzophenone.

Vibrational spectroscopy Fourier Transform Infrared (FTIR) and Raman spectroscopy are part of the collection of analytical techniques known as vibrational spectroscopy. Their strengths and limitations makes them complementary. FTIR allows to obtain the average concentration of a molecule in a plastic sample by a fast non-de-

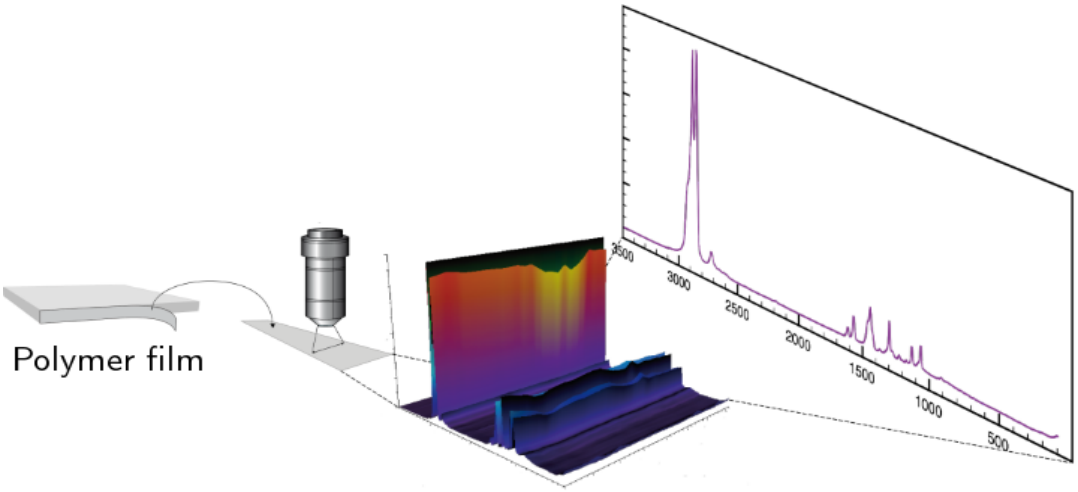

Figure 3: Schematic representation of how to get a concentration profile of a migrant through a polymer film by cross section with Raman microspectroscopy.

structive means. This allows to quantify the additive content in the sample before and after the treatment, accurately determining the amount of additive released or gained. It is also well known for its molecular selectivity, since it is relatively easy that a migrant contains a different chemical group that might absorb infrared light. However, a polymer like PET containing in its structure aromatic and ester groups that could hinder the detection of this chemical groups in migrants. The main disadvantage of FTIR is its relative lack of sensitivity, making it difficult to work on concentrations bellow 0.1 w/w.

There are two ways samples can be measured: the traditional transmission sampling or the Attenuated Total Reflectance (ATR). The traditional transmission sampling requires the dilution of the sample in a media. This was usually accomplished by preparing a KBr pellet or Nujol (oil) mull, but in case of polymer layers, the same polymer layer serves for this purpose. Traditional sampling provides a global measure on the thickness of the layer. Cava et al. 2004 Cava et al. 2005 used FTIR in transmission mode to measure diffusion coefficients of aroma compounds and limonene into commercial PE and Mauricio-Iglesias et al. 2009 Mauricio-Iglesias et al. 2010 for Uvitex OB in LLDPE. In ATR, the most common sampling method today the sample of interest must be in direct contact with the ATR crystal, and only a few microns are interrogated, which raises issues, like the strong absorption by the glass. A big advantage of ATR sampling is the possibility to couple an ATR plate to a heating source allowing measuring at a certain temperature. Examples of ATR sampling are abundant at the literature, like Fieldson and Barbari 1993, Fieldson and Barbari 1995 for water in polyacrylonitrile (first recorded use of FTIR-ATR to measure diffusion coefficients), acetone-polyproylene, methanol-polystyrene and methanol poly(methyl methacrylate); Sammon et al. 2000 for water and simple alcohol in PET films and more recently Fu and Lim 2012 for a multi-component study of 2-octanone, hexyl

acetate, octanal, limonene and linalool in LLDPE. Doppers et al. 2004 for water and acetone into poly(vinyl alcohol)-clay nanocomposites at 40 ^{o}C is the only record of heating ATR-FTIR (Figure 2). FTIR has also been used coupled to a microscopy to measure diffusion coefficients by obtaining local concentration profiles: Riquet et al. 1998, for olive oil in polypropylene, Xu and Fu 2004 for bovine serum albumin into a porous membrane of polyethylene. There is a record of conventional IR sources encountering a *S/N* limitation when apertures reach 20-30 μm of diameter (Carr 1999). In contrast to FTIR, which is an absorption technique, Raman is a scattering technique; however, in Raman, as in FTIR, fundamental vibrational modes are interrogated resulting in outstanding molecular selectivity with little dependence on physical properties such as particle size. Raman also allows sampling trough glass, plastic film and water, since they are very weak Raman scatterers, which are not permitted in FTIR.

The only record of using Raman to measure diffusion coefficients is by means of Raman microspectroscopy (the use of dispersive Raman spectroscopy coupled to a confocal microscope). A Raman microspectrometer employs detectors that contain many small elements that correspond to pixels in the final image. The result of an imaging experiment is a chemical picture (spectrum) of the sample derived from thousands of spectra. Spatial discrimination is achieved by the detector elements themselves, rather by an aperture. The resolution of such systems is often incorrectly stated in terms of the pixel element size at the sample. However, this describes only the magnification of the system as opposed to its resolution. While it is true that the spatial resolution can never be less than the pixel size at the sample, other factors, primarily diffraction, actually control the resolution. Raman microspectroscopy gives the concentration profile in the thickness of the sample. There are two ways to accomplish this: depth-profiling (suitable for thin samples) and cross section (more appropriate for thick samples), which is represented in Figure 3. Depth-profiling demands a complete correction of experimental data since the variation of refractive index between the polymer and air distorts the data obtained (Tomba et al. 2007, Mauricio-Iglesias et al. 2011). Diffusion coefficients of Uvitex OB in LLDPE have been measured (Mauricio-Iglesias et al. 2009 Mauricio-Iglesias et al. 2011) by cross section and depth-profiling respectively. The same technique probed to be adapted to the determination of diffusivity in the glassy state as well by Martínez-López et al. 2014 (p-terphenyl in glassy amorphous PS).

Literature shows that FTIR has been traditionally more used to determine diffusion coefficients. Theoretically, every molecular species has a specific spectral fingerprint and is identifiable by any of these techniques. However, signal intensity spans in a large scale depending on the present functional groups, being a limiting factor on

their application. A note on the use of vibrational spectroscopy for this purpose has been made by Lagaron et al. 2004.

Gravimetry Gravimetric analysis, applied to determination of the diffusion coefficient, consists on measuring the weight variations caused by the gain or loss of the surrogate subject of study with a precision balance. There are some recent studies of these techniques available on literature: Krüger and Sadowski 2005, Mueller et al. 2012 for toluene in glassy polystyrene. They both report non-fickian diffusion behaviour below the glass transition temperature and slightly above. and Bernardo 2012 Bernardo et al. 2012 Bernardo 2013 who studied the diffusion of three different homologous series of tracers ranging between 32 to 240 $g{\cdot}mol^{-1}$ in amorphous polystyrene: alkanes, carboxylic acids and alcohols respectively, on temperature ranges from 35 to 165 ^{o}C. The latter is also complemented with NMR measures for certain acids that show non-fickian diffusion behaviour.

Other techniques Three spectroscopic techniques that lay out of the classification proposed in this work have been found in literature. The first one is the Forward Recoil Elastic Spectrometry (FRES), a non-destructive technique that can be used to measure depth concentrations of hydrogen or deuterium in solids. It has been used by Gall and Kramer 1991 to measure the diffusion coefficient of deuterated toluene in glassy polystyrene from 20 to 35 ^{o}C, finding a non-fickian diffusion behaviour. The second one, is the spectroscopic ellipsometry, another non-destructive technique, appropriated for sorption studies in thin films, and based on measuring the change of polarization of reflected from the polymer due to the presence of the surrogate. It has been used by Ogieglo et al. 2013 to measure diffusion of hexane in polystyrene. Authors conclude that hexane shows a case II diffusion due to the swelling of the polymer along with the surrogate uptake. The last one is the use of a synchrotron with a specific excitation wavelength ranging from 275 to 295 nm, used by the already mentioned Fang et al. 2013 (homologous series of olygophenyls and diphenyl alkanes in PLA, PP, PCL and PVA).

3.4 Conclusions: development of a general methodology

It has been shown that the experimental determination of the diffusion coefficient has three key choices: the type of contact, the analytical technique and the mathematical solution. Depending on the combination, several parameters shall be fixed to allow an efficient determination of the diffusion coefficient. It is an upcoming work, to gather enough data on some polymeric matrices in order to develop general rules to dimension experimental methodologies that allow to determine diffusion coefficients in a fast, reproducible and, if possible, non-destructive way.

Today, with the increase of available computing power, new ways of modelling that have only existed on paper for years are finally becoming possible. By taking into account all interactions at microscopic level it could, in the future replace experimentation as the main way to determinate transport properties.

Author	D ($m^2 \cdot s^{-1}$)	System	Analytical Technique
Anandan et al. 2004a Anandan et al. 2004b	0.84 - 12.83 $\times 10^{-14}$	pyrene/silicone coatings	Fluorescence
Cava et al. 2005	4 - 419$\times 10^{-14}$	Limonene/LDPE	FTIR,Raman
Cava et al. 2004	5.5 - 18.5 $\times 10^{-13}$	Limonene, Linalool, pinene, citral in PE	FTIR-ATR
Cruz et al. 2008	1.1 - 8.7$\times 10^{-12}$	DPDB, BHT and triclosan/LDPE	HPLC
Dole et al. 2006	2.77$\times 10^{-19}$ - 33 $\times 10^{-9}$	DPDB, BHT and triclosan/LDPE	GC-HPLC
Dong and Gijsman 2010	2e$\times 10^{-15}$ - 5.7$\times 10^{-14}$	Irganox 1098/PA 6	UV-Vis
Doppers et al. 2004	2.3 - 6.7$\times 10^{-11}$	Acetone/PVA clay	ATR-FTIR
Ferrara et al. 2001	0.7 - 163.2 $\times 10^{-16}$	Irganox 1010/poly(propylene-co-ethylene)	UV
Fu and Lim 2012	7.02 $\times 10^{-14}$ - 5.81 $\times 10^{-13}$	several surrogates/LLDPE	ATR-FTIR
Helmroth et al. 2003	1.1$\times 10^{-13}$	Irganox 1076/LDPE	GC
Jackson and Huglin 1995	0.09 - 1.63$\times 10^{-8}$	chlorobenzene/epoxy resins	reverse GC
Karbowiak et al. 2008	1e$\times 10^{-12}$ - 1$\times 10^{-15}$	fluorescein and t-Carrageenan	FRAP
Lazare and Billingham 2001	5$\times 10^{-17}$ - 2$\times 10^{-14}$	Tinuvin 234 in poly(ester-block-ether)	UV
Matsukawa et al. 1999	about 1$\times 10^{-13}$	Review paper	PGSE NMR
Mauricio-Iglesias et al. 2009 Mauricio-Iglesias et al. 2011	about 8$\times 10^{-14}$	Uvitex OB/LLDPE	FTIR,Raman
Mauricio-Iglesias et al. 2010	about 1$\times 10^{-14}$	Uvitex OB and Irganox 1076/LLDPE	FTIR,Raman
Neyertz and Brown 2008 Neyertz and Brown 2009	2.4 and 11$\times 10^{-11}$	Oxygen in polyimide	MD
Pickup and Blum 1989	about 1$\times 10^{-10}$	toluene in PS solution	PGSE NMR
Pinte et al. 2008 Pinte et al. 2010	3.9$\times 10^{-17}$ - 5.4$\times 10^{-13}$	NBD-based series/PS	FRAP
Sakakibara et al. 1990	9.34e-7 - 1.7e-5	Styrene and Ethylbenzene/PS	GC
Sanches Silva et al. 2007	about 1$\times 10^{-10}$	DPDB from LDPE into fatty foodstuffs	
Tseng et al. 2000	3.5$\times 10^{-18}$ - 6.3$\times 10^{-14}$	Rubrene/PS	FRAP
Sok 1994	2.1- 10 $\times 10^{-9}$	CH_4,He/PDMS	MD
Waharte et al. 2010	10 and 20$\times 10^{-12}$	fluoresceinisothiocyanate/biofilms	FRAP
Xu and Fu 2004	1.56 $\times 10^{-12}$	Bovine serum/ldpe membrane	FTIR

Table 1: Diffusivity data for common synthetic packaging polymers and different tracers.

4 Modelling of diffusion at microscopic scale

As already detailed in the second section, the classical concept of diffusivity is a macroscopic parameter dependent on the phenomenological Fick's law, applicable to length scales up to several microns and time ranges up to months or years. As seen, the existing predictive modelling approaches usually relate diffusivity to certain properties of the polymer/migrant system. However, these models are either too complicated for a direct application, usually requiring extensive and unintuitive experimental input (obstruction, hydrodynamic and free volume theories), or they need an update to take into account the diffusivity data published after they were originally proposed, and the new packaging materials (e.g. biopolymers for instance) that did not exist, like it is the case of the Piringer equation. Consequently, experimental determination of diffusivity is still preferred. However, time and money could be saved if accurate diffusivity predictions were possible. Therefore efforts are still put on the development of effective predictive models of diffusivity.

Since the last two decades, rapid improvements in the ability to model physical and chemical processes at the atomistic level permitted to provide, in addition to closer fundamental understandings of the matter, the prediction of properties that cannot yet be studied satisfactorily experimentally (Gubbins and Moore 2010). One example of the latter is the mobility of molecules at molecular or atomistic scale investigated using molecular modelling. At this level of detail, diffusion is understood as molecular displacement, result of Brownian motion (Brown 1827), and diffusivity is calculated as the mean-squared displacement of the centre of masses of the moving species. While it is generally accepted that the concentration gradient used to define the phenomenological diffusion coefficient is a macroscopic observation or consequence of the Brownian motion of molecules, it is still not clear whether phenomenological diffusivity and the mobility at microscopic scale would yield the same results due to the high computing power still required today for time scales at the order of the ps.

Therefore to avoid any confusion with the phenomenological, fickean diffusion coefficient the terms *molecular mobility* and *self-diffusion* will be indistinctly used in the present section instead of "diffusion" and "microscopic diffusivity" for the resulting mass transport coefficient calculated by the authors.

This section is intended as a brief introduction and overview of the different modelling strategies at microscopic scale, with a special emphasis on the studies dedicated to the determination of molecular mobility. Theories and modelling approaches can be divided into four groups depending on the length and the time scales to which they apply, as seen in Figure 4 the electronic scale of description, in which matter is regarded as made up of fundamental particles (electrons, protons, etc..) and is described by quantum mechanics; the atomistic level of description, in which matter is

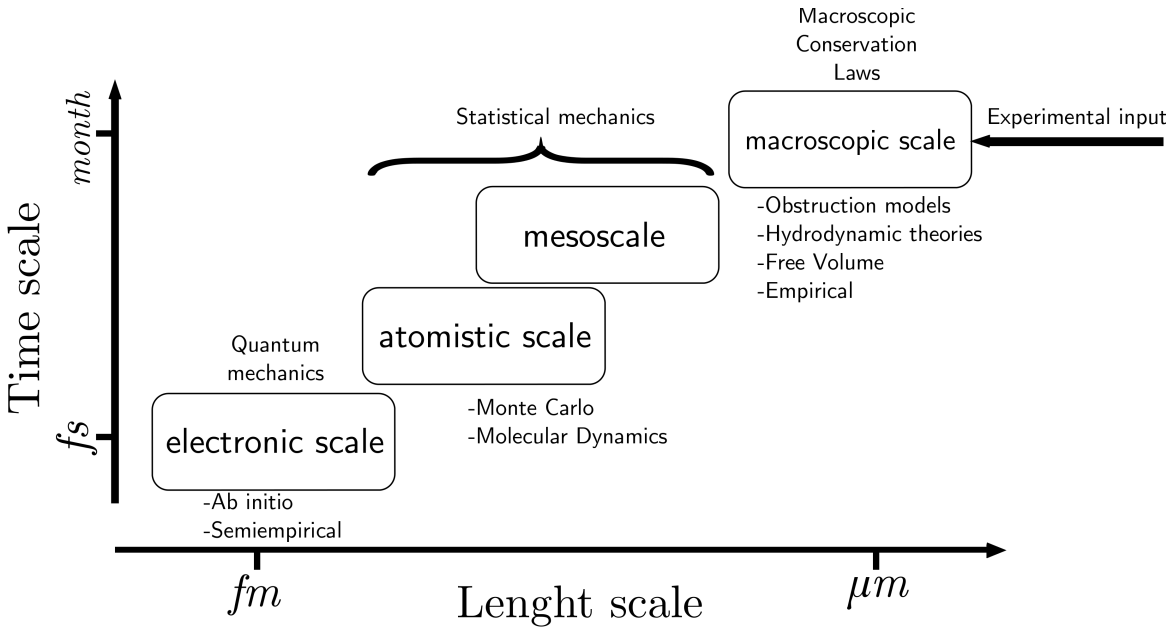

Figure 4: Modelling strategies according to the length and time and scale consideration of the system.

made up of atoms and the mesoscale level in which matter is regarded as composed of beads, each one containing a number of atoms; whose behaviour obeys the laws of statistical mechanics and the continuum scale where the matter is assumed to be a continuum where the conservation equations for mass, momentum and energy applied (e.g. Fick's law for mass transport as described in section 2). In the following, even though to the best of the author's knowledge, electronic scale was never, strictly speaking, used to calculate molecular mobility, it is presented for a better understanding of the atomistic scale and mesoscale.

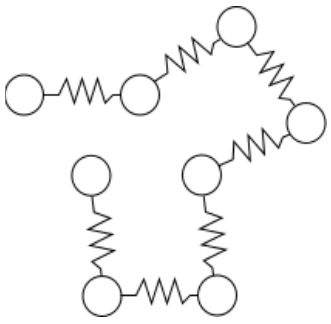

Figure 5: Schematic representation of a Rouse chain, as a linkage of beads and springs.

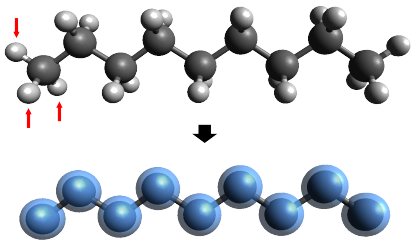

Figure 6: Fully atomistic (top) and coarse grained (bottom) models for Polyethyelene, a polymer commonly used in packaging industry. The hydrogen atoms are grouped along with the atoms of carbon into beads.

4.1 Modelling at Electronic scale

Electronic level of description is the most rigorous way to model matter structure and particle movement. This level of description is required when significant rearrangement of electrons or other fundamental particles occur, such as chemical reactions where chemical bonds are broken and formed. Today, these methods require significant computing power and their application is limited to systems having a relatively small number of atoms and to time scales up to 1 ps. In general, ab initio calculations give very good qualitative results and can give increasingly accurate quantitative results as the molecules become smaller; in practice, extremely accurate solutions are only obtainable when the molecule contains half a dozen electrons or less (Young 2002a). There are three remarkable methods at this scale, called "Ab Initio" (latin for "from the beginning"): the Hartree-Fock calculation, the Quantum Monte Carlo and the Density Functional Theory. Differences between them are due to simplifications introduced in the calculations and hence, accuracy of the results. Indeed simplifications are rapidly needed in such "Ab Initio" calculations. For example, the Hartree-Fock method scales as N^4, where N is the number of functions needed for the calculation of molecular orbitals. This means that increasing the number of needed functions by three would make the calculation take 81 times longer. As of today, this modelling scale is strictly reserved to matter description.

A second class of modelling approach at electronic scale are semi-empirical methods. They are not strictly fully electronic but fall between the electronic and the atomistic level of description. They are simplified versions of Hartree-Fock theory using empirical (experimental) data to improve performance. For instance, some parameters are directly obtained from molecules similar to the one under study, which may lead to very good results if it is similar to molecules in the database used to parametrize the method (Young 2002b). Hence their name "semi-empirical methods". Other additional

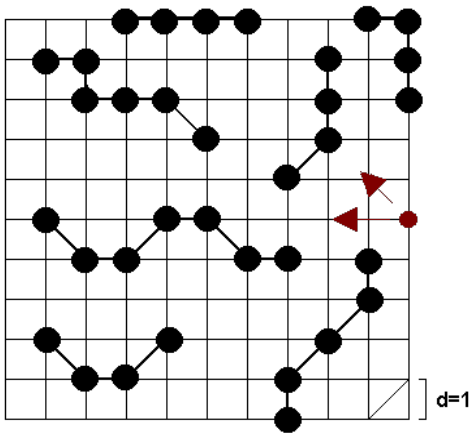

Figure 7: Schematic representation of the three-dimensional lattice described in Schulz et al. 2006 . Black circles represent the polymer beads and the red one represents the tracer.

approximations are usually made to speed up calculations like excluding core electrons from calculation. Compared to the *stricto sensu* electronic scale, all these simplifications make possible to deal with large systems such as biomolecules or nanostructured solid materials. However, taking this level of detail to a polymeric matrix is unattainable today. Consequently there is no record in literature at all of using none of the described above to monitor molecular mobility.

4.2 Atomistic Scale, and Mesoscale

Atomistic level methods are less computing power demanding than electronic ones because they deal with atoms and not anymore with electrons, allowing the study of systems of thousands or millions of atoms over time intervals of 10 to 100 ns, depending on system size and complexity (Gubbins and Moore 2010). Electronic detail is lost but for most physical processes, molecular mobility included, this is not important, since electronic perturbation is a priori small. Atoms or molecules interact with each other through a force field, or intermolecular potential energy, according to Newtonian dynamics. The two well known atomistic level methodologies are Monte-Carlo (MC) and molecular dynamics (MD) simulation. Atomistic treatment may not be feasible yet for systems of large molecules or for slow processes that occur over time scales greater than about a microsecond. For such larger systems, various mesoscale methods have been developed, based on what is loosely termed *coarse graining*. One common form of coarse graining is to replace the fully atomistic description of the molecules by united atom "beads", each "bead" being a group of atoms, as seen in Figure 6. Coarse graining reduces the number of interactions centres and the number of intermolecular pair interactions between molecules (Gubbins and Moore 2010). Consequently, it extends the length and time scale that are accessible, but at cost of reduced rigour and loss of both electronic and atomic detail. After having defined the "beads" and the interaction force fields between them, the resolution of the statistical mechanics equations can be done either by the Monte Carlo (MC) or by the Molecular Dynamics (MD) method. As atomistic and mesoscale theories used the same solving methodologies, both are treated together in the following. Simulations at the atomistic level and mesoscale had played and continue to play an important role in gaining fundamental understanding at the atomic scale of numerous phenomena such as protein unfolding, micelle formation, phase transition, diffusion in nanoscale porous networks, etc. to remain in the field of (bio)-material science. They have been also used to determine the validity of macrocospic law for small systems such as Fick's law of diffusion (Hahn et al. 1996, Percus 1974). The molecular mobility observed at atomistic level results in a random movement of the molecules, as a consequence of the Brownian Motion, (Brown 1827) made famous by Albert Einstein in

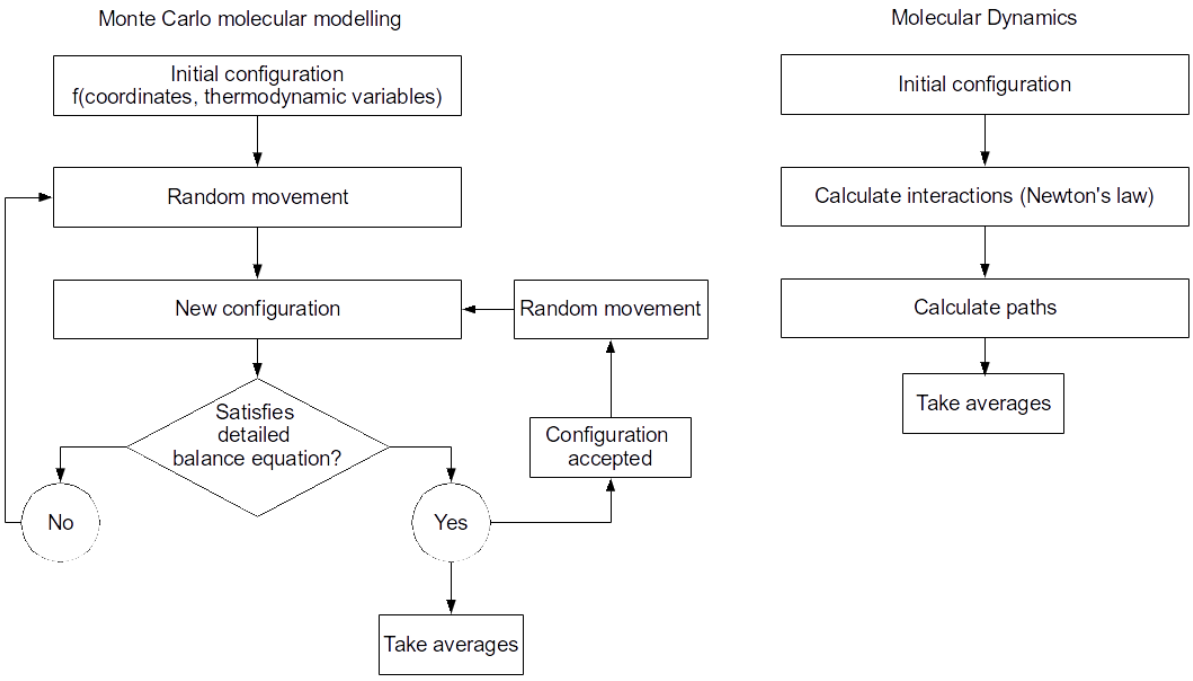

Figure 8: Differences between Monte Carlo and Molecular Dynamics modelling strategies. MC generates random states and check their validity a posteriori, instead of trying to reproduce the dynamics of the system.

one of his Annus Mirabillis papers (Einstein 1905). Brownian motion originated simple models for the motion of polymeric chains in solution, on which some models to determine diffusivity of small tracers in polymeric matrices are based.Rouse 1953, proposed a model to describe the behaviour of a single polymer chain in solution. It pictures a polymer chain as a linkage of beads and springs (Figure 5). The description, in terms of a linkage of Rouse segments is a simplifiation of the enormous number of degrees of freedom associated with all the chemical bonds of a long polymer chain, therefore falling in the category of mesoscale methods. In spite of being originally intended for describing the motion of a single polymer chain in solution, the

Rouse theory has been found valid for more concentrated polymer solutions supposing there were not any entanglements between chains. The centre of mass of the chains is the reference point for displacements. With these conditions, the self-diffusion constant of the centre of mass (the diffusion coefficient) is given by equation 14:

$$D = \lim_{t \to +\infty} \frac{1}{6t} \langle [r(t) - r(0)]^2 \rangle (14)$$

which is known as the mean square displacement of the particles. $\langle [r(t) - r(0)]^2 \rangle$ is the vector distance travelled by the centre of masses of the subject over the time interval. In the framework of the model:

$$\langle [r(t) - r(0)]^2 \rangle = 6 \frac{k_B T}{N\xi} \text{ (15);}$$

and hence:

$$D = \frac{k_B T}{N\xi} \text{ (16)}$$

Where k_B is the Boltzmann constant, T is the temperature, N is the number of monomers and ξ is the friction coefficient, which can be obtained by rheological measures. The model would be later updated in order to be valid for more concentrated regimes Rouse 1998.

Mobility or diffusion of a chain of polymer in a solution has been subject of numerous studies for monodisperse systems, where the polymer chains have the same number of monomers N. It appeared rapidly that diffusion depends on chain length, N, or more generally to the molecular weight, M of the diffusing molecule following a power law of the type $D \propto N^{-\alpha}$or $D \propto M^{-\alpha}$. In fact, as it can be noticed in the Rouse theory (equation 16), $D \propto M^{-1}$ with α=1. A previous theory (Einstein 1905), already stated that $D \propto M^{-1/2}$ with α=1/2, and the reptation theory by de Gennes 1971, which pic-

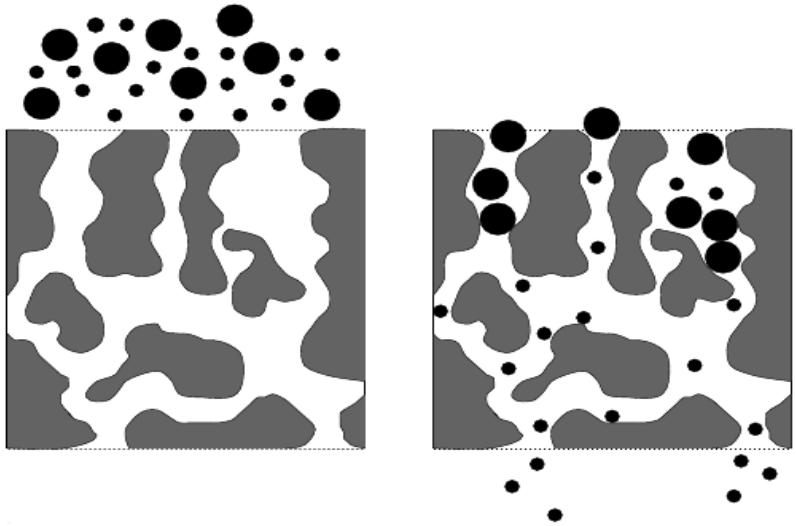

Figure 9: A static description of the diffusion process where the membrane acts as a sieve. The smaller particles have more accessible volume and thus will permeate faster according to the free volume behaviour detailed by Sok 1994. Reproduced with permission of its author, Dr Robert Sok.

tures the diffusion of a polymer chain constrained by fixed tubular obstacles, predicted a dependence of $D \propto M^{-2}$. The application of these theories can be found at Leger et al. 1981 displacement of a polymeric chain in an entangled polymer solution) Antonietti and Sillescu 1985 (diffusion of polystyrene chains in networks) and Von Meerwall et al. 1985 (diffusion of polystyrene in THF solutions. A compilation of α values for different systems can be found at Masaro and Zhu 1999.

All the aforementioned studies deal with the self-diffusion of polymer chain in polymer-solvent solution. Extrapolation of these theories to the diffusion of low-molecular weight molecule into dense polymeric phase should be done with caution. However, since tracer diffusion and polymer chain self-diffusion are equivalent from statistical mechanics point of view, $D \propto M^{-\alpha}$ is expected to be true, at least for molecules of the same family, provided that the increase in the molecular weight respects the pattern. Some efforts to prove $D \propto M^{-\alpha}$ true in the case of low-molecular molecule diffusing in polymeric materials and trying to identified the value of alpha can be found in the literature (Vitrac et al. 2006), even giving more detailed physical meaning to the parameter α Fang et al. 2013.

Now that basics of statistical mechanics of diffusion of a polymer chain into a polymer solution have been explained, it can be detailed how diffusivity can be calculated from the mean square displacement of the center of masses of the molecules by using Monte-Carlo or Molecular Dynamics simulations. Again, diffusivity found this way is a consequence of Brownian motion and it can be defined as molecular mobility or self-diffusion, different from the fickian phenomenological coefficient.

4.2.1 Monte Carlo Method

The Monte Carlo simulations were introduced by Metropolis et al. 1953 as a means to sample points in multidimensional space according to a probability distribution. It quickly found application in many scientific and engineering fields, like the prediction of thermodynamic and kinetic properties. In the Monte Carlo method, the system has an initial configuration that is given by the spatial coordinates of a constant number of particles and a set of external independent variables. These variables represent the thermodynamic state of the system and are chosen by convenience of the problem at hand. Additionally, all MC algorithms are subject to the condition of detailed balance. The condition of detailed balance states that for a system to remain at equilibrium, each elementary process should be equilibrated by its reverse process. One particle is chosen at random and moved by a random amount, generating a new configuration. This new configuration will be accepted or not according to the probability distribution law of statistical mechanics for the chosen set of variables provided that it satisfies the condition of detailed balance. The idea behind the Monte Carlo

simulations is to calculate hundreds of thousands or millions of accepted configurations and equilibrium properties. As stated, all MC algorithms must obey detailed balance regardless of the ensemble of variables used or the type of move made (Gubbins and Moore 2010). As deduced, these theoretical concepts can be applied to calculation of random walk of diffusing molecule in liquid or solid system such as polymeric matrices providing that the complexity and size of the diffusing molecule/polymer system is compatible with the computing cost. Some examples of application of MC simulations to measure molecular mobility and deduce some self-diffusion coefficients were found in literature and described in the following.

Schulz et al. 2006 studied the mobility of ions in polymer by Monte Carlo simulations. As it has been represented in Figure 7, they considered a generic polymer to be formed by polymer chains built by beads that occupy the sites of a three-dimensional simple-cubic substrate lattice of unit spacing. Successive beads are connected either by nearest-neighbour or second-neighbour lattice bonds. A bead can move along a nearest-neighbour bond, provided the target site is vacant and the move does not violate bond restrictions. With these rules, the system is considered to be equilibrated with a concentration c of occupied sites up to c=0.95. Generic diffusing ions are added in this system, and they perform nearest-neighbour hops among the lattice sites. Interactions between beads and ions are taken into account and exchanges between vacancies and nearest occupied neighbour are possible. This lattice concept is also used by the percolation theory that is described later.

They introduced two concepts of diffusion coefficient, the time-dependent diffusion coefficient, which is a self-diffusion coefficient or mobility in a given interval of time, directly calculated from equation 10 and the long-time diffusion coefficient, which is a self-diffusion coefficient considering time as infinite, and as according to what is understood from the paper, would be an equivalent to the phenomenological diffusion coefficient. It is given by the equation 17:

$$D = D_0(1-c)\ f(c,r) \quad (17)$$

Where D is in function of D_0 (the diffusion coefficient of the diffusing molecule in an empty lattice) and ion correlation factor $f(c,r)$ which depends on the length of the bead chain r and the proportion of occupied sites c. In this work, instead of specific values of the diffusion coefficient, understood as molecular mobility, authors show plots of its dependence on time and occupation level of the lattice.

Another example of the use of the Monte Carlo method for determining self-diffusion coefficient or molecular mobility is that of Nilsson et al. 2009, who studied the mobility of undefined punctual penetrants in polyethylene spherulites. Serving as an example of multi-scale modelling, this technique includes two sub-models; one used to build spherulites and other to simulate penetrant mobility through them. Regarding the simulations of the penetrant diffusion, the core of the algorithm consisted of two parts: a random generator providing the direction and the length of each walker jump; and the collision detection algorithms. Intermolecular forces were neglected. After a large number of simulations of the mean-square displacement, the penetrant self-diffusion coefficient was obtained from equation 10. Results show that the linear dependence of the mean square displacement and self-diffusion is isotropic, agreeing with experimental data. As already mentioned, this work is an example of multi-scale modelling: penetrant diffusion is simulated in a more detailed way than spherulite growth and works reasonably well while more computing power is not available.

4.2.2 Molecular Dynamics

The second main method used in atomistic simulations is molecular dynamics. If the origin of the moves in Monte Carlo was completely stochastic, particles in MD move naturally under their own intermolecular forces for every particle. Their initial position is chosen so the system is in or close to a local minimum in the potential energy. Applications of these simulations to diffusion of molecules are also available in the literature. Since the concepts are completely different, a schematic representation of their steps is presented in Figure 8.

Sok 1994 used molecular dynamics simulations to study the permeation process of small molecules through polydimethylsiloxane (PDMS), and to predict self-diffusion coefficient or mobility properties and evaluate their dependence on the penetrant size. In order to reduce necessary computing power and time, PDMS was *coarse-grained*, meaning that two or more atoms are modelled by only one united atom. The self-diffusion coefficient of the polymeric chains, as well as the self-diffusion coefficient of the tracers are, again, given by equation 10. The tracer is not confined to a limited region of space. As the tracer size increases, it becomes increasingly difficult to leave the hole it is situated in and jump diffusion starts to appear: tracer are stuck in a hole for some time and it picks up momentum from kicks of the polymer chains. When there is an opening in the direction of the momentum, the tracer moves to another hole. The time the tracer passes waiting for an opening that permits it to move is called residence time. The author simulates at first the PDMS matrix alone, without tracers. This simulation evaluates the polymer model and gives structural properties like chain/radial distributions and accessible volume distributions. Then, two types of PDMS samples containing tracers are simulated: a small system using

either *He* or CH_4 as tracer; and a larger system, using 7 sets of surrogates with increasing sizes and the same interaction parameter as *He*. The time needed by the tracer to diffuse through the whole thickness of the system seems to be exponentially dependent on their size, at least within the range investigated. The author concludes that the self-diffusion coefficient for molecules of small size (<0.4 nm) in PDMS can be evaluated with sufficient accuracy; getting values of 2.1×10^{-9} $m^2 \cdot s^{-1}$ (simulated) against 2×10^{-9} $m^2 \cdot s^{-1}$ (experimental) for *CH4*, and 18×10^{-9} $m^2 \cdot s^{-1}$ (simulated) against 10×10^{-9} $m^2 \cdot s^{-1}$ (experimental) for *He*.

As seen, the author (Sok 1994) relates diffusion to the probability of finding free holes, bringing up the concept of free volume, but this time from an atomistic point of view. The author states that a polymer has one specific free volume and for each tracer, an accessible volume that depends on both this free volume and the size of the tracer. Once the tracer has entered the polymer matrix, it can only diffuse through its accessible volume, but it also has to find a path of connected accessible volume throughout the complete polymer matrix (Figure 9).

Molecular dynamics have been recently extensively used for the determination of molecular mobility and self-diffusion coefficients of small molecules gases in polymeric membranes by the same group of co-workers (Neyertz and Brown 2008, Neyertz and Brown 2009, Neyertz et al. 2010, Neyertz and Brown 2013, Neyertz et al. 2014). The approach is always quite the same: MD simulations of the membrane, MD simulations of the diffusing molecule itself (for instance in their work on CO_2, it is modelled as a rigid three-site molecule) and its trajectory in the membrane as a function of progressive molecule loading, mimicking either a sorption/desorption or permeation experiment for the membrane. Analysis of the trajectories for each penetrant molecule permitted to the authors to analyse the diffusion mechanism and to calculate the penetrant mean square displacements.

In MD simulations, the mean square displacement is usually then used to evaluate the self-diffusion using equation 10. However this equation is valid under the assumption that the gas molecules follow a random walk, which is not the case of this work, because one of its originalities is that a difference in gas concentration on both sides of the membrane has been imposed. Random walk (and therefore self-diffusion) would be obtained in their case only once the membrane is in equilibrium with the migrant, i.e. within the framework of, what the authors call, a long-time Fickian diffusive limit. This equilibrium could not been reached with MD simulations (simulations are limited to 5000 up to 10000 ps in the study) despite the high mobility of CO_2 into their membrane.

In order to estimate a diffusion coefficient, they used the average MSDs values to estimate a local distribution profile of diffusing molecule within the membrane. Then they fitted this distribution using an analytical solution of Fick's law equation 18:

$$C(z,t) = C_0 \; erfc\frac{z}{2\sqrt{Dt}} \quad (18)$$

Where C is the concentration of the tracer within the medium, C_0 its concentration at the interface, D its diffusion coefficient in the medium, t the time-interval considered and z the coordinate in the reference system.

As expected, the diffusivity determined using this approach is not fully consistent with experimental, phenomenological values (30-40 $\times$ 10^{-11} m^2 s^{-1} instead of 1-2 $\times$ 10^{-11} m^2 s^{-1} for the experimental data) (Neyertz and Brown 2013). This is easily understandable due to the limited amount of time the simulation can reach. The same authors propose a simplification of their MD simulations, named bulk techniques that allow to extend the penetrant trajectories up to 10^7 ps (Neyertz et al. 2010). In that case, identified diffusivity values are much more consistent with the experimental one (3-4 $\times$ 10^{-11} m^2 s^{-1}).

This group of co-workers used the same approach on O_2 in their most recent paper, (Neyertz et al. 2014) to study the transport properties of oxygen in POSS (polyhedral oligomericsilsesquioxanes) membranes using classical molecular dynamics simulations over a timescale long enough to reach the Fickian regime for diffusion mimicking a sorption experiment. This study has brought new insights in the understanding of the diffusion mechanism; the O_2 molecules would permeate the organic phase and move through combinations of oscillations within available free volumes in the matrices and occasional jumping events.

In addition to the aforementioned papers, other recent studies could be find dealing with the determination of diffusion using MD such as for example the recent work of (Yang et al. 2013) who studied diffusion behaviour of seven several gases (hydrogen, carbon monoxide, carbon dioxide, methane, acetylene, ethylene and ethane) in oil and paper medium. Authors used molecular dynamics to reveal the diffusion mechanism of gas molecules in oil-paper insulation system at the microscopic level and, in particular, to in-depth understand the micro-mechanism of diffusion of the targeted molecules. They determined the diffusion coefficients of gas molecules in cellulose and in oil and demonstrated that free volume of gas molecules is the main factor that influences the diffusion behaviour in oil, whereas intermolecular interaction is the main influencing factor of diffusion behaviour in cellulose.

To conclude this section, it has been shown that at the time being, atomistic and mesoscale methods continue to be hampered by the computer cost of calculations and that only simple systems (homopolymers, small diffusing molecules such gases, etc.) were generally investigated by these methods. At the moment electronic scale methods remain dedicated to a description of the matter (association of atoms). First studies of molecular mobility appear with atomistic and mesoscale level. Both methods are based on either Monte-Carlo simulations or molecular dynamics. These simulations permits to calculated a mean square displacement of diffusing substance that could be used to calculate self-diffusion. The most promising results in the field of diffusion under concentration gradient were obtained with molecular dynamics and recent papers on the topic propose some calculations of diffusion coefficient, assimilate to a fickean, phenomenological diffusivity, of gases in simple polymeric, dense membranes with an acceptable computing time. However, simulation time scale for MD is still too low to permit the representation of long-diffusion time and for diffusing molecule more complex than gases.

5 General conclusions

As seen, and repeated several times through the text, predictive modelling of the phenomenological diffusion coefficient is still far from ready for direct application. Models yielding macroscopic diffusivity are still too complicated, or require abstract and extensive experimental input. Approaches developed specifically for an industrial application, like the Piringer equation, while potentially useful, rely too much on diffusivity data obtained experimentally, and hence require an update in order to take into account the data published since they were first presented.

Regarding the experimental methodologies, it is clear what are the main points on which it must be built: contact system, mathematical solution according to its geometry, and appropriate analytical technique to monitor the migrant concentration evolution; there is not a simple method for measuring diffusion coefficient of low molecular weigth molecules in polymer. As of today, and as it has been seen, the experimental setup depends on the system under investigation.

The increase in the computing power in the last thirty years, has made possible the application of modelling strategies allowing rigorous description of mobility of molecules at the microscopic scale, that were pure theory when they first came out, like Monte Carlo or Molecular Dynamics. Unfortunately, as of today these strategies only allow to simulate a very small section of the system (on the scale of the pm) for a very small time (on the order of the ps). It is to expect that computing power will continue to increase and to become exponentially cheaper in the next years, which

will allow rigorous simulation of the system at space and time scales that will make them useful for industrial applications like the prediction of diffusivity in food packaging systems. As well, it will be finally possible to compare the macroscopic or phenomenological concept of diffusivity with the microscopic mobility as a result of Brownian motion. Until then, packaging industry will have to rely mainly on experimentation to obtain reliable values of diffusivity.

Chapter III

This chapter summarises the experimental methods, numerical schemes and statistical treatment of data developed for the determination of transport properties. It presents the applicability of the vibrational spectroscopy tool Raman microspectroscopy to determine the diffusion coefficient and the solubility limit in a high barrier polymer in glassy state (Publication II), and an identifiability analysis to determine the conditions for the determination of both diffusivity and mass transfer coefficient by different methodologies (Publication III). More specifically, Publication II shows the application to a system where only diffusive transport is considered, hence $D_{App}=D$; differently from Publication III, where the system under investigation was chosen in order to study the contribution of both diffusion and desorption to D_{app}.

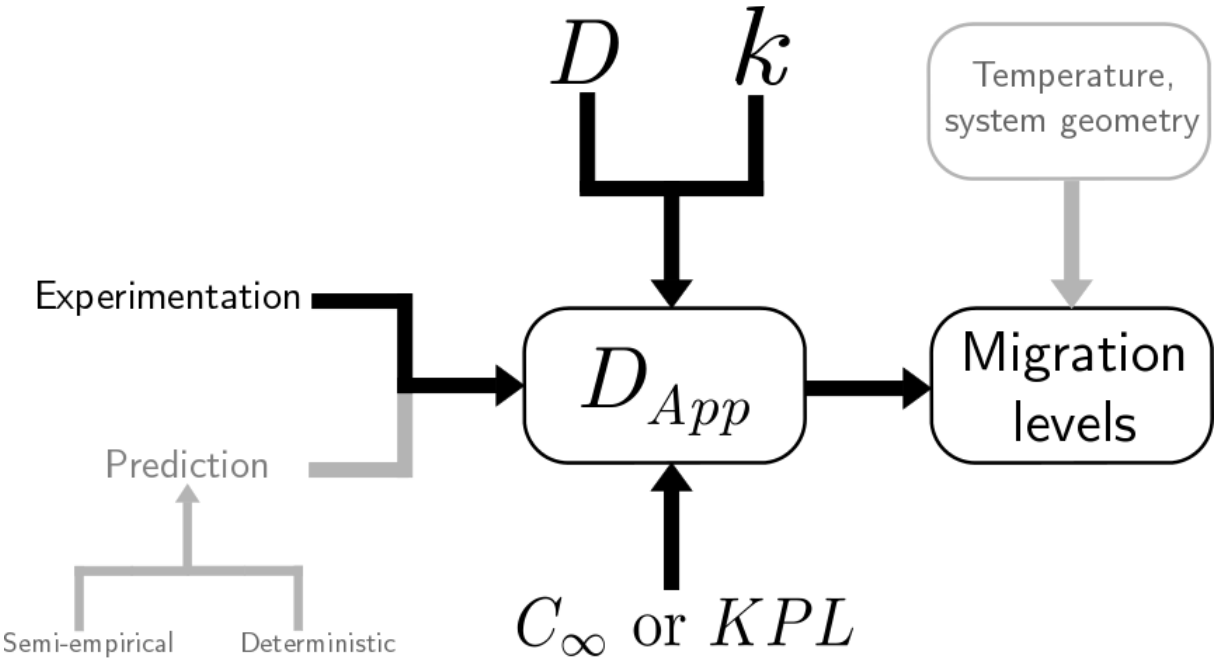

Publication II: Determination of mass transfer properties in food/packaging systems by local measuring with Raman microspectroscopy.

Brais Martínez-López, Pascale Chalier, Valerie Guillard, Nathalie Gontard, Stephane Peyron

Abstract

A fast, non-destructive method, based on the determination of local concentration profiles in the polymer thickness with Raman microspectroscopy is presented here and used to assess diffusivity of a model molecule (*p*-terphenyl) in amorphous polystyrene films at 95 °C ($2.38 \pm 1.08 \times 10^{-17}$ $m^2 \cdot s^{-1}$). This methodology is validated by comparison with a more classical destructive approach based on monitoring concentration evolution in the whole of the film with gas chromatography (89.4×10^{-17} $m^2 \cdot s^{-1}$). These values are in agreement with data available in the literature for molecules on the same molecular weight and temperature range determined with local measuring while significantly lower than those determined by global measuring. Raman microspectroscopy is found to be adapted to slow diffusion speeds, typically found in high barrier polymers, allowing to obtain diffusivity long before the equilibrium is reached, and thus, without the need of the partition coefficient.

Keywords: diffusion in polymers, confocal raman microspectroscopy, polystyrene, packaging.

In press. *Journal of Applied Polymer Science* **2014**, *131*, 40958.

1 Introduction

Food Contact Materials (FCM) must comply with the European Regulation 1935/2004 that can be summed up in two main requirements: Packaging materials shall not transfer their constituents to food in quantities which could (1) endanger the human health and (2) bring about deterioration in the organoleptic characteristics. To ensure the safety of consumers, the European regulation 10/2011 translates the requirements of regulation 1935/2004 to plastic materials and lays down the procedure for their compliance. In addition to the requirement of inertia for plastic FCM, the regulation 10/2011 provides guidelines on the testing procedure for migration assessment. An important aspect of the regulation is that it allows the use of "generally recognized diffusion models based on experimental data [...] under certain conditions" to determine overestimated migration levels, thereby avoiding expensive and time-consuming experiments. In this way, the existing models, used to describe migration, are based on Fick diffusion equation that involves at least two key parameters: (i) the diffusion coefficient (D), and (ii) the partition coefficient (KPL). Little attention has been paid though to the assessment of the partition coefficient and a commonly accepted approach is to use a KPL value of 1 if the migrant is soluble in the food or 1000 otherwise (Simoneau 2010). Contrary to the KPL coefficient, the diffusion coefficient or diffusivity, must be determined for each couple polymer-migrant because it depends on physical characteristics of both (molecular mass, molecular volume, polarity of the diffusing molecule, glassy or rubbery state of the polymer matrix). Besides experimentation, diffusivity can be determined via predictive modelling; generally based on empirical or semi-empirical relationships like the one developed by (Piringer 2007) or more recently by Welle 2013. Special attention should be paid to Piringer semi-empirical relationship, which does not try to accurately predict, but to give worst-case scenario diffusivity values. This strategy based on purported overestimation proved to be an efficient strategy for the safety evaluation of FCM but may be inappropriate in other cases such as plastics decontamination, inherent to recycling process. In this case, overestimation of the diffusivity of migrants could lead to an overestimation of the efficiency of the decontamination, which would endanger consumer health. Experimental determination of diffusivity remains therefore indispensable for reliable prediction of migrant diffusion within polymer.

The experimental determination of D consists on two steps: (1) monitoring diffusion of a molecule through a polymer resulting of the imposition of a concentration gradient and (2) identification of the diffusivity value from experimental data by comparison with a mathematical model using a dedicated optimization algorithm. Experimental data can be of two kinds, depending on the analytical tech-

nique used to monitor the migrant: (1) concentration profile in function of the polymer thickness (local measuring or local profiling) (2) average concentration in the whole film in function of time (global measuring, global concentration evolution or global kinetics). Identification of a diffusivity value necessitates to reach the equilibrium or to know the KPL coefficient between the polymer and the medium in contact with it. Since KPL data is scarce, and considering the time required to reach equilibrium for high barrier polymers, determination of diffusion coefficient in the latter is made difficult. As consequence, most published D values have been collected on polymers that are rubbery at room temperature (Ferrara et al. 2001, Helmroth et al. 2003, Cava et al. 2004, Doppers et al. 2004, Cruz et al. 2008, Fu and Lim 2012). Diffusivity values for the two high barrier polymers most used in packaging industry (PS and PET) are rare, and there are often for low-medium molecular weight and presumably highly volatile molecules. In the case of amorphous PS, there are diffusivity values for cyclohexane (86.2 $g{\cdot}mol^{-1}$, Ogieglo et al. 2013); linear alkanes (from 114.3 to 226.4 $g{\cdot}mol^{-1}$) (Bernardo 2012); carboxylic acids (from 60.1 to 256.4 $g{\cdot}mol^{-1}$) (Bernardo et al. 2012), alcohols (from 32 to 242.4 $g{\cdot}mol^{-1}$) (Bernardo 2013); toluene (92.4 $g{\cdot}mol^{-1}$), chlorobenzene (112.6 $g{\cdot}mol^{-1}$) and phenyl-cyclohexane (160.26 $g{\cdot}mol^{-1}$, Dole et al. 2006),homologous series of fluorescent tracers (from 230 to 1120 $g{\cdot}mol^{-1}$, Pinte et al. 2010) and Rubrene (532.7 $g{\cdot}mol^{-1}$, Tseng et al. 2000); being the majority of values determined in the rubbery state. More abundant is literature on PET (Pennarun et al. 2004a,b, several molecules with different functional groups from 78 to 431 $g{\cdot}mol^{-1}$) and Franz and Welle 2008 (several molecules with different functional groups from 92.4 to 298.5 $g{\cdot}mol^{-1}$) amongst others. Some of these approaches make possible to determine diffusion coefficient in a faster-non destructive way, by obtaining local concentration distribution profiles through the thickness of the material. For example, non-invasive FRAP techniques (fluorescent recovery after photobleaching) proved to be well adapted to the investigation of diffusion of high molecular weight surrogates in high-barrier polymers but is limited to transport of fluorescent molecules (Axelrod et al. 1976). Applied to a specifically designed set of model probes ranging from 230 and until 1100 $g{\cdot}mol^{-1}$, FRAP technique was used to determined diffusion (reaching 10^{-19} $m^2{\cdot}s^{-1}$) into amorphous PS (Pinte et al. 2010). Second example of promising non-destructive method is Raman microspectroscopy, which turned out being a powerful method to provide spatially resolved information about the chemical composition of materials. With confocal collection optics, the method was well suited to the characterization of diffusion in rubbery polymers (Mauricio-Iglesias et al. 2009) In this work, it permitted the determination of diffusivity in the studied polymer in less than 24h of contact with the food simulant after one profile acquisition taking

4h whereas the determination of D using classical method based on global average profile required 26 days to obtain the full kinetics in function of time.

The objective of this study is to explore the potential of Raman microspectroscopy as analytical device adapted to the fast characterization of mass transport properties of molecules in high-barrier polymers at glassy state for which diffusion speeds are usually very slow. *p*-Terphenyl was selected as model molecule to follow the diffusion phenomena in amorphous PS in glassy state. A Moisan test was used as experimental set up for inducing mass transfer phenomena into virgin PS films. Raman microspectroscopy was used to determine local concentration profiles through the thickness of the polymer after a given time of contact. Diffusivity value identified from the local distribution profile was compared to that determined by global evolution concentration measuring assayed by GC analysis. Difference in resulting diffusivities was discussed in term of usability and relevance of each method.

2 Materials and methods

2.1 Chemicals

Amorphous polystyrene with a molecular weight of approx. 285000 g·mol^{-1} and a glass transition temperature (case II transition) of approx 105 °C was purchased from Polyone France. Ultra Low Molecular Weight Polyethylene (ULMWPE), with a dropping point around 115 °C was kindly provided by TER France. *p*-terphenyl (purity ≥ 99.0%) CAS n. 92-94-4 with a molecular weight of 230.3 g·mol^{-1} , and internal standard butyl hydroxyl toluene (BHT) (purity ≥ 99.0%) CAS n.128-37-0, with a molecular weight of 220.35 g·mol^{-1} were purchased from Sigma-Aldrich (France).

2.2 Fabrication of films and sources

Virgin Polystyrene films were made by thermoforming PS pellets (hot press) at 200 bar and 165 °C during 5 min. Polystyrene films with 0.5, 1, 2 and 4 %wt of *p*-terphenyl were made by solvent-casting method, solving PS pellets (0.2 g/mL) along with *p*-terphenyl in THF and spreading it into a plexiglass surface. 0.5, 2 and 10 %wt *p*-terphenyl ULMWPE sources were made by mixing ULMWPE pellets with *p*-terphenyl at 135 °C using a 5 cm petri dish as mould. Liquid wax and *p*-terphenyl were mixed by stirring manually and left to solidify. p-Terphenyl pellets were made by pressing *p*-terphenyl powder at 7.5 ton using an evacuable pellet die purchased from Eurolabo (Paris, France). The PS film thickness was measured by using a micrometer (Braive Instruments, Chécy, Fr) in quintuplicate.

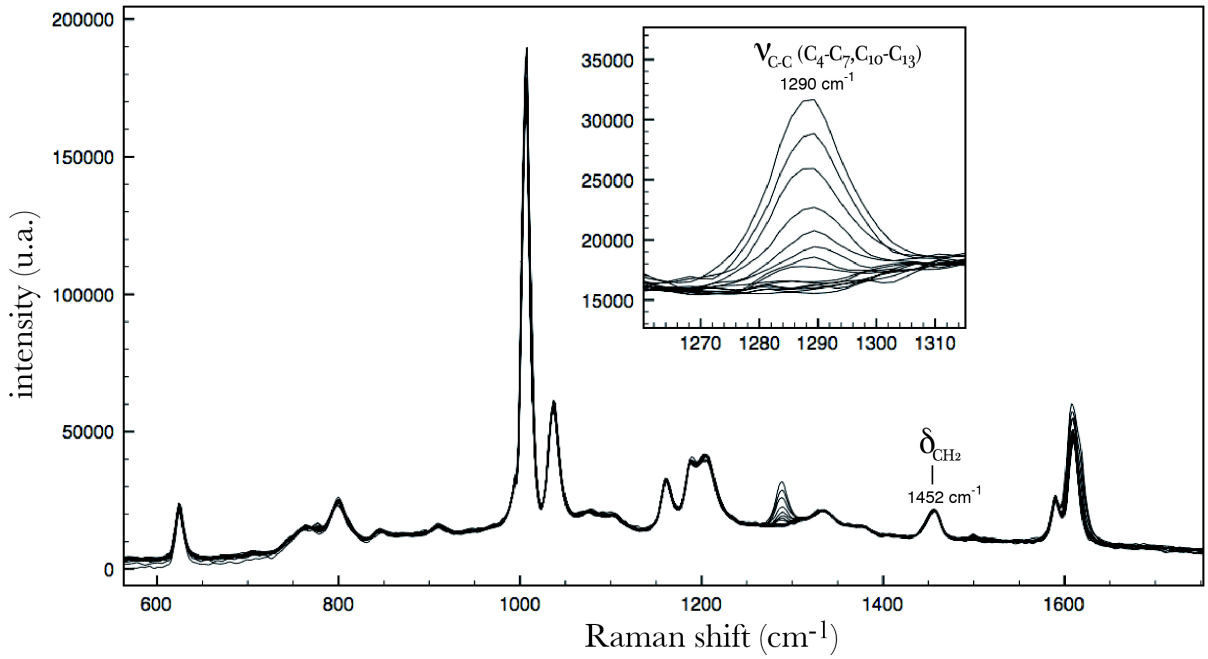

Figure 10: Raman spectral fingerprint of PS+p-terphenyl. Focused region shows the peaks selected tofollow p-Terphenyl concentration variation in the thickness of the film.

2.3 Diffusion assay

Diffusion assays of *p*-terphenyl from a spiked Ultra low molecular weight polyethylene (ULMWPE) source, as well as a pure *p*-terphenyl pellet placed in contact with a virgin PS film were conducted by the Moisan method (Moisan 1980, Reynier et al. 1999, Dole et al. 2006) at 95 °C. Before each measurement, the PS film was removed and wiped with ethanol. Raman measurements were performed once after 72 h of contact with the pellet and 30 days of contact with ULMWPE spiked at three different concentration levels (0.5, 2 and 10 %wt). The GC measurements were done after 4 *h*, 17 *h*, 24 *h*, 48 *h*, 72 *h*, 1 week, 2 week, 3 week and 4 week of contact with a 0.5 %wt ULMWPE source. PS films in contact with the source had to be replaced after each GC measurement due to the destructive nature of the method.

2.4 Raman measurement

p-Terphenyl concentration profiles were determined as follow. Thin slices of PS were prepared using a razor blade and stuck on a microscope slide. Raman spectra were recorded between 800 and 3500 cm^{-1} Raman shift using a confocal Raman microspectrometer Almega (Thermo-Electron) with the following configuration: excitation laser He-Ne 633 nm, grating 500 grooves/mm, pinhole of 25 μm, objective x50. The resultant spectra were the mean of two acquisitions of 25 s each. Measure-

ments were carried by triplicate in the cross-section of the sample with a spacing of 1 µm.

2.5 Raman calibration

All spectra pre-treatments were performed with Omnic v7.3 (Thermo-Electron). Processing included: (i) a Multipoint linear baseline correction, (ii) normalization according to the area of the PS specific band at 1452 cm^{-1} assigned to the CH_2 bending mode (δCH_2). The relative content of *p*-terphenyl was assessed according to the area of the specific band (1290 cm^{-1} , Bower and Maddams 1989) assigned to the inter-ring *C-C* stretching band (νC_4-C_7, C_{10}-C_{13}). PLS regression was applied to quantify the concentration of *p*-terphenyl in PS. Calibration procedure was performed on the basis of 1290/1452 area ratio and concentration of *p*-terphenyl in PS was established by repeatedly taking measures of spiked *p*-terphenyl/PS films at 0.5, 1, 2 and 4 %wt concentration levels with TQ analyst software (Thermofisher). Calibration performance was calculated as the multiple regression coefficient (R^2) and root-mean-square error ($RMSE$) of calibration. The root mean square error ($RMSE$) was used to evaluate the goodness of the fit, according to equation 19.

$$RMSE = \sqrt{\frac{(y_{exp} - y)^2}{N - p}} \quad (19)$$

Where y_{exp} and y are respectively the experimental and predicted *p*-terphenyl concentration values, N is the number of measurements and p is the number of identified parameters. Since in this case it is only used to evaluate the goodness of the fit and not to identify any parameter of the model, p is equal to 0. The ratio of standard error of prediction to standard deviation (RPD) was calculated as Equation 20:

$$RPD = \frac{SD_{cal}}{RMSE} \quad (20)$$

where SD_{cal} is the standard deviation of the *p*-terphenyl percentage in the calibration data set.

2.6 Additive extraction and GC measurement

PS films were dissolved under agitation in 5 mL of dichloromethane for 1.5 h, during which 80 μL of a solution of a 1 mg mL^{-1} solution of BHT was added. After that, PS was re-precipitated by adding 5 mL of ethanol under agitation during 30 min. In order to remove the PS that was still in the aqueous phase, the organic extract was placed under N_2 gas to evaporate a small amount of dichloromethane. The reprecipitated PS was completely removed by filtration, and the aqueous extract was concentrated again under N_2 gas to reduce the volume of solvent to 2 mL.

1 µL of organic extract was injected in an Agilent technologies 7890A GC equipped with an Agilent automatic liquid sampler an HP 5 column (30m x 0.32 mm, film thickness 0.25 µm, J & W scientific) and a flame ionisation detector (FID; hydrogen, 30 $mL \cdot min^{-1}$; nitrogen 30 $mL \cdot min^{-1}$; air, 300 $mL \cdot min^{-1}$). Hydrogen was the carrier gas at a flow rate of 1.5 $mL \cdot min^{-1}$. The temperature was set at 250 $^{\circ}C$ for the injector and 300 ℃ for the detector. The temperature ramp of the oven ranged from 40 to 250 ^{o}C at 4 ^{o}C min^{-1} and maintained at 250 ^{o}C during 15 min. *p*-terphenyl concentration in the vial was determined by reporting the peak area of *p*-terphenyl to the peak area of the BHT, which had been previously calibrated with solutions of known concentrations to take into account all stages in the extraction-reprecipitation process. The calculated response factor of the calibration was of 0.93 and the extraction performance, calculated on the basis of the data points used on the determination of diffusivity was of 37 ± 4.4 %.

2.7 Identification of diffusivity

The internal diffusion of a migrant in the packaging is given by Equation 21 (Fick 1855) where x is the distance (m), C, the polymer concentration in diffusing substance (mass diffusing substance/mass of polymer) and D the diffusivity of the molecule in the packaging ($m^2 \cdot s^{-1}$). D is assumed independent of the concentration of the diffusing substance, so the system is said to follow Fickean kinetics. Equation 21 can be solved with the initial and boundary conditions that apply to the case, in order to obtain an expression for the concentration distribution.

$$\frac{\partial C}{\partial t} = D\frac{\partial^2 C}{\partial x^2} \quad (21)$$

The analytical solutions of equation 21 that are used in this work are given by Equation 22 and Equation 23 (Crank 1980). Equation 22 is used when the thickness of

the system is several orders of magnitude greater than the region of the system in which diffusion occurs or can be detected. This kind of solutions (called semi-infinite or short-time solutions) is easily recognized because of the use of the error function as a result of the integration of the original differential equation. It allows following the evolution of a local concentration profile in time. Equation 22 represents the concentration evolution in time in the whole thickness of the film. The different conditions to which each solution applies can be noticed by the variables present on them: Equation 23 lacks of the variable x (position in the film), since the concentration distribution on the film is not taken into account. However, since the integration has been made considering the system as finite, it does take in to account the parameter L (thickness of the film).

It is to be pointed that, in both solutions, C_∞, the concentration of the diffusing substance at equilibrium or solubility limit of the diffusing substance in the diffusing medium is required.

$$\frac{C}{C_\infty} = erfc\left(\frac{x}{2\sqrt{Dt}}\right) \quad (22)$$

$$\frac{C}{C_\infty} = 1 - \frac{8}{\pi^2}\sum_{n=0}^{\infty}\frac{1}{(2n+1)^2}e^{-\frac{(2n+1)^2\pi^2 Dt}{4L^2}} \quad (23)$$

Both solutions describe sorption kinetics into an originally virgin medium, from a source, or medium spiked with the diffusing substance. *p*-Terphenyl diffusivity was identified from experimental data by minimizing the sum of the squared residuals between experimental and predicted profiles and by using an optimization method (Levenberg-marquardt algorithm, optimization routine predefine from Matlab software). The root mean square error (RMSE) was used to evaluate the goodness of the fit, according to Equation 19. Since one parameter is being identified (the diffusion coefficient), p=1.

2.8 Estimation of *p*-terphenyl solubility in PS

The content of *p*-terphenyl in PS at equilibrium (C_∞) was determined by assuming that the region immediately adjacent to the source reaches equilibrium in a very short time. This way, the *p*-terphenyl/PS characteristic peak area ratio of the first point of several concentration profiles after 30 days of contact with the ULM-WPE sources where measured with Raman, and then converted into concentration units with the chemometric model detailed above (§2.6). In order to confirm that C_∞ is independent of the source concentration, sources spiked at three differ-

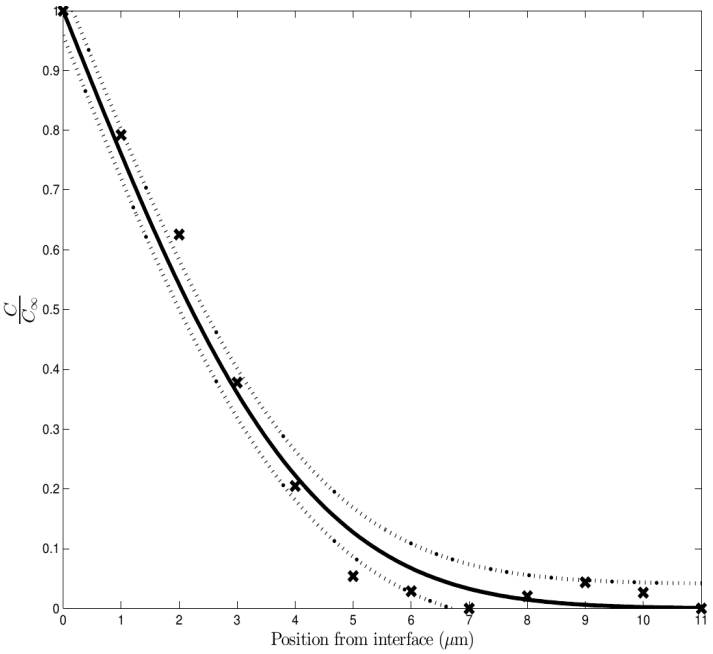

Figure 11: Concentration profile of p-Terphenyl through the thickness of PS film submitted to a contact with a p-terphenyl pellet during 72 h. The continuous line represents the profile with the predicted value of diffusivity and the dotted lines, the predicted concentration ratio ± RMSE, which in this case was of 0.0124.

ent *p*-terphenyl concentration levels (0.5, 2 and 10 %wt) were used. Three measures were taken for each source concentration level to ensure repeatability.

2.9 Uncertainty propagation and impact on identified diffusivity.

A Monte Carlo sampling was applied to obtain 95 % confidence interval of the diffusion coefficient for each one of the methodology. The Monte Carlo sampling consists on adding artificial noise to one or more of the variables used in the identification of diffusivity. One way to do this is to introduce variations on the variable subject of study within a certain interval that imitates the error that can be present in an actual measure. This process is repeated many times, and each of these times the diffusivity is identified.

At the end, a diffusivity distribution can be built, where the mean of the distribution would be the searched diffusivity and the confidence interval may be determined as those values that enclose the 95% of the distribution around the mean. For the determination from local concentration profiles, artificial noise was added by introducing variations on the position of each experimental point, within the interval ± 1 μm, according to the resolution of the Raman microscope. In the case of determination from concentration evolution in time, variations were introduced on the equilibrium concentration, C_∞ within the interval of the standard deviation derived from its de-

termination. The process was repeated 10000 times for each methodology. A Lilliefors test was applied to the parameter distribution to verify the hypothesis of diffusivity following a normal distribution. If the test was positive, the confidence intervals were calculated using the formula for a normal distribution. If no known probability distribution fits the data correctly, instead of a confidence interval, the incertitude is given by manually discarding the 2.5% of the upper and lower values (Penicaud et al. 2010).

3 Results and discussion

3.1 Test conditions

Since one of the goals of the study is to show that the local measuring methodology is well adapted to high-barrier polymer in glassy state, amorphous PS which is also well representative of the food-packaging industry was selected. The polymer being in glassy state means that transfer will occur at very low speeds. A robust determination of diffusivity requires at least 4 data points and the maximum resolution of the Raman microscope is of 1 μm; which means that if the diffusing substance does not penetrate at least as deep as 4 μm, the diffusivity value found this way may not be representative of the process. In order to be able to get enough data points in a reasonable time, diffusion must be accelerated by means of performing the test at a high temperature while the polymer remains at glassy state, hence the choice of 95 ^{o}C. Instead of using an actual additive present in commercial packaging, the study was carried on with a model molecule. *p*-Terphenyl was chosen because of its strong Raman signal even within the PS matrix.The thickness of the PS films is also important for the correct application of the methodology, in two ways. The first is an experimental limitation: above 350 µm it becomes difficult to obtain a clean cut that will ensure usable concentration profiles. Second is related with the semi-infinite hypothesis: in order to consider a system as semi-infinite, the region in which diffusion occurs must be significantly smaller than the size of the system; otherwise it must be considered finite, which changes the boundary conditions that apply in the integration of Equation 2 1 and thus, the analytical solution to use in the diffusivity determination, hence the need of knowing the exact thickness.

3.2 Determination of diffusivity of Terphenyl in PS from local concentration profiles.

Raman microspectroscopy was applied to establish the local concentration profile of *p*-terphenyl in the thickness of PS film. The Figure 10 shows the Raman spectra acquired from the surface to the centre of the PS film after 72 *h* of contact with the pellet. The signal of the characteristic peak of *p*-terphenyl at 1285 cm^{-1} is of high intensity and was well suited to follow the sorption of *p*-terphenyl. On this basis, four concentration profiles were separately plotted and used to evaluate the diffusivity of *p*-terphenyl using Equation 22. An example of these profiles is plotted in Figure 11. The ratio C/C_∞ is assumed to be represented by a signal ratio A/A_0, where A is the *p*-terphenyl/PS peak area ratio at each of the points and A_0 is the *p*-terphenyl/PS peak area ratio at the position $x=0$. Therefore, no quantification of the concentration was required at this stage for diffusivity identi-

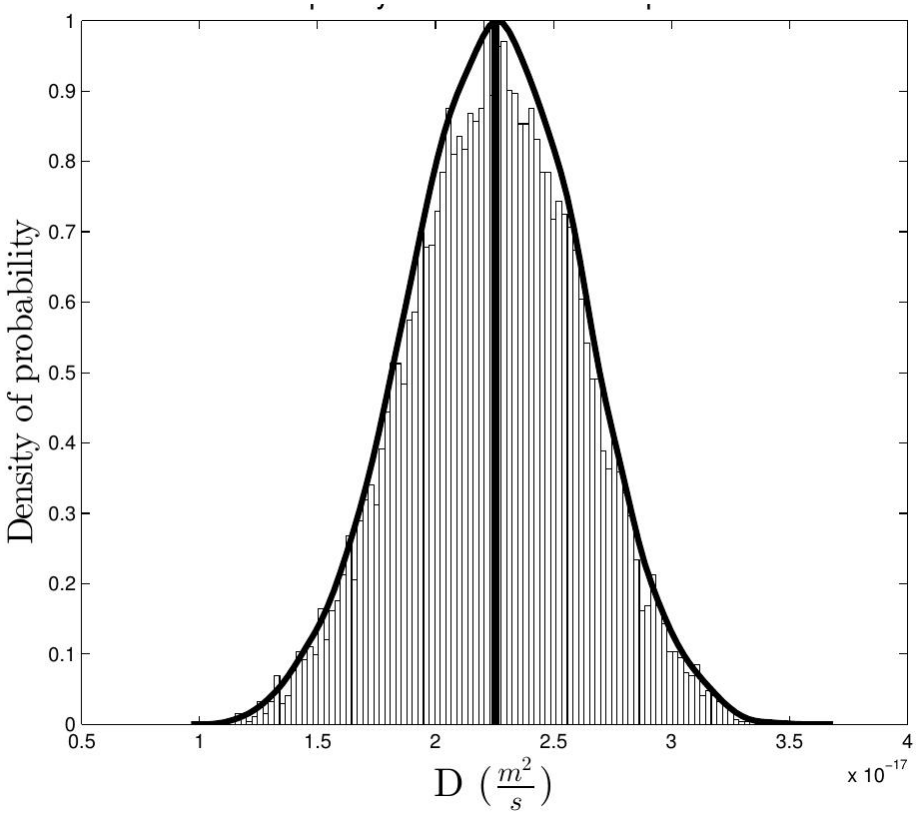

Figure 12: Normal distribution resulting from noise addition within the range ± 1 μm to the experimental points obtained with Raman. The solid curve represents the modelled normal distribution and the black vertical line the mean of the distribution.

fication. The average value of diffusivity obtained for the 4 profiles was found equal to 2.17 ± 0.76 × 10^{-17} $m^2 \cdot s^{-1}$ proving the good repeatability of the measure. As shown in Figure 11 *p*-terphenyl sorption is only detectable in a region as little as 6 µm from the interfaceof a 260 µm PS film, but this depth was sufficient enough to gain a reliable diffusivity value as regard to the Raman microscopy resolution. Also, 6 µm out of 260 µm is well in agreement with the semi-infinite consideration of the system. The same procedure was applied to three other samples after 30 days in contact with ULMWPE spiked at three different concentration levels (0.5, 2, 10 %wt). A value of 2.26 ± 1.13 × 10^{-17} $m^2 \cdot s^{-1}$ was obtained independently of the source content of *p*-terphenyl, on the basis of three concentration profiles taken for each concentration level. This value is not significantly different from the value obtained after 72 h of contact, so a final value of 2.38 ± 1.08 × 10^{-17} $m^2 \cdot s^{-1}$ will be considered. This low diffusivity is representative of the slow diffusion process that was to expect in a high barrier polymer below its glass transition temperature. From a practical point of view, an uncertainty in the interface location during the Raman measurement may be pointed out. In order to assess the impact of a possible error related to interface location, error during D identification was computed by introducing variations within the interval of ± 1 μm in the location of each measurement point. As shown in Figure 12, the sensitivity analysis showed that diffusivity values followed a normal distribution, according to the Lilliefors test, with a mean of 2.25 × 10^{-17} $m^2 \cdot s^{-1}$ and a confidence interval of (2.24 × 10^{-17}, 2.26 × 10^{-17}) $m^2 \cdot s^{-1}$. The mean of the distribution is consequently, almost exactly the same value than the measured diffusivity. The narrow confidence interval means that the misplacement of the points does not represent a main source of error in the determination of diffusivity. The determination of diffusivity from local concentration profiles obtained with Raman microspectroscopy has already been applied to low barrier polymers above their glass transition temperature. For example Mauricio-Iglesias et al. 2009 reported a diffusivity value of 8 × 10^{-14} $m^2 s^{-1}$ for optical brightener Uvitex OB (molecular weight of 430.6 $g \cdot mol^{-1}$) in linear low-density polyethylene. It has been here evidenced that this analytical strategy can also be successfully applied to a high-barrier polymer such as PS below its glass transition temperature, even if diffusion occurs significantly slower.

3.3 Determination of diffusivity of Terphenyl in PS by following global concentration evolution in time.

In order to clarify the impact of the way of characterization in diffusivity, the same system (p-terphenyl in amorphous PS at 95 °C) was submitted to diffusivity determination by global concentration evolution measuring in time, which can also be called kinetics reconstruction or simply global measuring. The classical global concentrations

approach consists on following the diffusing molecule mass gain in an originally virgin film until equilibrium is reached. As expressed by Equation 23, knowing the value of the concentration at equilibrium, represented by the variable C_∞ is absolutely mandatory. However, according to the value of diffusivity obtained above, equilibrium would be reached after more than 600 years of contact. Since this is unattainable in the practice, other way to find this parameter must be developed, which implies that this technique alone is not sufficient to accurately determine diffusivity, at least for slow systems, which are the case of high barrier polymers such as amorphous polystyrene.

3.3.1 Determination of p-terphenyl solubility in PS.

Since equilibrium in the whole film is unattainable in the period of time of the study, the assumption that the region of the film immediately adjacent to interface reaches equilibrium in a reasonable time was made. The Raman microscope was used to measure the local concentration of *p*-terphenyl at the film surface (which is the first point or *x=0* in the concentration profile) in contact with the spiked ULMWPE.

The PLS regression applied to quantify the concentration of *p*-terphenyl in PS gave a 0.97 regression coefficient for calibration and validation. The root-mean square error of calibration (*RMSEC*) that refers to the uncertainty of calibration for selected data was 0.246 and *RMSEP* value for prediction data is 0.196. These two values attest to the low differences between nominal concentration and values predicted by the model. RPD value calculated from the validation data set is 4.8 that can be

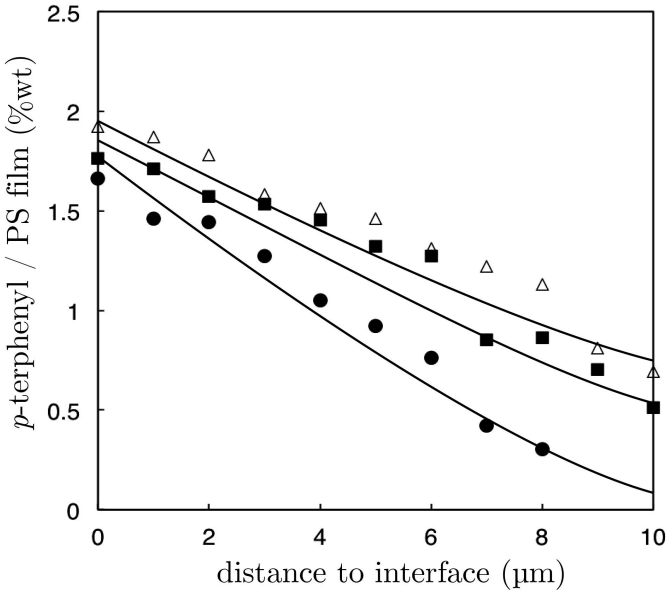

Figure 13: Experimental (symbols) and predicted (solid lines) local concentration profiles in originally virgin PS films resulting from 30 days of contact with ULMWPE spiked with respectively 0.5 %wt (■), 2 %wt (●) and 10 %wt (Δ) concentration levels of p-terphenyl.

considered as a good indicator of prediction purpose. Using the PLS regression, the sorption of *p*-terphenyl in the thickness of the PS film can be plotted as a function of concentration (%wt). The Figure 13 shows examples of profiles obtained with different source concentrations of 0.5, 2 and 10 %wt after 30 days of contact. It can be pointed out that concentration of *p*-terphenyl in PS at interface, obtained from 9 measures with the three different source concentrations provided a repeatable value of 1.74 ± 0.5 %wt, as it can be seen in Figure 13. This value can be considered as the solubility limit of *p*-terphenyl in PS and consequently represents the concentration value (C_∞) reached in the PS at the equilibrium state after a long-time period of contact with spiked ULMWPE.

3.3.2 Determination of D.

The sorption kinetics of p-terphenyl from ULMWPE to PS were followed by analysis of p-terphenyl mass uptake by the PS film using gas chromatography after extraction. Figure 14 shows the concentration ratio after one week of contact. As seen, representation in function of the square root of the elapsed time, gave a straight line, which clearly indicates a fickian mechanism of diffusion. However, it must be noted that an extended period of test up to four weeks resulted in a mild decrease and stabilization of p-terphenyl content on PS film that could be explained by imprecisions in the extraction process that are not correctly represented by the internal standard. The quantification method was developed on the basis of weak concentrations that were to expect if the affinity of p-terphenyl for PS was low. This affinity turned out to be higher than expected and consequently the concentrations found in the actual material lay out of the concentration range for which the quantification method was successfully tested.

Besides, the low performance of the extraction (37 ± 4.4%) might indicate re-precipitation of p-terphenyl, either at the moment of the ethanol addition (re-precipitation along with the PS), or after the re-concentration (solvent volume below solubility limit of p-terphenyl). Because of these observations, the methodology was found not to be adapted to amorphous polymers like PS that cannot support extraction without dissolution, which might cause diffusing molecule losses at the moment of the addition of the re-precipitating solvent; or for volatile compounds that might get lost during solvent purge. Probably because of these issues the evolution of the measured quantities of p-terphenyl as function of time, the sorption phenomena seems to reach a plateau, suggesting to be close to the equilibrium after one week of contact. Taking into account the diffusivity value of 2.38×10^{-17} $m^2 \cdot s^{-1}$ previously obtained on the basis of local concentration profiles, the mass of p-terphenyl transferred into the polystyrene film after 1 week of contact should reach an estimated value of less than 1.5 % of the maximum admissible or equilibrium value. It can be deducted with the equi-

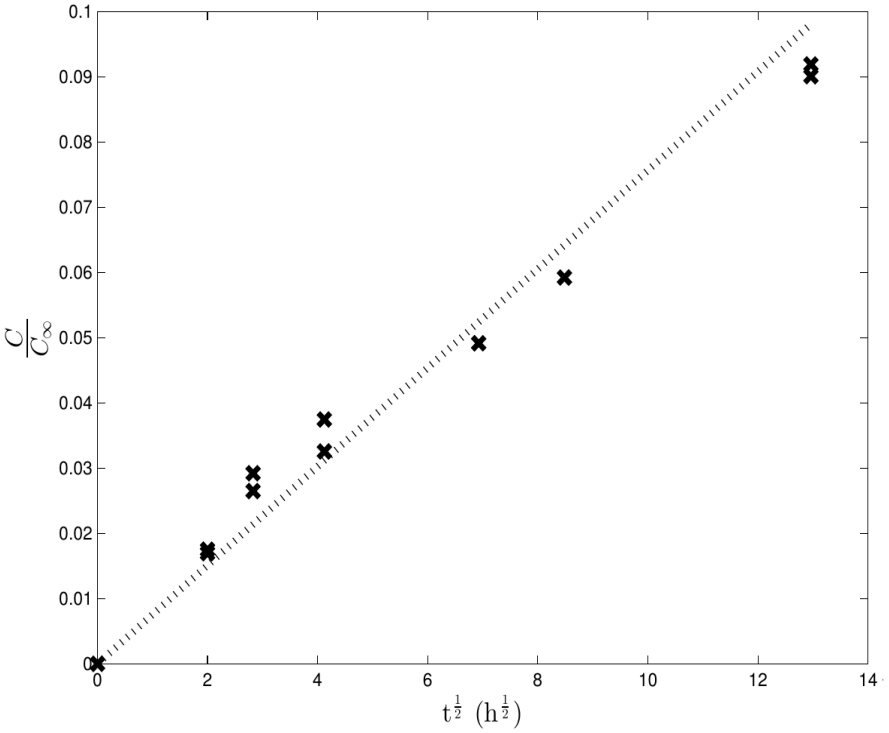

Figure 14: Experimental (X) and predicted (solid line) global concentration profile in PS film, submitted to contact with an ULMWPE source spiked with 0.5 %wt of p-terphenyl.

librium value determined with Raman (1.74% of PS) that after one week, the concentration of p-terphenyl in the PS film is only of 0.025%. Moreover, considering the last data point as equilibrium (as suggested by the pseudo-plateau shape of the curve) would give a diffusivity value of an order of magnitude around 10-12 $m^2 \cdot s^{-1}$ which is more than 10000 times greater than the value determined from local concentration profiles. Therefore, in order to prevent such a huge overestimation of the diffusion coefficient, attention should be paid to verifying that the last data points describe an effective plateau, indicative of an actual equilibrium state. Using Fick's Law for one sided sorption in a flat film, represented by Equation 23, with a value of C∞ of 1.74 ± 0.5 % deducted from the interface concentration using Raman calibration, the fitting of experimental data produces a diffusion coefficient of 89.4 × 10^{-17} $m^2 \cdot s^{-1}$. In order to give an estimation of the extreme importance of the value of C∞, the latter should be of around 10.5 % in order to obtain a diffusivity value of exactly 2.38×10^{-17} $m^2 \cdot s^{-1}$ with the data points obtained with this method, which represents 10 times the value of C_∞ obtained with Raman. As well, an uncertainty propagation analysis performed by introducing random variations on C_∞ from within the standard deviation derived from its determination produced a diffusivity distribution that could not be satisfactorily fitted to any known probability distribution, so the 2.5 % lower and upper percentiles were removed manually, which correspond to an interval between 54.5

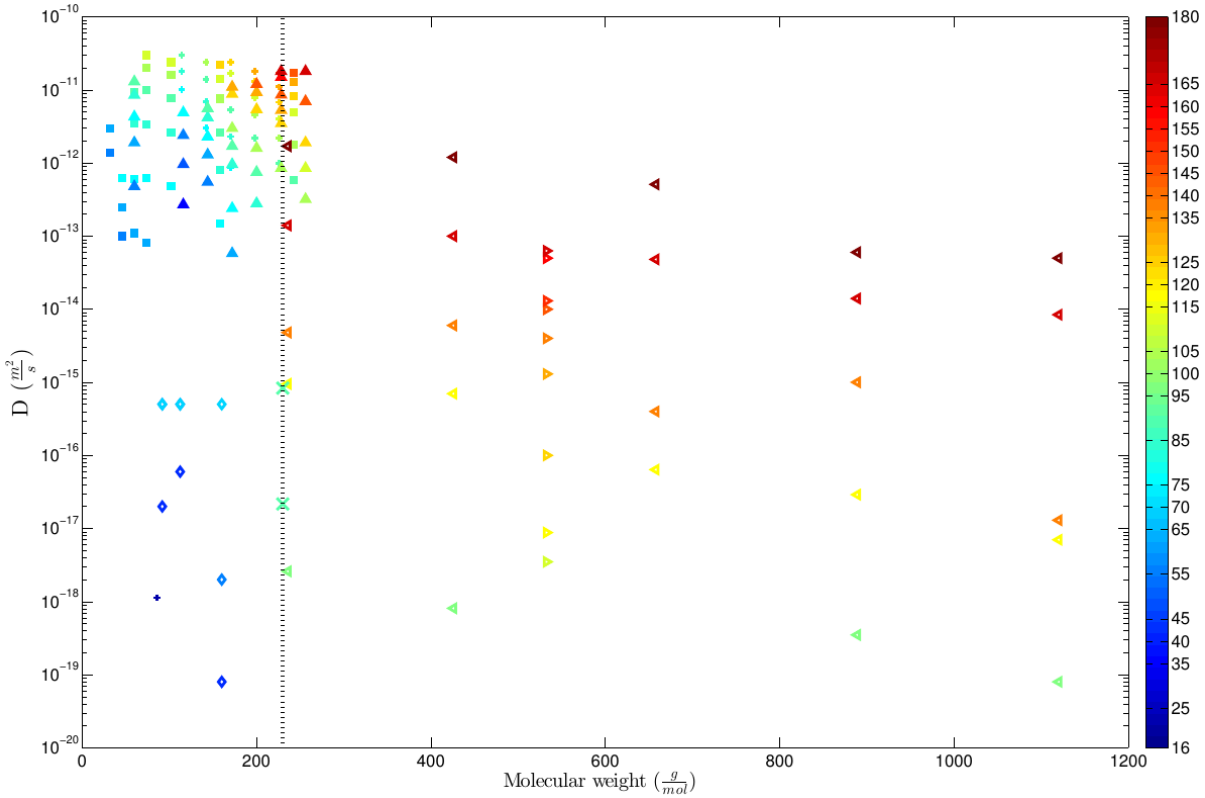

Figure 15: Representation of the dependence of the values of diffusivity found in literature for amorphous polystyrene on molecular weight and temperature. + Alkanes, NMR and gravimetry (Bernardo, 2012) and Spectroscopic ellipsometry (Ogieglo et al., 2013), ■ Alcohols, NMR and gravimetry (Bernardo, 2013), ▲Carboxylic acids, NMR and gravimetry (Bernardo et al., 2012), ◊ Toluene, Phenylcyclohexane and Ethylbenzene (Dole et al., 2006), ◄ Homologous series offluorescent tracers, FRAP (Pinte et al., 2010), ►Rubrene, FRAP (Tseng et al., 2000). The values obtained for p-terphenyl on this work are represented by X. The dotted line delimits diffusivities determined by global (left) and local (right) measuring.

$\times$ 10^{-17} and 178 $\times$ 10^{-17} $m^2 \cdot s^{-1}$. The error got from the determination of C∞ may represent an under or overestimation of diffusivity of up to 2 times its value.

The fact that the value of 89.4 $\times$ 10^{-17} $m^2 \cdot s^{-1}$ found by global measuring relatively near to the one determined from local concentration profiling (2.38 $\times$ 10^{-17} $m^2 \cdot s^{-1}$) demonstrated the necessity to use an accurate value of C_∞ in the determination of the diffusion coefficient by global measuring. In this way, the present strategy based on Raman microspectroscopy proved to be more adapted than global measuring to the characterization of both diffusion coefficient and solubility of low molecular weight molecules in high barrier polymers. Although there are no diffusivity values in literature for p-terphenyl in amorphous PS, other molecules with comparable molecular weights and at comparable temperatures have been studied. This bibliographical review, represented in Figure 15 as function of molecular weight and temperature, yields two well differentiated groups of values: conforming a first group, values in the range of 10^{-13} to 10^{-12} $m^2 \cdot s^{-1}$ are reported for alkanes, alcohols and carboxylic acids,

toluene, phenylcyclohexane and ethylbenzene, ranging from approx 30 to 230 g·mol-1, measured between 35 to 160 °C and determined by monitoring global concentration evolution in time with several analytical techniques: gravimetry and NMR (Bernardo 2012, Bernardo et al. 2012, Bernardo 2013) spectroscopic ellipsometry (Ogieglo et al. 2013 and GC-FID (Dole et al. 2006) It should be pointed that due to the analytical techniques used by Bernardo and Oglielo, their data is free from the error source derived from the extraction process described previously. Separately from this first group, values of a homologous series of fluorescent model molecules (Pinte et al. 2010 and Rubrene, a sensitiser used in chemoluminiscence (Tseng et al. 2000) ranging from 230 to 1100 g·mol-1 and measured between 95 to 180 °C which go from 10^{-19} to 10^{-12} are found. It is important to point out that this second set of values has been determined from local concentration profiles, and more concretely by using time-resolved fluorescence recovery measurement after photobleaching (FRAP), which is a technique used to follow diffusion of molecules that exhibit properties. Figure 15 consequently highlights a differentiation in diffusivity values that appears related to the experimental strategy: local or global profile. Taking into account the molecular weight of p-terphenyl (230.3 g·mol-1) and the temperature at which the experiment has been performed (95 °C), one might expect a diffusivity value in agreement with the first group of values. The significant deviation between the value found in the present work and the reported D values measured on molecules of similar molecular weight with global measuring raise a dual issue about the possible over-estimation of the diffusion coefficients determined by monitoring global concentration evolution with time or an underestimation by the methodology based on concentration profile. Since the data got from local measuring contains spatial information, besides the time information also present on the data got global measuring; the latter is considered to be less precise for diffusivity determination. It could be assumed that the most probable cause of such difference is the overestimation of the values obtained by the methodologies based on global measuring. Of course, this reasoning is valid if only molecular weight and temperature and not any other physicochemical characteristics of the systems are taken into account as factors influencing diffusion, but nevertheless, it gives an idea of the kind of imprecision inherent to global measuring when dealing with very slow kinetics that are characteristic of high barrier polymers.

4 Conclusions

Raman vibrational microspectroscopy proved to be accurate to characterise the diffusivity of an additive in a commercial plastic used in packaging industry from local concentration profiles. This method had been originally used for a low barrier polymer above its glass transition temperature (Mauricio-Iglesias et al. 2009) and was applied here to a high barrier polymer below its glass transition temperature with satis-

factory results. This methodology is compared with a classical approach consisting on monitoring the concentration evolution in time, based on global measurement of average concentration using gas chromatography. The methodology based on local measuring gives a fast, precise and non-destructive characterisation of diffusivity. The classic methodology based on global measuring is time consuming, less precise considering its destructive implementation, needs of extraction of additives from the polymer, and is especially not self-sufficient for very slow kinetics, but is potentially applicable to any molecule and even to several molecules at once, while the methodology based on Raman can only be used in the case of molecules that are detectable with it. The diffusivity values obtained with each methodology, while not identical, are comparable ($2.38 \pm 0.76 \times 10^{-17}$ $m^2 \cdot s^{-1}$ for local measuring and 89.4×10^{-17} $m^2 \cdot s^{-1}$ for global measuring).

Considering the values obtained with diffusing molecules exhibiting similar molecular weight and at comparable temperature, large difference in diffusivity can be observed depending on local or global measuring. The projection of the values obtained in this study showed that diffusion coefficient issued from sorption kinetics integrating reliable estimation of equilibrium concentration match with value deducted from local concentration profiles. Because a minor under-estimation of the value of the equilibrium concentration of the migrant result in a large overestimation of diffusion coefficient, the implementation of Raman micro spectroscopy additionally emerges as a useful tool to characterize diffusivity and maximum solubility in high barrier polymers in glassy state. The study of other molecules with common structural properties (a homologous series of molecules) on the same polymeric matrix with the same method might allow relating differences on the diffusivity values with molecular properties; and could be subject of further research

Acknowledgements: This work has been possible thanks to the funding provided by the French funding agency Association Nationale de la Recherche within the framework of the Research Project Safe Food Pack Design. Special thanks to Dr Ignacio Echeverria, from CIDCA-CCT LaPlata-CONICET (National University of La Plata, Argentina) for the fabrication of the p-terphenyl/PS spiked films.

Publication III: Practical identifiability analysis for the characterization of mass transport properties in migration tests.

Brais Martínez-López, Stéphane Peyron, Nathalie Gontard, Miguel Mauricio-Iglesias.

Abstract

A robust experimental setup for determination of diffusivity in a food/packaging system is required in order to use the estimated value to predict migration levels. However, the common assumption of considering external mass transfer resistance as negligible can lead to a systematic bias that underestimates the actual diffusivity value. In this context, the suitability of two methods and the possible experimental setups (global or local concentration measurements) for determination of both diffusivity and mass transfer coefficient is discussed. The assessment was based on the experimental results of the desorption of Uvitex OB from LLDPE into the food simulant Miglyol 829. It was seen that estimating the two parameters sequentially requires several experiments and that the proper determination of both parameters cannot be ensured for viscous liquids or slurries. Simultaneous determination of the parameters was possible but required measurements of local concentration. In order to formalise these results, practical identifiability analysis of each of the methods and experimental setups was carried out, hence demonstrating that the increased amount of information provided by local measurement methods allows a better identification of the parameters. As a conclusion, local measurement methods (e.g. Raman microspectroscopy) can be used for simultaneous estimation of the mass transfer coefficient and diffusivity, thereby reducing the experimental work and providing an unbiased method for determination of diffusivity.

Keywords: Identifiability analysis; mass transfer coefficient; Raman microspectroscopy; FTIR; migration.

To be submitted to *Industrial Engineering and Chemistry Research.*

1 Introduction

The use of numerical simulation to replace or complement migration tests in polymers was first introduced in the European regulation on plastic materials and articles intended to come into contact with food over ten years (regulation 2002/72/EC), thus replacing costly experiments in cases where the predicted migration is well below the regulatory threshold. Yet, the following physical parameters are generally needed to simulate mass transfer in the food/packaging system: diffusivity of the migrant in the polymer (D), food/polymer partition coefficient (K) and, for liquid or semisolid food products, the mass transfer coefficient (k). The lack of a diffusivity database fostered the development of methods to determine the diffusivity of migrants in polymers (Moisan 1980, Tseng et al. 2000, Ferrara et al. 2001, Helmroth et al. 2003, Lagaron et al. 2004, Martinez-Lopez et al. 2014)

In most experiments aimed at determining diffusivity, it is assumed that the mass transfer resistance is negligible (i.e. k is high), which is a good approximation in case the food or food simulating liquid is a stirred liquid with relatively low viscosity. Otherwise, the determined parameter (often called apparent diffusivity, D_{app}) is always lower than the actual diffusivity value, since it represents the inverse of the resistances, both to external and internal transfer. Hence, D_{app} is not a *worst case* estimation of D. If D_{app} is used to simulate migration in conditions where k is higher than those when D_{app} was determined, the level of migration will be underestimated. As a consequence, it is of great importance to estimate both k and D in experiments aiming at the determination of the diffusivity.

The determination of k in desorption experiments is, however, not straightforward, which may partly explain why this parameter has been frequently overlooked in migration modelling. One of the reasons of this difficulty lies in the fact that variations of k and D give similar macroscopic results (i.e. more desorption when they increase and less when they decrease). In other words, k and D have a poor *practical identifiability* when estimated from desorption kinetics measuring the amount of migrant that has been transferred (either as uptake by the liquid medium or loss by the polymer). In order to improve the simultaneous estimation of D and k, Vitrac and Hayert 2006 propose a reparametrization of the mass transfer equation which aims at isolating the effect of k at the beginning of the desorption experiment. Nevertheless, the influence of the analytical setup on the determination of D and k and their identifiability is rare in literature (Vitrac et al. 2007). As a result, data available in literature for mass transfer coefficients in food packaging systems is even scarcer(Gandek et al. 1989a, Gandek et al. 1989b, Vergnaud 1995).

The aim of this contribution is to explore the use of three different analytical methods for the simultaneous determination of D and k in a polymer/food simulating liquid system. The desorption kinetics is monitored by measuring i) the remaining concentration of migrant in the polymer by FTIR, ii) the concentration of migrant in the liquid by fluorescence spectroscopy and iii) the profile of concentration along the polymer thickness direction by Raman microspectroscopy (Mauricio-Iglesias et al. 2009). In this way a model system composed of low density polyethylene (LLDPE) including Uvitex OB, an optical brightener and UV stabiliser commonly used in polyolefin was set in contact to Miglyol used as fatty food simulating liquid.

The paper is organized as follows: first, there is a brief explanation of the mass transfer model taking into account both internal and external transfer. The materials and methods sections, besides detailing the fabrication of the LLDPE/Uvitex films and how the measurements were made, it also gives information about the principles of a practical identifiability analysis that allows to regress more than one parameter of a model from the experimental data. The results section states the differences between both characterization methodologies (sequential determination and simultaneous determination), as well as the values obtained with each one. In the next section, the differences between the values obtained with the different methods as a result of their practical limitations are discussed. The article ends with general conclusions and perspectives for future work.

2 Mass transfer model.

The mass transfer in a polymer-liquid system is a combination of transport phenomena, governed by the molecular diffusion, as it has been represented in Figure 16. Assuming no interactions between the liquid and the polymer, the one-dimensional transport of a molecule can be expressed by Equation 24, which represents the mass balance of the diffusing migrant (Fick 1855) where t is the time (s) x is the distance (m), L is the plastic polymer thickness (m) C, the concentration in diffusing substance (mass diffusing substance/mass of polymer) and D the diffusivity of the molecule in the sheet material ($m^2 \cdot s^{-1}$). D is assumed independent of the concentration of the diffusing substance, so the system is said to follow Fickean kinetics. Equation 24 can be solved with the initial and boundary conditions that apply to the case, in order to obtain an expression for the concentration distribution.

$$\frac{\partial C}{\partial t} = D\frac{\partial^2 C}{\partial x^2};\ with \begin{cases} t > 0 \\ -L \leq x \leq L \end{cases} \quad (24)$$

The rate at which the diffusing substance is transferred into the liquid is equal to the rate at which this substance reaches the surface of the polymer sheet by internal diffusion. This rate can be expressed by a simple mass balance at the polymer/liquid interface (Equation 25):

$$-D\frac{\partial C}{\partial x} = k(C_{x=L,t} - C_{x=L,\infty});\ with \begin{cases} t > 0 \\ -L \leq x \leq L \end{cases} \quad (25)$$

where k is the mass transfer coefficient ($m{\cdot}s^{-1}$), $C_{x=L,t}$ is the concentration at the interface at time t, and $C_{x=L,\infty}$ is the concentration at the interface at equilibrium ($kg{\cdot}m^{3}$). For convenience, the following dimensionless numbers were introduced, namely the Fourier number (Fo) or dimensionless time, and the Biot number (Bi) which represents the ratio of the external over the internal transfer.

$$Fo = \frac{Dt}{L^2} \text{ Dimensionless time } (26)$$

$$c = \frac{C}{C_0} \text{ Dimensionless concentration } (27)$$

$$X = \frac{x}{L} \text{ Dimensionless space } (28)$$

$$Bi = \frac{kL}{D} \text{ External/internal transfer ratio} (29)$$

Which can be substituted in Equations (24) and (25) obtaining:

$$\frac{\partial c}{\partial Fo} = -D\frac{\partial^2 c}{\partial X^2} \ (30)$$

$$-\frac{\partial c}{\partial X} = Bi(c - c_{inf}) \ (31)$$

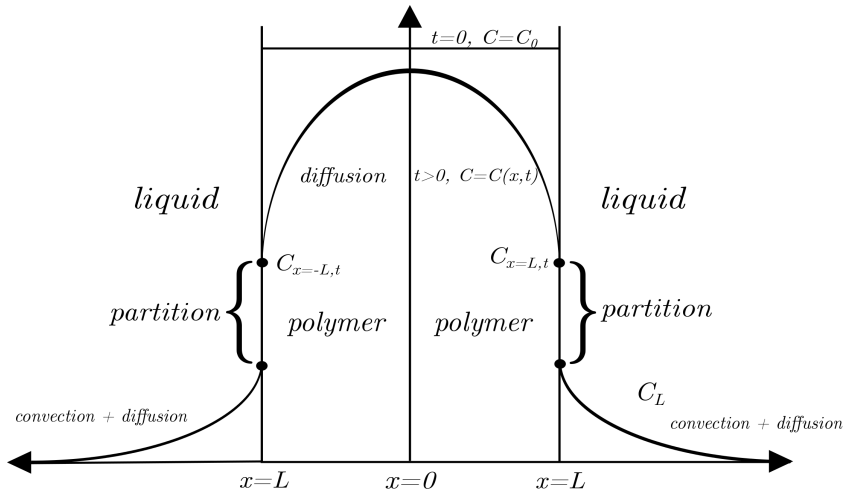

Figure 16: Schematic representation of mass transport phenomena in a polymer-liquid system

At equilibrium, the relation between $C_{x=L,\infty}$ and the concentration in the liquid C_L is given by Equation 32:

$$K = \frac{C_{x=L,\infty}}{C_L} \quad (32)$$

where K is the partition coefficient between the polymer and the liquid. For the system studied, the migrant is much more soluble in the liquid than in the polymer and the liquid volume is considerably larger to the polymer volume (around 350 times larger). The liquid is considered to have infinite capacity to absorb the migrant hence, $C_L = 0$.

Equation 24 was solved numerically for every boundary condition by the method of lines, i.e. discretization of the space (x, the polymer thickness), and numerical approximation of the space derivatives, in order to obtain a system of ordinary differential equations (ODEs). A number of 100 was found to be sufficient. The model was implemented and solved in Matlab R2013a (The MathWorks, Natick, MA).

3 Materials and methods

3.1 Materials

LLDPE pellets (density 920 kg·m^{-3}) were purchased from Sigma-Aldrich. 2,5-Bis-(5-tert.-butyl-benzoxazol-2-yl)-thiophen (Uvitex Optical Brightener, 430.6 g·mol^{-1}) was purchased from Fluka. Miglyol 829, a triglyceride of the fractionated plant fatty acids C_8 and C_{10} combined with succinic acid, with a density between 1-1.02 g·cm^{-3} and a viscosity about 230 mPa·s was purchased from Sasol.

3.2 Films fabrication

LLDPE pellets were mixed with Uvitex OB at 140 °C (50 rpm) during 5min. The dough material obtained after mixing was then thermoformed using a hot press at 150 bar during 5min at 140 ∘C. The nominal concentration of the films was 0.2 % (w/w). The actual film thickness was of 240 ± 40 μm, and was measured by using a micrometer (Braive Instruments, Chécy, Fr) in quintuplicate.

3.3 Experimental setup

LLDPE film samples of 3.5 cm^2 were fully immersed in 15 mL Miglyol 829 at 40 °C . For each analysis, 1 duplicate was just immersed, while the other was placed under a stirring of 350 rpm. Fluorescence measures were performed after 15 min and 30 min of contact. FTIR measures were done 4 times after 0, 3, 15 and 24 h, while Raman measurements were done once after 1 h of contact.

3.4 FTIR measurements

LLDPE film samples were analysed by transmission FTIR. Spectra were recorded using a Nexus 5700 spectrometer (ThermoElectron Corp.) equipped with *He-Ne* beam splitter and cooled MCT detector. Spectral data were accumulated from 128 scans with a resolution of 4 cm^{-1} in the range 800-4000 cm^{-1}. Two for each agitation level were employed for the measure and three spectra were recorded for each sample. All spectra treatements were performed using Omnic 7.1 and TQ Analyst v7.2 software (ThermoElectron). Processing included a multipoint linear baseline correction and a normalization according to the area of the LLDPE doublet (1369-1378 cm^{-1}) due to the CH3 symmetric deformation vibration. To avoid imprecisions derived from the inhomogeneity of the initial concentration and the lack of sensitivity of the FTIR, a different sample was used for each data point, its concentration being measured before and after the contact; and then normalized in relation to the concentration value before the contact (C_0). The dispersion of the concentrations and thickness of the Uvitex OB/LLDPE confirmed this hypothesis: 2.31 ± 0.92 wt% and 231.83 ± 39.5 μm for the unstirred contact; 2.37 ± 0.77 wt% and 251.83 ± 36.9 μm for the stirred contact on the basis of a triplicate for each data point at 3, 6, 15 and 24 h

3.5 Raman spectroscopy

Uvitex concentration profiles were determined as follow. Thin slices of LLDPE were prepared using a razor blade and stuck on a microscope slide. Raman spectra were recorded between 95 and 3500 cm^{-1} Raman shift wavenumber using a confocal Raman microspectrometer Almega (Thermo-Electron) with the following configuration: excitation laser He-Ne 633 nm, grating 500 grooves/mm, pinhole 25 μm, objective ×50. The collection time was about 1 min 40 s (5 scans of 20 s each). Measurements were carried out in the cross-section of the sample with a spacing of 5 or 15 μm. All spectra pre-treatments were performed with Omnic v 7.1 (Thermo-Electron). Processing included a multipoint linear baseline correction, normalization according to the area of the LLDPE specific band at 1129 cm^{-1} representing the symmetric C-C stretching of all-trans PE chains. The relative content of Uvitex OB was assesed using the area of the specific doublet (1569-1614 cm^{-1}) assigned to the aromatic $C{=}C$ and $C{=}N$ bands. Two concentration profiles, with a spacing of 5 or 15 μm were taken from each stirred and unstirred duplicate, making a total of 4 concentration profiles for each desorption experiment. For the experiment at high stirring, the sample thicknesses were 200 and 165 μm, while for the unstirred experiment, they were of 200 and 210 μm.

3.6 Practical identifiability analysis

In order to be able to identify the parameter set of a model, it must fulfil two conditions. First, the output of the model must be sensitive enough to changes on each of the parameters of the set. Second, changes in the model output due to changes in single parameters may not be cancelled by changing the values of other parameters. If the sensitivity of a model with relation to a parameter is defined as the variation of the model output (y) with relation to the variation of a predictor variable (θ), a sensitivity matrix S_a can be defined (Equation 33) as matrix conformed by the variation of the model output with relation to the variations of each of the parameters (Brun et al. 2001):

$$S_a = \{S_{a,ij}\} \;\; where \; S_{a,ij} = \frac{\partial y_i}{\partial \theta_j} \quad (33)$$

This sensitivity matrix can be nondimensionalised, and normalised, according to Equation 34 and 35 respectively:

$$S_{nd} = \{S_{nd,ij}\} \;\; where \; S_{nd,ij} = \frac{\Delta \theta_j}{SC_i} \frac{\partial y_i}{\partial \theta_j} \quad (34)$$

$$S_{norm} = \{S_{norm,ij}\} \;\; where \; S_{norm,ij} = \frac{S_{nd,ij}}{\|S_{nd,ij}\|} \quad (35)$$

where $\Delta\theta_j$ is the reasonable span of parameter θ_j, SC_i is a scale factor with the same physical dimension as the corresponding observation and $\|S_{nd,ij}\|$ the Euclidean norm of S. Since the parameters D and k can span over several decades, their logarithm was used as a parameter instead of their actual value. Hence, the initial guesses for their values were *log(D)* = -13 and *log(k)* = -6 and the scaling factors ($\Delta\theta_j$) equal to 6 for both. Since the only output was the measured migrant concentration, the scaling factor used was equal to the initial concentration. The derivatives $\frac{\partial y_i}{\partial \theta_j}$ were obtained by finite differences. If a column of the dimensionless sensitivity matrix S_j is linearly or nearly linearly dependent, the parameters are said to be collinear or nearly collinear. A common metric for characterising the collinearity of parameters is the collinearity index γ_k *;* which can be defined according to Equation 36 (Brun et al. 2001):

$$\gamma_k = \frac{1}{\sqrt{min\lambda_m}} \; where \; \lambda_m = eigen(S_{norm}^T S_{norm}) \quad (36)$$

The effect of the variation of parameter θ_j on the measurable output y_i can be compensated up to a value of $1/\gamma$ by a change in another parameter $\theta_{k\neq j}$. For example, a value of γ=20 would indicate that a change in a parameter can be compensated up to 1/20 or 5% by changing another parameter. Exceeding a value of γ of 10-15 is often considered as an indication of a poorly identifiable parameter set (Sin et al. 2010).
Another useful metric is the so-called the determinant measure $\rho_{k,}$ (Brun et al. 2002), the determinant measure ϱ_k is defined as in Equation 37:

$$\rho_m = det(S_a^T S_a)^{\frac{1}{2}} \quad (37)$$

where m is the number of parameters considered. This metric combines the information about the sensitivity of the outputs to the parameters and their collinearity. For ρ to be large, the sensitivities must be large and γ must be low (since γ is the inverse of the smallest eigenvalue λ, a large γ would imply a low λ and consequently a low ρ). Unfortunately, since ρ depends on the scaling factors used, a threshold cannot be given. It should be used instead to compare different parameter subsets or experimental setups.

3.7 Parameter estimation

Uvitex diffusivity and mass transfer coefficient were identified from experimental data by minimizing the sum of the squared residuals (Equation 38)between experimental and predicted profiles and by using a nonlinear least square minimisation method

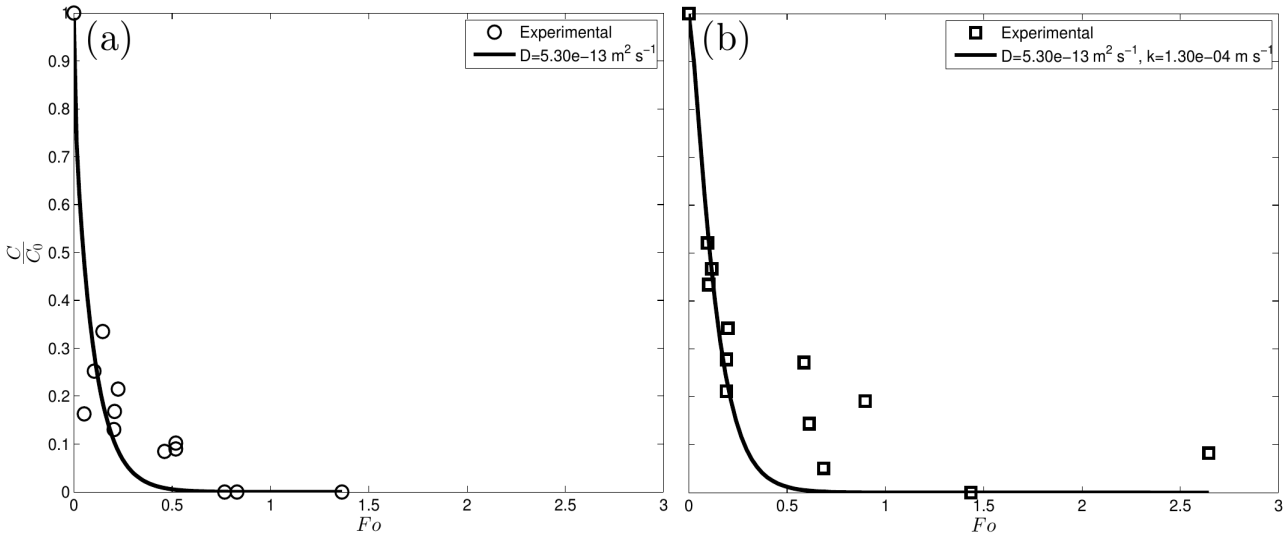

Figure 17: Desorption curves in function of the Fourier number or dimensionless time obtained with FTIR. (a) Stirred contact used to obtain diffusivity (5.3 $\times 10^{-13}$ $m^2 \cdot s^{-1}$) . (b) Unstirred contact used to evaluate the mass transfer coefficient (1.3 $\times 10^{-4}$ $m^2 \cdot s^{-1}$) by fixing the value of diffusivity obtained from the stirred contact.

(*lsqnonlin* command predefined from Matlab software) combined with the *multistart* routine, which uses different starting guesses to ensure that global solutions were obtained:

$$SSQR = (y_{pred} - y_{exp})^2 \quad (38)$$

To ensure the robustness of the parameters estimated and determine their confidence intervals, each determination was iterated 200 times following a bootstrap method with Monte Carlo resampling algorithm.

4 Results

The implemented approach consist on characterizing the mass transfer coefficient following two distinct methods: the sequential estimation method and the simultaneous estimation method. The sequential estimation method relies on using conditions when one of the resistances to mass transfer (internal or external) is negligible. The simultaneous estimation method requires the measured outputs to be sensitive to both parameters in the experimental conditions.

Sequential estimation of *D* and *k*. The rationale behind this approach is that k depends strongly on the stirring rate of the fluid and, as consequence, D can be estimated at a high stirring rate so that the resistance to external transfer is negligible. Then, the stirring rate is increased until the estimation of D converges to a given value assumed to be the true diffusivity. The experiment is then repeated at the actual stirring rate (or with stagnant liquid) in order to determine k with known diffusivity.

Simultaneous estimation of *D* and *k*. To apply this method, equations 24 and 25 are integrated and the variation of concentration with time and space is determined and dependent of both D and k. The sequential and the simultaneous estimation of the parameters were carried out in this work by using two different experimental setups. In one of the setups, the average concentration (so-called *global concentration method*) of migrant remaining in polymer was followed by FTIR. Global concentration methods, where the migrant is measured in the liquid and/or in the polymer, are probably the most common way to determine diffusion coefficients. The other setup consisted on measuring the profile of migrant concentration along the thickness of the polymer (so-called *local concentration method*) by Raman microspectroscopy.

4.1 Sequential determination of D and k.

4.1.1 Global measuring.

The estimation of apparent diffusivity was done at high stirring rate Figure 17a by following the desorption by FTIR. Fixing the value at $D = 5.3 \times 10^{-13}$ $m^2 \cdot s^{-1}$, the mass transfer coefficient without stirring was determined Figure 17b. Despite the lack of sensitivity of FTIR, the effect of stirring on the desorption rate is appreciated on the curves. However, the scattered experimental data lead to a wide confidence interval of the estimated apparent diffusivity. As an inherent limitation of the sequential determination, the error in the estimation of the apparent diffusivity is a burden for an accurate estimation of the mass transfer coefficient, since k is determined fixing a previously estimated value of D.

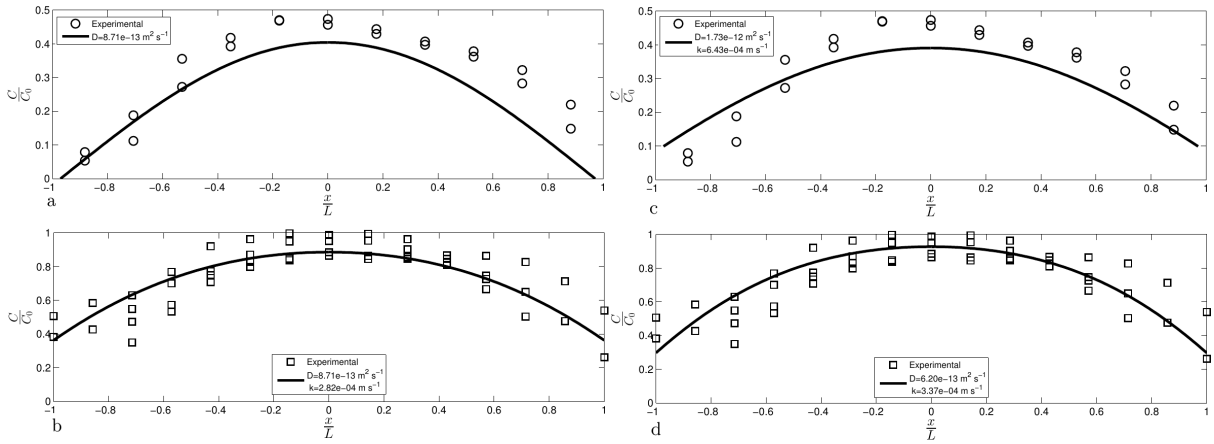

Figure 18: Concentration profiles in the thickness of the LLDPE films. (**o**) represent data got from stirred contacts, and (□) from unstirred contacts. The solid line represents the best fit as follows: (a) Single regression of D under stirring, (b) single regression of k using the value of D got from (a); (c) simultaneous regression of D and k using the same experimental data as in (a);(d) simultaneous regression of D and k using the same experimental data as in (b).

4.1.2 **Local measuring.**

The local concentration profiles were determined after 1h of contact time with Raman microspectroscopy, shorter than required by FTIR As for the global measurements, the local concentration profiles were fitted to estimate the apparent diffusivity (Figure 18a) and, fixing the estimated value, the mass transfer coefficient was determined for the unstirred case (Figure 18b). All the estimated values are gathered in Table 3 While the values found by local measuring are not significantly different from those determined by global measuring, it is noticeable that confidence intervals are significantly narrower when determined by local measuring. This may be caused by several reasons, partly due to the sensitivity difference between FTIR and Raman and partly due to the higher number of measurements obtained. In general, as more measurements are collected by the local experiments, the variance of the estimates should decrease. However, the information collected by the FTIR and the Raman microspectroscopy are inherently different and cannot be compared straightforwardly. Rigorously, the variance of estimates obtained by different methods can be compared by comparing the elements of the Fisher Information Matrix (FIM) which are related to the sensitivity of the observables to the model parameters. The elements of the FIM will increase because more measurements are available and/or because the measurements are more sensitive to a change in the parameters, hence it seems likely that the Raman microspectroscopy can outperform the FTIR. In any case, the properties of the FIM for each of the methods have not been analysed here, but will be the object of upcoming work.

4.2 Determination of transport properties by simultaneous regression.

4.2.1 Global measuring.

Using the same experimental data issued from global measuring and presented previously, D and k were determined by simultaneous regression. It was observed that the value of the estimates depended strongly on the initial guess, indicating the identifiability problems could be present. The problem of the unique estimation of D and k was further investigated mapping the residuals (Figure 20 left). The plot of $SSQR$ (equation 38) for different estimates of D and k, revealed a region of infinite pairs of parameters that minimise the $SSQR$ As a consequence, in the conditions of this experiment the parameters are non-identifiable. This analysis can be generalised if the collinearity index (γ) is represented for numbers of Fourier and Biot that virtually represent the whole space of application of plastics in food packaging (Figure 18a). It can be seen that for an experimental setup equivalent to this one (5 global measurements distributed in time) no region presents a $\gamma < 15$, which can be considered as the threshold for practical identifiability. As discussed previously, the identification of

the parameters becomes difficult and largely dependent on the initial guess and hence, the obtained value of D and k only calibrate the model but cannot be extrapolated in any other system.

4.2.2 Local measuring.

The same estimation steps were done for local measurements, using the data previously presented. For the local measurements it was possible to determine a pair of D and k that did not depend of the initial guesses. In effect, representing the residuals (Figure 20), it can be seen that the $SSQR$ contours converge to a point with a unique minimum.

In more general terms, the collinearity index of the local measuring setup is lower than for the global measuring one. As shown in Figure 19c, there is a region of space corresponding to high Bi and low Fo where $\gamma<15$, which indicates that, a priori, the parameters may be identifiable. The values estimated are displayed in Table 3. Indeed, the identifiability of the parameters can be improved if more information is provided about the system. As an example, decreasing the spacing between the local measures then leading to a higher number of measurements within the polymer results in a larger region where $\gamma<15$ (Figure 20 middle, right). However, the information provided about the system does not grow indefinitely increasing the number of measurements, whether global or local, due to sensitivity limitations of every analysis method.

4.3 Validity of the estimated parameters and methods

The main hypothesis supporting the sequential method is that it is possible to reach a stirring rate that makes that mass transfer resistance as negligible. While this is a common statement, in order to confirm or reject this hypothesis, the evolution of the global mass transfer coefficient along with the stirring level should have been observed. Regarding the simultaneous determination, logic dictates that the diffusion coefficients should not be significantly different regardless of the stirring, while mass

	D_{app} stirred contact $(m^2 \cdot s^{-1})$	k unstirred conctact $(m \cdot s^{-1})$
Global measuring (FTIR)	5.3×10^{-13}, $(3.7, 14.6) \times 10^{-13}$ (a)	1.3×10^{-4}, $(0.85, 1.9) \times 10^{-4}$ (b)
Local measuring (Raman)	9.1×10^{-13}, $(8.4, 9.8) \times 10^{-13}$ (a)	3.0×10^{-4}, $(2.8, 3.3) \times 10^{-4}$ (c)

Table 2: Values of diffusivity and mass transfer coefficient, as well as their associated 95 % confidence intervals and significance, measured from the difference between a stirred and an unstirred contact.

transfer coefficients should. Since there is not data at more than one stirring level, the values may be validated by comparing both methodologies between them. This way, the diffusivities obtained by simultaneous determination should not be significantly different from the apparent diffusivity regressed from the stirred contacts. As well, the mass transfer coefficients obtained from unstirred contacts (sequential and simultaneous determination) should be different from the one obtained from the stirred contact (only simultaneous determination).

Results show that all the unstirred mass transfer coefficients (1.8, 2.8 and 3.4 $\times 10^{-4}$ $m \cdot s^{-1}$) significantly different by very small margins; while very different from the stirred one, which almost doubles the value of the greatest of them (6.5 $\times 10^{-4}$ $m \cdot s^{-1}$). It might be then concluded that stirring increases as much as twice the value of the

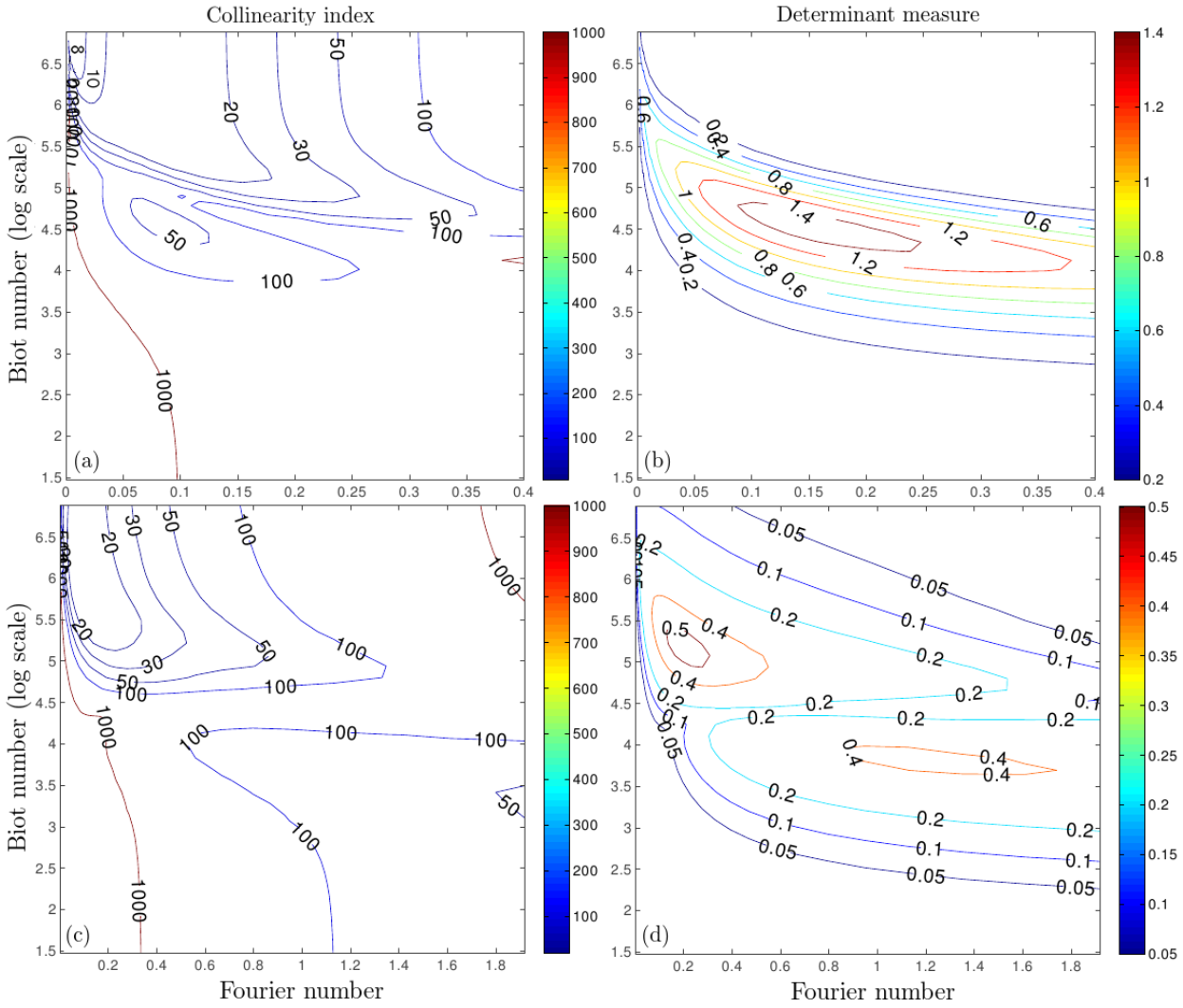

Figure 19: Contour plots made according to the sampling rate and spacing of the data used in the determination from the difference between a stirred and an unstirred contact: 5 measures in 24h, taken at 0, 3, 6, 15 and 24h for global measuring with FTIR and 12 measures equally spaced (15 μm) taken at the end of the experiment (1h), for local measuring with Raman.

mass transfer coefficient. Contrary to long-accepted ideas, the resistance to transfer may be not negligible in the case of a viscous liquid.

Regarding the internal transport, apparent diffusivity determined by sequential fitting under stirring from both global and local measurement can be considered the same (5.3 and 8.7 $\times 10^{-13}$ $m^2 \cdot s^{-1}$), and similar to the value of true diffusivity determined from local measures by double regression from an unstirred contact (6.2 $\times 10^{-13}$ $m^2 \cdot s^{-1}$). On the other hand, values of true diffusivity obtained by simultaneous regression are different by almost a factor 3 (17 and 6.2 $\times 10^{-13}$ $m^2 \cdot s^{-1}$ stirred and unstirred conditions respectively), which suggests that stirring might influence the internal mass transport as well. This result is also confirmed by the contour plot of $SSQR$ w.r.t. D and k. The contours close to the minimum $SSQR$ also show that an ellipse is formed with a long semiaxis almost parallel to the horizontal axis (where D is represented). In principle, the error would be comparatively larger when estimating D than when estimating k but no evidence allows extrapolating this observation to other conditions. This difference may be explained by the effect of the solvent uptake, which has been reported to influence diffusivity of migrants in polymers. The evidence of such an effect is non-conclusive for polyolefins and olive oil, while literature using miglyol as a simulant is till scarce (Begley et al. 2004, Begley et al. 2008, Franz and Brandsch 2013).

Regarding the global mass transfer coefficient or apparent diffusivity, values are in the range of those determined by the same global and local methodologies by (Mauricio-Iglesias et al. 2009) using olive oil as simulant (8 $\pm$ 0.25 $\times 10^{-14}$ $m^2 \cdot s^{-1}$). More difficult is the comparison of the mass transfer coefficient, since literature values are really scarce for food-packaging systems. (Vitrac et al. 2007) report values spread between approximately 6 -20 $\times 10^{-8}$ $m \cdot s^{-1}$ and diffusion coefficients between 10^{-14} and 10^{-12} $m^2 \cdot s^{-1}$ for low molecular weight families of alkanes, alcohols and other commercial molecules in a LDPE/ethanol system followed by global concentration measuring with GC-FID until equilibrium. While diffusivities stay in range, mass transfer coefficients are significantly lower for a less viscous liquid, which appears theoretically contradictory. This might be explained because of all the three coefficients being determined by

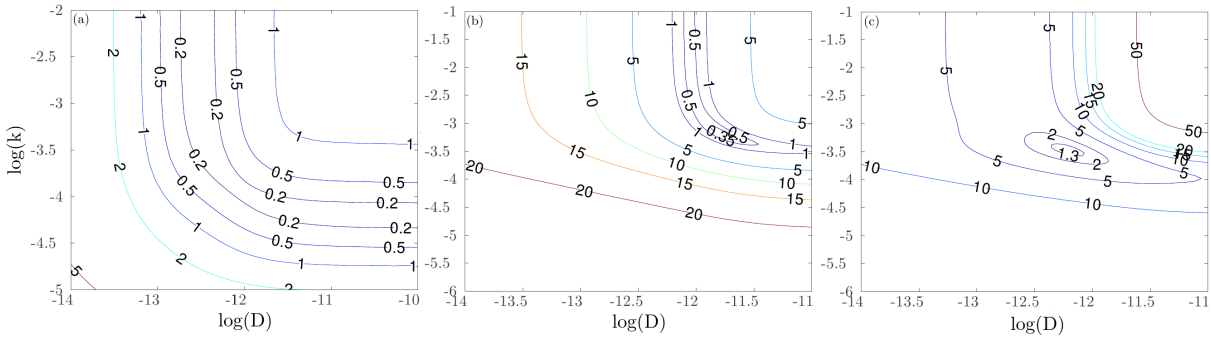

Figure 20: SSQR contour plot for global measuring with FTIR (left), Stirred contact(middle) and unstirred contact (right) local measuring with Raman.

global measuring until equilibrium was reached. If, as it is shown by the practical identifiability analysis (Figure 19), global measures taken at the beginning of the kinetics increase the sensitivity to the mass transfer coefficient, measures taken at very high numbers of *Fo* (near equilibrium) may increase the sensitivity to the partition coefficient, but may also decrease the sensitivity to the mass transfer coefficient dramatically, leading to a less robust estimation, that might be reflected by this difference of approximately three orders of magnitude. More in agreement are values by (Gandek et al. 1989b), for desorption of BHT (220.4 $g{\cdot}mol^{-1}$) from LLDPE into water, going from 10^{-5} to 10^{-7} $m{\cdot}s^{-1}$ with a model that also takes into account the BHT degradation reaction.

4.4 Result discussion and comparison of methods

Global and local measurements give comparable results if the coefficients are determined by the sequential method. Each of the methods has its own pros and cons that make them more suitable in a case by case basis. For instance, global methods require more samples and follow the kinetics at different desorption times for a comparative accuracy in the estimation of D. On the other hand, measurements can be taken online or in an automatized way and is adapted, not only to FTIR, but also to a number of well-known analytical techniques such as UV, fluorescence spectroscopy, chromatography, etc making it very versatile. Local measurements, such as those obtained by Raman (Mauricio-Iglesias et al. 2011), FRAP (Pinte et al. 2008) or gravimetry after cutting the sample with a microtome (Reynier et al. 2002) give valuable insight from the inside of the polymer, such as crystallinity or solvent uptake and can also be used in a non-destructive way . However the sample preparation and experimental setup is usually more complex.

The main disadvantage of the sequential method is that, to be reliable, it requires a number of repetitions of the experiment until the estimated diffusivity value converges to a given value. Even then, it cannot be ensured that the experimental setup will lead to a completely negligible external mass transfer resistance if the fluid is very viscous or if diffusivity is very high.

	D $(m^2{\cdot}s^{-1})$	k $(m{\cdot}s^{-1})$
Stirred contact	17.1×10^{-13}, $(13.8, 21.4)\times 10^{-13}$ (a)	6.5×10^{-4}, $(5.3, 8.1)\times 10^{-4}$ (c)
Unstirred contact	6.2×10^{-13}, $(5.3, 7.6)\times 10^{-13}$ (b)	3.4×10^{-4}, $(3, 3.8)\times 10^{-4}$ (d)

Table 3: Values of diffusivity and mass transfer coefficient got from simultaneous regression of locally measured data from stirred and unstirred contacts. Significant differences are found between both types of contacts.

In principle, the simultaneous method is more suitable since the determination of both parameters does not require any repetition of experiments. On the contrary, an obvious limitation is the poor identifiability that has been demonstrated for global measuring methods.
In theory, the sequential method would always be able to determine both parameters, also with global concentration measurements since it is assumed that the true diffusivity can be known. In practice, the relatively large errors that involve the determination of diffusivity may be a serious obstacle to determine the mass transfer coefficient, in particular at large Bi.
A low collinearity index γ is a necessary but not a sufficient condition for practical parameter determination. It is also important that the measurements are sensitive to the outputs what makes the determinant measure (ρ) a more interesting metric to elucidate the differences between the global and local measuring methods. Even though it is not possible to give absolute thresholds to ρ, it can be regarded as a comparison among methods provided that the measured outputs and parameters have the same dimensions. The two regions where ρ is high for global measurements Figure 19b indicate conditions where the mass transfer resistance is limiting (centred in Bi = $10^{3.5}$ and Fo=1.2) or where diffusion is limiting (centred in Bi = $10^{5.5}$ and Fo=0.2) at time scales where the measurements provide diverse information (i.e. different concentrations). As for the local measuring method (Figure 19d), it outperforms the global measuring method for experiments with a similar time demand given that ρ has a higher value for the whole space of Bi and Fo. It is important to note that the previous discussion assumes the validity of Fickean diffusion, which is accepted as the main framework for modelling migration in food packaging. Currently, the effect of solvent uptake and plasticization in polymers remains unclear. While there is evidence of plasticization effects in PVC (Fankhauser-Noti and Grob 2006), reports are not conclusive for polyolefins (Mauricio-Iglesias et al. 2009). If plasticization caused by solvent uptake is possible, the sequential method becomes less reliable. In effect, the solvent uptake would depend on the diffusivity of the solvent and the mass transfer coefficient, which would, in turn, affect the diffusivity of the migrant. Changing the mass transfer coefficient would influence the migrant diffusivity. To what extent or which experimental setup would allow to determine the parameters of such a complex system is not tackled here.

5 General conclusions.

Methods for parameter estimation and the corresponding experimental setup were compared with the aim of elucidate the best conditions to determine the mass transfer coefficient and the diffusivity of a compound commonly used by packaging in-

dustry. The system subject of study was optical brightener Uvitex OB from LLDPE into food simulant Miglyol 829 at 40 °C .

The methods were based on utilization conditions where the external where only the internal mass transfer is limiting (sequential method) or treating both simultaneously (simultaneous estimation method). Each of the methods can be based on measuring the average concentration in the polymer (global measuring) or the concentration profile along the thickness (local measuring).

The sequential method can be used with both local and global measuring analyses. It requires a number of experiment repetitions to ensure that only the internal resistance to diffusion is limiting; which can be cumbersome or impossible for very viscous liquids.

The simultaneous method cannot be used with global measuring analyses because of poor parameter identifiability, except for narrow experimental conditions and a large number of samples. The analytical method should also be relatively sensitive. Local measuring analyses, such as Raman microspectroscopy, could be used in both sequential and simultaneous methods as the information provided by the measurements gave place to good identifiability (γ) and sensitivity (ρ).

Regarding the experimental setup, it can be concluded that local measuring methods should be selected whenever possible. As discussed previously, it is possible to achieve narrower confidence intervals, a better identifiability thanks to, both higher sensitivity and lower collinearity, and hence carry out a simultaneous identification of D and k, hence ensuring that the external mass transfer resistance is taken into account.

The design of the experimental conditions (number of measurements, when they must be taken) has not been tackled in this paper but it was shown to be of great importance. In an upcoming contribution, these results will be formalised and systematised in order to provide the conditions needed for an optimal experimental design for the determination of the mass transfer and diffusion coefficient.

Chapter IV

This chapter applies the diffusivity characterisation methodology developed in Publication II to two families of homologous molecules in order to relate molecular geometry to diffusion behaviour. Particularly, it tries to lay the foundations of a predictive model of diffusivity by relating it to molecular compressibility, describing the molecules as springs-beads systems. This chapter fits in the main goal of this dissertation as shown in the following scheme:

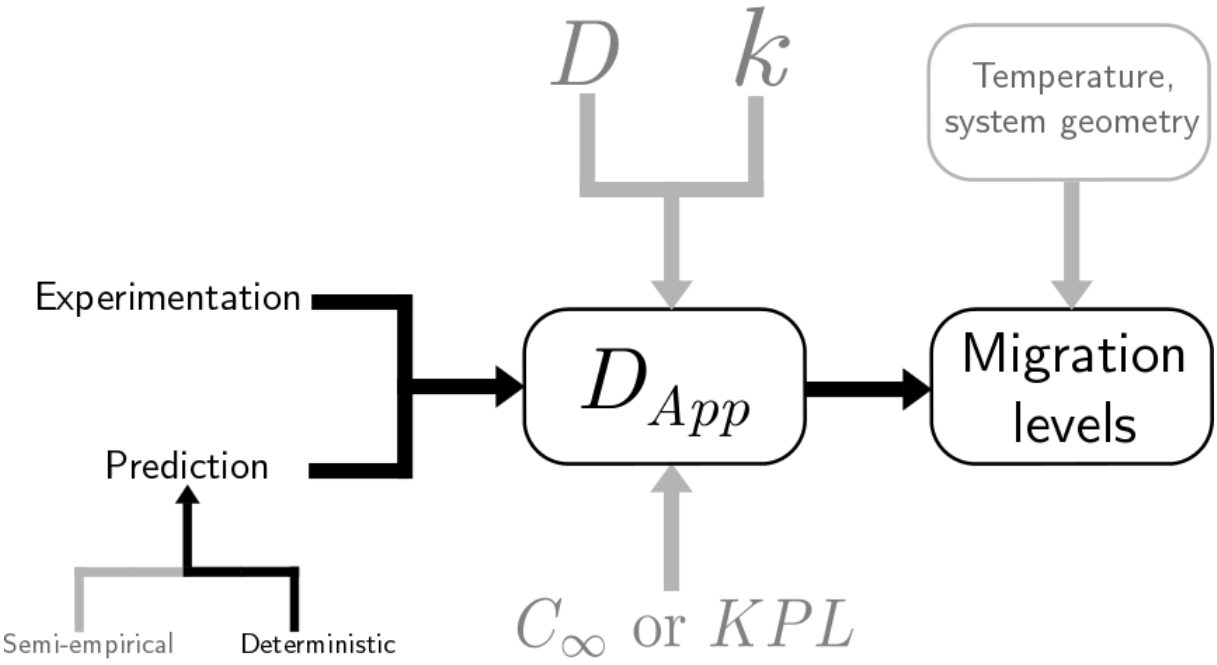

Publication IV: Setting up a mechanical model of molecules diffusion in polymers in the rubbery state.

Brais Martínez-López, Patrice Huguet, Nathalie Gontard, Stéphane Peyron

Abstract

A methodology based on Raman microscopy and dedicated to the determination of diffusivity of low molecular weight molecules was successfully applied to homologous series of tracers diffusing through amorphous polystyrene above its glass transition temperature. Results showed that the influence of temperature on diffusivity was different for both series suggesting that molecular mobility is controlled by both the volume of the diffusing substance and its flexibility in conditions under which the movement of polymer chains can generate stress-induced deformation of molecules. In order to evaluate the ability of molecules to undergo a deformation and considering that these potential deformations could influence their mobility, the compressibility of both homologous series composed of oligophenyl and diphenyl-alkenes was assessed according to the newtonian mechanics, where the molecules were considered as springs-beads systems. The good regression observed between the measured diffusion coefficient and the variables defined in order to quantify the molecular compressibility supports the hypothesis that diffusion behaviour in rubbery state, which presents variations in the shape of the free volumes shall not be regarded only on the basis of the most stable conformation of the molecules but also according to their flexibility.

Keywords: diffusion in polymers, modelling, Raman microspectroscopy.

To be submitted to *Macromolecules*.

1 Introduction

Accurate determination of diffusivity remains indispensable for reliable prediction of migrant diffusion within polymer. Significant advances have been made in understanding the fundamentals of molecular mobility and predicting diffusion coefficients, but the identification of the mechanisms by which diffusion occurs in polymeric systems remain a scientific challenge. The main factors that are known to influence the diffusion comprise: (1) the size or bulkiness of the diffusing molecule, (2) the morphology of the polymer that determines the segmental mobility of the polymer chains and (3) interactions between the diffusing molecule and the polymeric matrix, as a result of polarity or the presence of different functional groups. One of the oldest theories accepted to accurately describe the diffusion of solutes in solid-state polymers is the so-called free-volume theory (Cohen and Turnbull 1959). This theory is based on the assumption that the amorphous fraction of a semi-crystalline polymer may be regarded as a network of polymer chains containing free spaces between them with different sizes and shapes. This so-called free volume is redistributed continuously since the thermal agitation makes the polymer molecules move so that the distribution and location of the spaces changes. Inside these local gaps, the diffusing molecules vibrate at much higher frequencies than the polymer chain motion. According to the free volume theory, a molecule will diffuse by "jumping" through these holes, only if the hole reaches a volume equal to or larger than the volume of the diffusing molecule. On the other hand, the idea of the "jump" was refined including the fact that molecules did not only jump but also had a slithering-like movement between the polymer chains (Molyneux 2001). There is a number of models based on the free volume theory (Fujita 1961). The most famous is, by far, the model of Vrentas and Duda, which spans several publications (Vrentas and Duda 1977a, Vrentas and Duda 1977b, Vrentas and Duda 1977c, Vrentas and Duda 1977d) and was refined nearly two decades later (Vrentas and Vrentas 1994, Vrentas and Vrentas 1995, Vrentas et al. 1996, Vrentas and Vrentas 1998) Unfortunately, these models usually take into account several macroscopic parameters of different nature that are too abstract for a direct application, and often describe diffusion in polymer solutions instead of polymeric matrices. It is well established that the diffusion coefficient of a molecule depends on both the size and shape of the molecule. As of today, most of the predictive models available in literature are empirical relationships between D and the molecular weight of the migrant. This is understandable because of two reasons: on one hand, molecular weight is a descriptor very easy to find or to calculate. On the other hand, there is a theory that has been refined over time, stating that diffusivity and molecular weight are related by a scaling relationship of the kind $D \propto M^{-\alpha}$. This theory is the result of the application of statistical mechanics to the self-diffusion of a polymer

chain in dilute or semi-dilute regimes (Rouse 1953, Rouse 1998). Some authors have related the value of the coefficient α to the transport mechanism (Lodge 1999). For example, de Gennes 1971 states that a value of $a=2$ means that the polymer chain diffuses through the matrix by crawling through a tube conformed by the neighboring chains. Since the self-diffusion of a polymeric chain in a semi-dilute regime and the diffusion of a small molecule through a solid polymeric matrix are equivalent from the statistical mechanics point of view, some authors have tried to extrapolate this scaling relationship to this kind of system. This is why it is possible to find studies giving the coefficient α a more meaningful sense (Fang et al. 2013). Although most of the authors evidenced a strong relationship between D and the molecular weight of the migrant or the actual volume occupied by the molecule, like the Van der Waals volume, bulkiness as represented by M does not appear to be sufficient to fully describe the diffusion behaviour through polymeric matrices. It may be assumed that the flexibility of the diffusing substance influences its easiness to get through the free volume of polymers (Reynier et al. 2001b). The molecular flexibility that translates the intramolecular degree of freedom is a descriptor difficult to evaluate. In the specific case of molecular structure composed of repeating units, flexibility proved to be related to the time-averaged molecular conformations (Rouvray and Kumazaki 1991 or the end-to-end distance distribution (Jeschke et al. 2010).

On this basis, current work aims to contribute to the clarification of the influence of the molecular structure on diffusion phenomena. Using a method based on local measuring with Raman microspectroscopy that has been probed successful for polymer in rubbery (Mauricio-Iglesias et al. 2009) and glassy state (Martínez-López et al. 2014), diffusivity data of two homologous series of molecules that share the phenyl group as main unit, was evaluated in amorphous polystyrene above glass transition. The homologous series were selected to display a broad range of size and flexibility, while remaining linear. Several trends in the diffusivity data were identified, by using the classical descriptors molecular weight and volume, and by following a new strategy based on the evaluation of compressibility of molecules in amorphous polymers based on a mechanical approach that considers molecules as springs-beads systems; each phenyl group being equated with a rigid bead, and the bond or series of bonds between them with a spring.

2 Materials and methods

2.1 Chemicals.

2.1.1 Polymer and sources.

Amorphous polystyrene with a molecular weight of approx. M_w 285000 g mol^{-1} and a glass transition temperature (case II transition) of approx 105 °C was purchased from Polyone France. Vestoplast 891, an amorphous poly-alpha-olephin rich in propene, generally used as hot melt adhesive, with a glass transition temperature of -33 °C, a softening point of 162 °C and a molecular weight M_w of 85000 g mol^{-1} was purchased from TER France.

2.1.2 Diffusing molecules

Biphenyl (CAS n 92-54-4, molecular weight 156.2 g mol^{-1}), p-Terphenyl (CAS n. 92-94-4, molecular weight 230.3 g mol^{-1}), trans-stilbene (CAS n 103-30-0, molecular weight 180.3 g mol^{-1}), diphenylbutadiene (CAS n 538-81-8, molecular weight 206.28 g mol^{-1}) and diphenylhexatriene (CAS n 1720-32-7, molecular weight 232.32 g mol^{-1}) were purchased from Sigma-Aldrich (France). p-Quaterphenyl (CAS n 135-70-6, molecular weight 306.4 g mol^{-1}) p-quinquephenyl (CAS n 3073-05-0, molecular weight 382.5 g mol^{-1}) and p-sexiphenyl (CAS n 4499-83-6, molecular weight 458.6 g mol^{-1}) were purchased from TCI-Europe (Belgium). These molecules have been chosen in order to be able to relate the differences on the values of D with their geometries. This is represented by the use of two homologous series of surrogate molecules that share the phenyl group as primary unit. This way, the first of the homologous series, from now on the olygophenyl series consists on the addition of phenyl groups in the para-position with respect to the others at each step. It is conformed by biphenyl (or phenyl-benzene, two phenyl units), p-terphenyl (or p-diphenylbenzene, three phenyl units), p-quaterphenyl (four phenyl units), p-quinquepheyl (five phenyl units) and p-sexiphenyl (six phenyl units). The other series, from now on the diphenyl-alkene series, starts also by biphenyl, but instead of adding more phenyl units, it increases the distance between them by adding an ethylene group at each step. This series is then, conformed by biphenyl, trans-stilbene (or 1,trans-2-diphenylethylene, one ethylene group between the phenyl units), diphenylbutadiene (or trans,trans-*1*,4-diphenyl-*1*,3-butadiene, two ethylene groups) and diphenylhexatriene (or 1,6-Diphenyl-*1*,3,5-hexatriene, 3 ethylene groups).

2.2 Fabrication of films and sources.

Virgin Polystyrene films were made by thermoforming PS pellets (hot press) at 200 bar during 5 min at 165 $^{\circ}C$. The actual PS film thickness was measured by using a micrometer (Braive Instruments, Chécy, Fr) in quintuplicate, resulting in 200 ± 23 μm.

Vestoplast 891 sources (from now on, Polypropylene or PP sources) were made by thermoforming vestoplast pellets (hot press) at very low pressure during 5 min at 165°C in order to obtain a vestoplast surface of approximately 5 mm of thickness. Then, 20 mg of surrogate were deposed on 2 cm^2 of this surface while on a hot plate, also at 165 °C. In the case of Biphenyl and trans-stilbene, being very volatile, the deposition was made at room temperature.

2.3 Diffusivity assay.

PP source and PS virgin film were put into contact at 105 (T_g), 115, 125, 135, 145 °C). After contact and previously to Raman measurement each measurement, the virgin film was removed and wiped with ethanol. Measurements were done once after certain time of contact, that was fixed in function of the size of the molecule and the temperature of the test.

2.4 Raman measurement.

Surrogate concentration profiles were determined as follow. Thin slices of PS were prepared using a razor blade and stuck on a microscope slide. Raman spectra were recorded between 800 and 3500 cm^{-1} Raman shift wavenumber using a confocal Raman microspectrometer Almega (Thermo-Electron) with the following configuration: excitation laser He-Ne 633 nm, grating 500 grooves/mm, pinhole 25 um, objective x50. The resultant spectra were the mean of two acquisitions of 25 s each. Measurements were carried out in the cross-section of the sample with different spacings, raging between 1 and 15 μm depending on the temperature of the assay. All spectra pretreatments were performed with Omnic 7.3 (Thermo-Electron). Processing included: (i) a multipoint linear baseline correction, (ii) normalization according to the area of the PS specific band at 622 cm^{-1}, indicative of the substituted benzene ring (Nishikida and Coates 2003).

2.5 Estimation of diffusivity.

The internal diffusion of a migrant in a plane sheet is given by equation 39 (Fick 1855) where x is the distance (m), C, the concentration in diffusing substance (mass diffusing substance/mass of sheet) and D the diffusivity of the molecule in the sheet

material(m^{2-} s^{-1}). D is assumed independent of the concentration of the diffusing substance, so the system is said to follow Fickean kinetics. Equation 39 can be solved with the initial and boundary conditions that apply to the case, in order to obtain an expression for the concentration distribution.

$$\frac{\partial C}{\partial t} = D\frac{\partial^2 C}{\partial x^2} \quad (39)$$

The analytical solutions of equation 39 applied in this work are given by equation 40 and 41 (Crank 1980). Equation 40 represents a thickness several orders of magnitude greater than the region of the system in which diffusion occurs or can be detected. This kind of solution(called semi-infinite or short-time solution) is recognized because of the use of the error function and the absence of the thickness of the film L, as a result of the integration of the original differential equation. In some cases, the molecules have shown greater diffusing speeds than expected, leading to diffusing penetrations that almost reach the thickness of the film. This results in the system being considered as finite instead of semi-infinite. For those cases, the analytical solution of equation 39 is given by equation 41. Differently from equation 40, equation 41 takes into account the thickness of sheet, represented by L. Both solutions allow following the evolution of a local concentration profile in time.

It is to be pointed that, in both equations 40 and 41, the concentration of the diffusing substance at equilibrium or C_∞ is required.

$$\frac{C}{C_\infty} = erfc\left(\frac{x}{2\sqrt{Dt}}\right) \quad (40)$$

$$\frac{C}{C_\infty} = \frac{x}{L} + \frac{2}{\pi}\sum_{n=1}^{\infty}\frac{-1}{n}sin\left(\frac{n\pi x}{L}\right)e^{-\frac{n^2\pi^2}{L^2}\ Dt} \quad (41)$$

As stated in previous work (Martínez-López et al. 2014), for this kind of system, the parameter C_∞ can be obtained from the Raman area ratio immediately adjacent to the source/film interface.

Diffusivity was identified from experimental data by minimizing the sum of the squared residuals between experimental and predicted profiles and by using an optimization method (Levenberg-marquardt algorithm, optimization routine predefined from Matlab software).

3 Results.

3.1 Geometrical descriptors of molecules.

The diffusing molecules or surrogates used in this study belong to two homologous series of oligomer that have in common the phenyl group as primary unit. These series are the olygophenyl series, conformed by biphenyl, p-terphenyl, p-quaterphenyl, p-quinquepheyl and p-sexiphenyl; and the diphenyl-alkene series, conformed by biphenyl, trans-stilbene, diphenylbutadiene and diphenylhexatriene. By using homologous series of molecules, the differences in diffusivity can be related to their geometry. This choice has been made in order to be able to relate the differences on their diffusivities to their molecular structures. As previously stated, most authors describe the diffusivity differences using as main molecular descriptor the molecular weight, which might not be sufficiently representative of the steric hindrance. This way, other geometric descriptors, are proposed, such as the molecular or Van der Waals volume

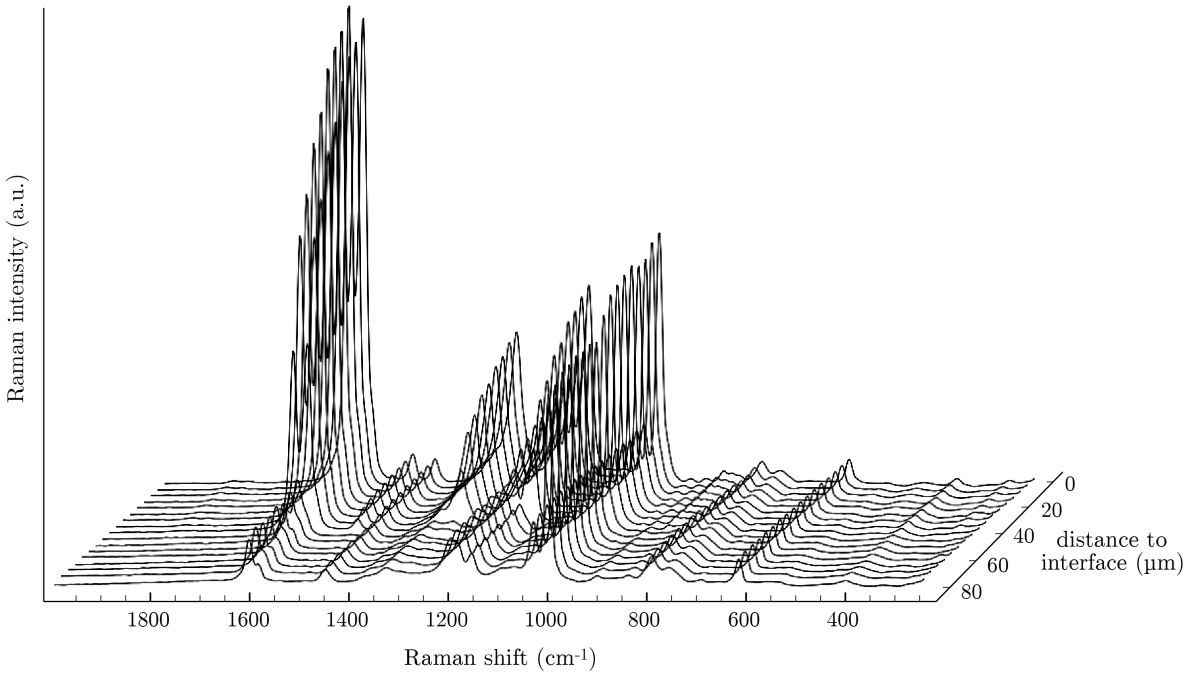

Figure 21: Raman normalised spectral fingerprint of PS+trans-stilbene, showing the decrease on the peak at 1295 cm-1 used to follow the evolution of the concentration of trans-stilbene on the thickness of the PS film.

(V_m) which corresponds to the volume enclosed by the Van der Waals surface; the latter being an imaginary surface of the union of spherical atom surfaces defined by the Van der Waals radius (Whitley 1998) the minimum area that can be projected by the molecule (A_{min}). The values of these descriptors, presented in Table 4, were gathered on the free internet site www.chemicalize.org, developed by chemaxon.

While there is an increase in the molecular weight and Van der Waals volume in both series, it is more noticeable in the case of the olygophenyl series. The chain enlongation of the olygophenyl series is made by adding one phenyl ring, while in the case of the diphenyl-alkene series, it is made by the addition of one ethylene group. In terms of molecular weight/volume, the addition of one phenyl ring is equivalent to the addition of three ethylene groups; which means that the difference between the two smallest molecules of the olygophenyl series is equivalent to the difference between the first and last molecule of the diphenyl-alkene series. As well, the volume/weight increase that each molecule represents with respect to the previous one in the same series becomes smaller in the case of the olygophenyl series, while remaining practically the same for the diphenyl-alkenes. For example, p-terphenyl is 1.46 times bigger than biphenyl, but p-sexiphenyl is only 1.19 times bigger than p-quinquephenyl. In the case of diphenyl-alkenes, trans-stilbene is 1.17 times bigger than biphenyl, while diphenylhexatriene is 1.13 times bigger than diphenylbutadiene. Also, if only Van der Waals volume and molecular weight are taken into account, both series have a common point, represented by p-terphenyl and diphenylhexatriene, which have fairly comparable values of both properties.

3.2 Springs-beads representation of the system.

Both molecule series used in this work can be considered as springs-beads systems. Each phenyl group is assimilated to a rigid bead, and the bond or series of bonds between them, to a spring. This way, three types of springs can be defined, the first represented by the bond *Ph-Ph* between two phenyl groups; a second one represented by the *C-C* single bond between a phenyl group and a *C=C* double bond; and a third one represented by the *C=C* double bond between two *C-C* single bonds. The first one is present in the olygophenyl series, while the second and the third ones are present in the diphenyl-alkene series. Each kind of individual spring has an associated force or elasticity constant k, which will be denominated k^{ph} for the *Ph-Ph* bond, k^{-} for the *C-C* single bond between the phenyl group and the double bond; and $k^{=}$ for the *C=C* double bond between two single bonds. These single constants can be calculated with the Hooke law, according to newtonian mechanics, and assuming that the spring

	$M\ (g\ mol^{-1})$	$V_m\ (Å^3)$	V_m increase	n	$L_{seq}\ (Å)$	$k_{eq}\ (N\ m^{-1})$	$A_{min}\ (Å^2)$
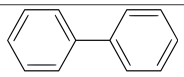 biphenyl	156.2	152.5	1	2	6.9	2210	27.0
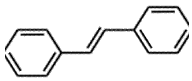 trans-stilbene	180.2	179.1	1.17	2	9.2	619.9	24.8
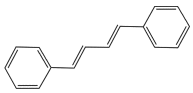 diphenylbutadiene	206.3	205.6	1.35	2	11.5	432.9	22.6
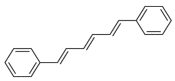 diphenylhexatriene	232.3	231.8	1.52	2	13.9	341.6	28
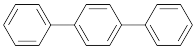 p-terphenyl	230.2	223	1.46	3	16.1	1105.3	31.8
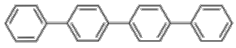 p-quaterphenyl	306.4	293.6	1.92	4	24.2	736.9	33.4
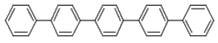 p-quinquephenyl	382.5	364.2	2.39	5	32.3	552.7	37.9
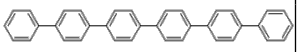 p-sexiphenyl	458.6	434.6	2.85	6	40.4	442.1	40.6

Table 4: Summary of geometric magnitudes of both homologous series of tracers, including molecular weight (M), molecular volume (V_m), increase of molecular volume respect to the first molecule in the series (always biphenyl), number of phenyl units (n), length of the equivalent spring (L_{seq}), elasticity constant of the equivalent spring (k_{eq}), Area of the minimal projection (A_{min})

is attached to the centre of mass of two punctual masses, represented by the phenyl rings of the extremes. The elasticity constant of the single spring can then be calculated according to equation 42:

$$f = \frac{1}{2\pi}\sqrt{\frac{k}{\mu}} \Longrightarrow k = \mu(2\pi f)^2 \quad (42)$$

Where μ is the reduced mass of the phenyl rings, and f is the frequency of the stretching vibration mode of the atomic bonding. The reduced mass allows to describe the relative motion of two objects that are acted upon by a central force as if they were a single mass and can be calculated according to equation 43:

$$\mu = \frac{m_1 \cdot m_2}{m_1 + m_2} \qquad (43)$$

where m_1 and m_2 are the values of both masses. Given that in this case both masses have a value equal to that of the phenyl ring, the reduced mass makes for half of the latter. The stretching vibration frequencies of the bonds were found by reconstructing the theoretical spectra of the molecules with the molecular modelling software Gaussian (Gaussian Inc. USA).

Resulting from the elasticity constant of all three kinds of single springs, the stiffness tensor of the whole molecule can be deduced by calculating the elasticity constant of the associated equivalent spring (k_{eq}). The equivalent spring is a simplification of the backbone of the molecule, derived from the series association of all the single springs, attached to the centre of masses of two punctual masses μ. This calculation allows to evaluate and to compare the compressibility of all molecules. The same way, the length of the associated equivalent spring (L_{seq}), defined as the length of the straight line binding the centre of masses of the phenyl groups situated at the extremities of the molecules can be easily deducted just with simple trigonometrical relationships. These calculations are made under different assumptions and simplifications depending on the geometry of the molecule, which is shared by the molecules of their same family. The olygophenyls are series combinations of rigid spheres of a ratio equivalent to that of the Van der Waals volume of a phenyl ring, attached between them by phenyl-phenyl springs. The equivalent elasticity constant of a spring series combinations in the same axis is given by equation (44):

$$k_{eq} = \frac{k^{Ph}}{m} \qquad (44)$$

where k^{ph} is the elasticity constant of the phenyl-phenyl bond and m is the number of phenyl-phenyl bonds (1 for biphenyl, 2 for terphenyl, etc...). The length of the equivalent spring (L_{seq}) can be expressed by equation (45):

$$L_{Seq} = mL_{Ph-Ph} + 2r_{Ph}(n-1) \qquad (45)$$

where m is the number of phenyl-phenyl bonds, $L_{Ph\text{-}Ph}$ is the length of the phenyl-phenyl bond, r_{Ph} is the ratius of a sphere of a volume equivalent of that of a phenyl ring, and n is the number of phenyl rings present in the molecule. The use of *(n-1)* instead of *(n-2)* is made to consider that the equivalent spring is attached to the centre of masses and not the surface of the phenyl groups situated at the extremes.

The case of the diphenyl-alkenes is more complex. Due to the geometry of the of the phenyl-phenyl bonds, the stretching was assumed to occur in the same axis for all

bonds, but that is not the case of the *C-C* single and the *C=C* double bonds. In fact, considering that the centre of masses of the left phenyl ring is in the origin of the system, the carbons conforming the *C-C* single and the *C=C* double bonds are bent approximately 55 ° with respect to the horizontal reference axis. All single bonds are assumed aligned in parallel to the longitudinal reference axis, while all angles of the carbons between single and double bonds were considered the same for each molecule of the series. As well, the *C-C* single bonds between the *C=C* double bonds of diphenylbutadiene and diphenylhexatriene were considered to vibrate at the same frequency as the double bonds, according to the simulation results, which might be due to the electron delocalization due to their placement between two double bonds. Distance between atoms, as well as the angles were measured after geometry optimization with the free, cross-platform, open-source molecular editor package Avogadro (Hanwell et al. 2012).

This way, two force constants may be calculated for each molecule, a series combination of the longitudinal contributions k_{eqH}, and a series combination of the radial contributions k_{eqV}, which are respectively given by equation 46 and 47:

$$k_{eqH} = \frac{k^{-}k^{=}cos(\alpha)}{k^{-}[p + (p-1)cos(\alpha)] + 2k^{=}cos(\alpha)} \quad (46)$$

$$k_{eqV} = \frac{k^{=}sin(\alpha)}{p} \quad (47)$$

where k^{-} is the elasticity constant for the *C-C* single bond between the phenyl group and the *C=C* double bond; $k^{=}$ the elasticity constant for the double bond between two single bonds, p is the number of nominal double bonds present in the molecule (1 for trans-stilbene, 2 for diphenylbutadiene, 3 for diphenylhexatriene), and α the angle of the carbon between the single and the nominal double bond.

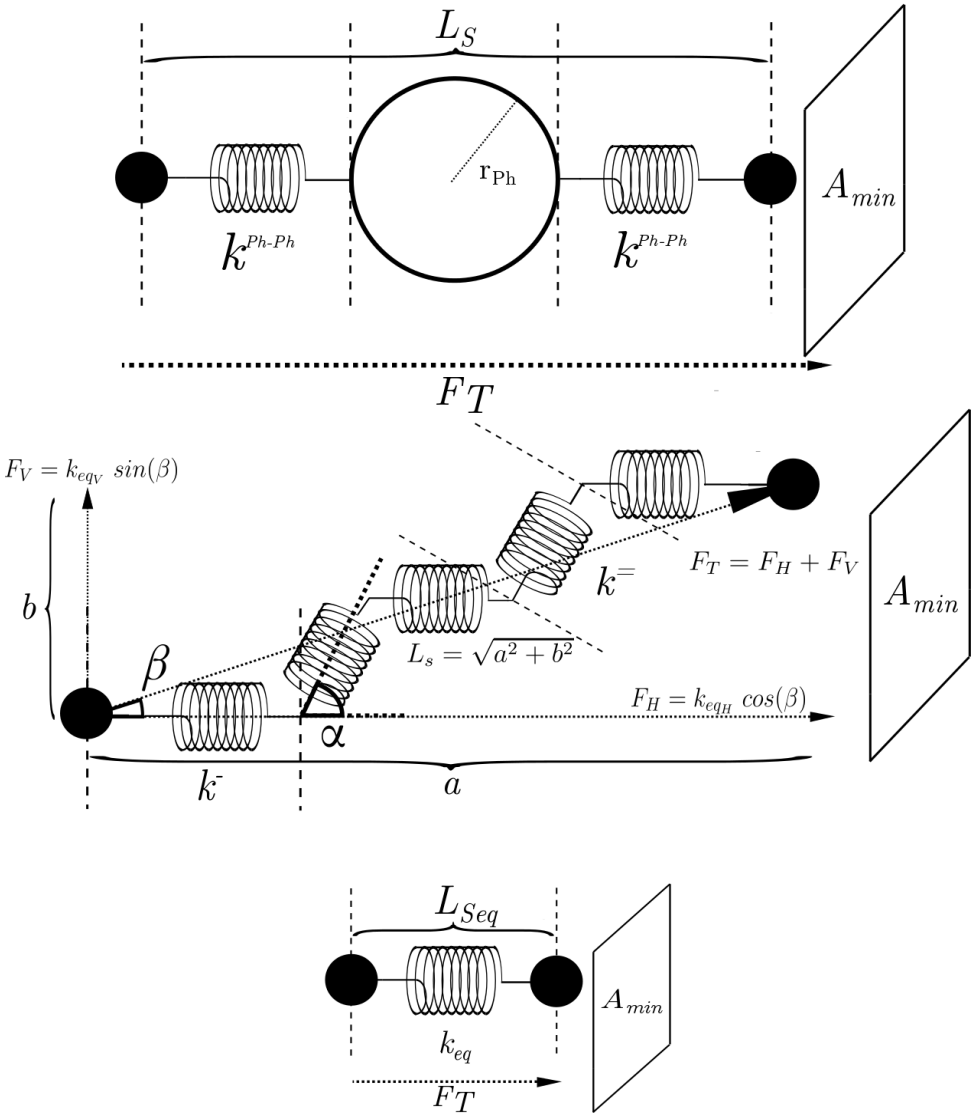

Figure 22: Representation of the molecules as springs-beads systems. p-terphenyl (up), diphenylbutadiene (center), and their simplification into the equivalent spring (bottom). Each kind of bond has its single force constant: $k^{ph\text{-}ph}$ for the phenyl-phenyl, k^{-} for the single bond between a phenyl group and a double bond, and $k^{=}$ for double bonds. The equivalent spring is defined by the distance between the center of masses of the extreme phenyl groups, called length of the equivalent spring (L_{seq}), and the force constant of the equivalent spring (k_{eq}), which takes into account the series association of the individual springs. In the case of the diphenyl-alkenes, the calculations of k_{eq} and L_{seq} are made taking into account the angles α and β, since, differently from the olygophenyls, the springs are not in the same axis.

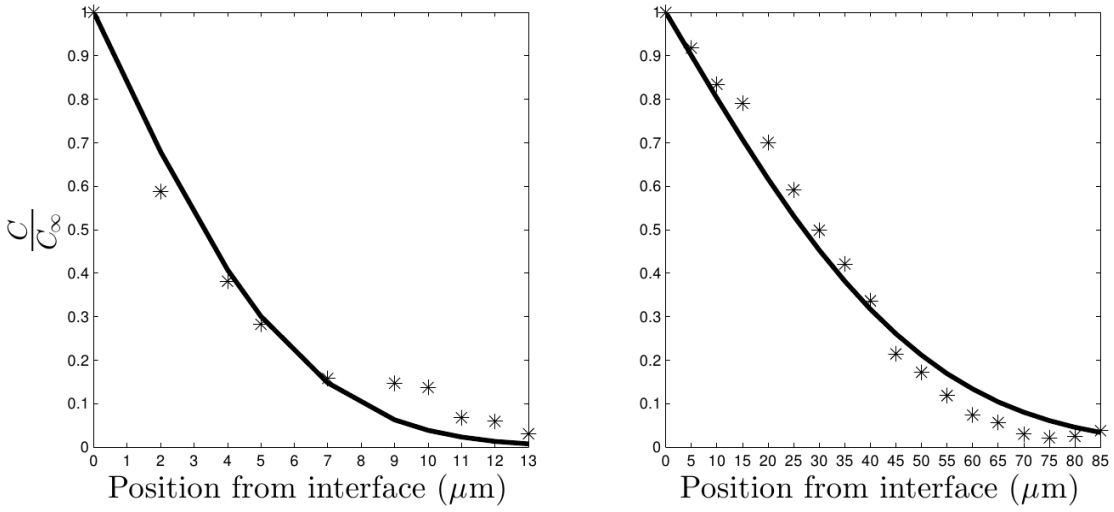

Figure 23: Evolution of the concentration of diphenylhexatriene in the thickness of the PS film. On the left at 105 $^{\circ}C$ after 48 h of contact, and at 135 $^{\circ}C$ after 2 h of contact on the right. The scatter represents the experimental points, and the black solid line the best fit, from which diffusivity was determined.

This way, the elasticity constant can be deducted from the expression, which gives the total force of the system F_T in function of its horizontal F_H and vertical F_V compounds, given by equation (48):

$$\begin{aligned} F_T = F_H + F_V = k_{eq}\ L_{Seq} = ... \\ ... = k_{eqH}\ L_{Seq}\ cos(\beta) + k_{eqV}\ L_{Seq}\ sin(\beta) \end{aligned} \tag{48}$$

where β is the angle between the centre of masses of the phenyl bead set at the origin and the horizontal reference axis. In this case, given that all bond lengths and angles were known, β as well as L_{seq} could be calculated with trigonometric relationships. For the sake of clearness, all values of the molecular descriptors are included in Table 4, while the springs-beads systems are represented in Figure 22. It can be noticed that, due to the torsions and the nature of the bonds of both series, a longer molecules are not always more flexible.

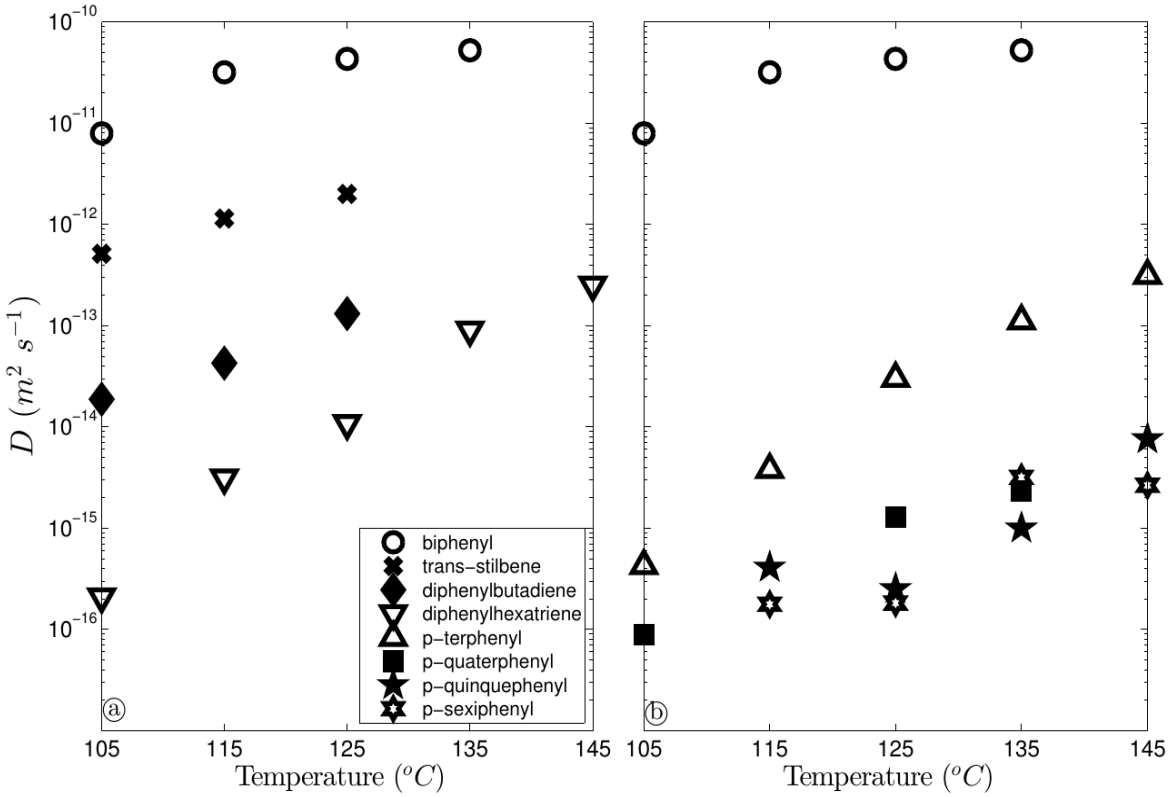

Figure 24: Plot of the dependence of diffusivity with temperature of the diphenyl-alkene series (a) and the olygophenyl series (b). Since biphenyl is the starting molecule for both series, it has represented in both subplots.

3.3 Diffusivity of diphenyl-alkenes

Raman microspectroscopy was applied to establish the concentration profiles of biphenyl, *trans*-stilbene, diphenylbutadiene and diphenylhexatriene in the thickness of PS films. The Raman fingerprint of diphenyl-alkenes exhibits a specific peak of high intensity at 1250 cm^{-1} assigned to (with an increasing signal according to the number of double bonds in the chain) which was well suited to follow the sorption of the molecule (Figure 21).

Three concentration profiles per molecule and temperature were separately plotted, as the ones shown in Figure 23, and used to evaluate the diffusivity using equation 40 or 41. As shown in Figure 24a, the evolution of D along with temperature can be described as linear with a possible slope break at the glass transition temperature for biphenyl and diphenylhexatriene. It can be pointed out that the molecule elongation influence in a large extent de diffusivity with a difference higher than one decade in D value between the different molecules of the series. The variation in temperature highly impacts diffusivity with, in general, a 10 $^{\circ}C$ increase in temperature resulting on an increase on diffusivity of 5×. In addition, the slope of D vs T curves appears

noticeably different according to the size of the molecules suggesting an activation energy increasing with the molecule length. As well, influence of temperature on the diffusion coefficient does not appear related to the molecular weight or volume: at a given temperature, the diffusivity difference between biphenyl and trans-stilbene is comparable to that between diphenylbutadiene and diphenylhexatriene. This is also shown by the shapes of the concentration profiles: concentration profiles of biphenyl or trans-stilbene are almost straight lines, while diphenylhexatriene shows a decreasing exponential curve.

3.4 Diffusivity of olygophenyls.

The relative content on olygophenyl molecule was assessed according to the area of the specific band at 1290 cm^{-1} assigned to the inter-ring C-C stretching band (νC_4-C_7, C_{10}-C_{13}). The intensity of this signal, which increases with the number of phenyl groups in the chain was used to establish the concentration profile through the thickness of the PS film.

Diffusivity was identified using Equation 40 or 41, on the basis of three concentration profiles per molecule and temperature. Figure 24b shows the evolution of diffusivity with temperature, which can be described as linear with the exception of biphenyl, which exhibits a slope break at the glass transition temperature (105 ℃). In contrast with the results observed on the diphenyl-alkene series, the molecule size appears to impact only biphenyl and p-terphenyl, which show a difference of about two or three decades between them and w.r.t the bulkiest molecules, p-quaterphenyl, p-quinquephenyl and p-sexiphenyl, which present low diffusivity (reaching 10^{-16} m^2s^{-1}) disregarding the temperature. More specifically, p-quaterphenyl and p-terphenyl displayed a size variation of only 1.3×, while the difference between their diffusivity is of 5× at 105 $^{\circ}C$ and reach up 100× at 135 $^{\circ}C$. Between p-quaterphenyl and p-quinquephenyl, being the latter 1.24 times bulkier, diffusivity differences do not generally reach 10×; and between p-quinquephenyl and p-sexiphenyl, being the latter 1.19 times bigger, diffusivity differences are so small that are difficult to quantify. In consequence, plotting D in function of the molecular weight or molecular volume would result in a decreasing exponential curve at any temperature. As well, the differences found in the values of the diffusion coefficient are well reflected in the shape of the concentration profile since, as an example at 125 $^{\circ}C$, biphenyl which manages to traverse the whole film thickness in 10 min, ($D = 4.32 \times 10^{-11}\ m^2\ s^{-1}$), while p-sexiphenyl penetrates just 6 μm after 9 h of contact.

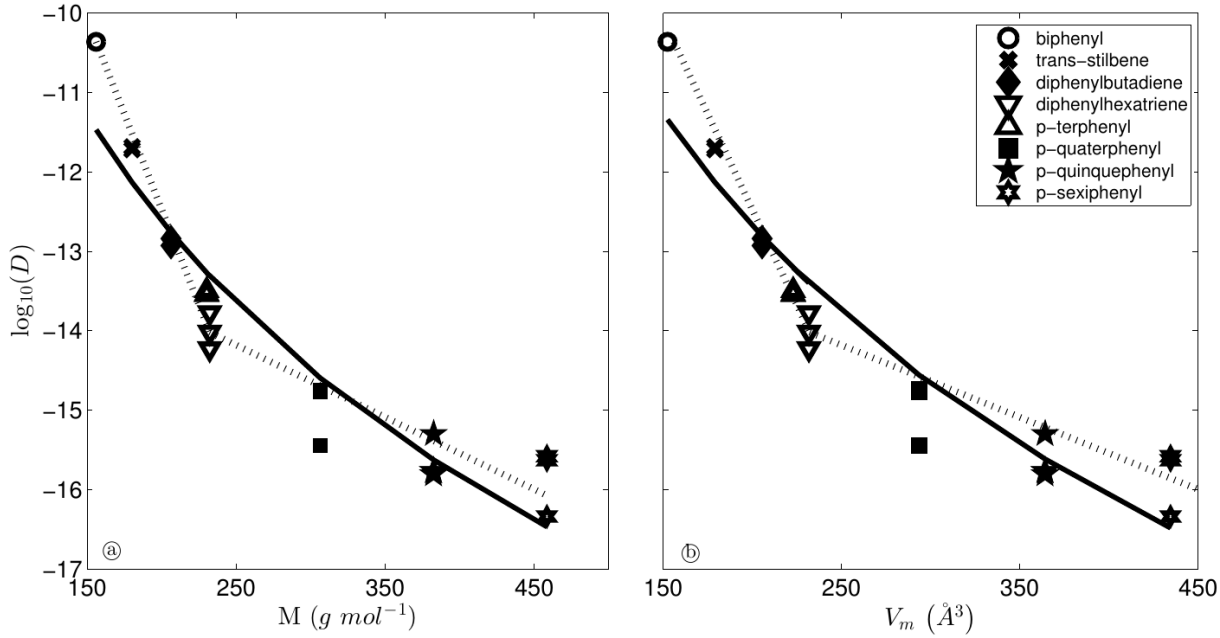

Figure 25: Representation of the log_{10} of experimental diffusivity got at 125 ^{o}C in function of the classical descriptors M (a) and V_m (b) for all molecules used in this work. The black line represents the best fit, of the form $D = A\ F^{\gamma}$, where F corresponds to the descriptor M or V_m, given by the parameters A and γ on Table 5, while the dotted lines represent the best fit considering a different diffusion behaviour for each homologous series.

At first approximation, Comparison of the results obtained on both series seems to confirm the major influence of the molecular weight since diphenylhexatriene and p-terphenyl which displayed similar molecular weights, show diffusivities on same order of magnitude. However, the impact of temperature appears slightly different with, in particular, a slope of the D vs T curve sligthy higher for p-terphenyl. Further to the fact that this translates in a higher activation energy, this statement could additionally suggest difference in diffusion mode depending of the temperature.

Comparative analysis of this diffusivity data with literature is difficult due to the lack of investigation performed on similar amorphous polystyrene. Bernardo 2012, Bernardo et al. 2012, Bernardo 2013 report values in the same range of temperature for homologous series composed by linear alkanes, alcohols and carboxylic acids ranging from 32 to 256 g·mol^{-1}, while Pinte et al. 2010 used polycyclic aromatic compounds as fluorescent probes for the determination of diffusion coefficient using FRAP (fluorescence recovery after photobleaching). Regarding the results obtained with surrogates of high molecular weight, diffusivities values obtained on the quater-, quinque- and sexiphenyl are in agreement with the value reported on fluorescent probes (10^{-14} - 10^{-15} m^2·s^{-1}) displaying molecular weight of 236 and 426 g·mol^{-1}. For molecules of lower molecular weight, diffusivity of biphenyl (156.2 g·mol^{-1}) above the glass transition temperature of PS fits relatively well in the trend of values, which is measured around 10^{-11} m^2 s^{-1} at 105 °C for the aforementioned linear alkanes, alcohols

and carboxylic acids. However, diffusivity of trans-stilbene (around 10^{-13} $m^2.s^{-1}$), is of the same order of magnitude of that of alkanes or alcohols of comparable molecular weight at temperatures of 75 °C and lower. This comparison suggests that bulkiness may not be sufficiently described by the molecular weight, despite its major influence on diffusivity.

3.5 Description of D by M or V_m.

Most of the comparisons between the diffusion coefficients of different molecules found in literature are made using molecular weight as the main descriptor, or molecular weight and temperature at most. This is possibly due to the fact that molecular weight is a parameter very easy to find or to calculate while other parameters that would yield more accurate descriptions, like the aforementioned molecular volume require more complex calculations, sometimes even with molecular modelling software that was not generally available. Figure 25 reports the experimental values of diffusivity of all of the surrogates at 125 °C as a function of M and V_m. Since biphenyl as the starting molecule *i.e* the most elementary molecule for both homologous series, data were plotted altogether and resulting in a curve apparently described by a decreasing power law. These projections show good correlations, with adjusted R^2 coefficients of 0.89 and 0.90 for M and V_m respectively. This behaviour is not surprising taking into account the base postulates of variation described by the relation $D \propto M^{-\alpha}$, and the fact that in this particular case Vm varies linearly with M. The existence of a simple relationship of the type $D \propto M^{-\alpha}$ has been subject of research for many years Durand et al. 2010 , Vitrac et al. 2006 and it has its origins on the use of the statistical mechanics to describe the self-diffusion of polymeric chains in dilute solutions

Shape factor	A	95 % CI A	γ	95 % CI (γ)
M	9.12×10^{11}	(0.0012, 72400) $\times 10^{11}$	-10.68	(-12.28, -9.07)
V_m	2.14×10^{13}	(0.00028, 20000) $\times 10^{13}$	-11.3	(-12.94, -9.65)
$\frac{L_{Seq}}{V_m}$	3.39×10^{-32}	(0.0068, 1740) $\times 10^{-32}$	-15.13	(-17.45, -12.8)
$\frac{L_{Seq}}{k_{eq}}$	3.55×10^{-21}	(0.11, 120) $\times 10^{-21}$	-4.26	(-5.24, -3.3)
$\frac{L_{Seq}}{k_{eq}} \times A_{min}$	8.13×10^{-15}	(4.5, 15)$\times 10^{-15}$	-3.81	(-3.74, -2.1)

Table 5: Parameters, as well as 95% confidence intervals issued from their determination. All models are decreasing power laws the kind: $D = A\ F^{\gamma}$, where F is the involved shape factor.

(Rouse 1953) or more concentrated regimes (Rouse 1998, de Gennes 1971). The meaning of the parameter a would express the transport mechanism. For example, de Gennes postulates that a value of $a=2$ indicates that the polymeric chain reptates through a tube conformed by the neighouring ones. While this has been probed accurate for self-diffusion of polymer chains in polymeric networks, it might not be accurate for general application to any other kind of diffusing molecule, an increase in the molecular weight can lead to increases of molecular volume of different kinds, depending on the size/weight of the atoms that are added. This way, other theories, studying the influence of parameters other than M, and with a more meaningful concept of the coefficient α have been recently developed (Fang et al. 2013), aiming to find a general model to predict diffusivity in polymeric matrices. However, the application of these relationships (Table 5) to predict diffusivity of the molecules found in literature generates contradictory results with, in particular, inaccurate predictions for molecules such as alkenes, carboxylic acids and alcohols of small molecular weight while the prediction of diffusion coefficient of rubrene (532.7 $g\ mol^{-1}$) based on such relation is fairly in agreement with the value found experimentally (Tseng et al. 2000). Therefore, it can be observed that despite the a priori good values of the R^2 coefficients, a logarithmic scale in the diffusivity axis does not result in linear regression, sign of deviation of the power law, particularly on the low molecular weight range. Another sign of inaccuracy is given by the width of the confidence intervals derived from the fit (Table 5). In-depth analysis of the results suggests distinct constitutive behaviour for both homologous series. In particular, the shape of the olygophenyl D vs M or V_m regression is a decreasing exponential, while the one of the diphenyl-alkene series is a straight line. Another lecture of the plot would be to consider two straight lines with a slope break at diphenylhexatriene/p-terphenyl, being p-terphenyl slightly smaller and lighter. Such interpretation of the results leads to most accurate regression of diffusivity data (with $R^2 > 0.9$) and consequently confirms that a description solely based on M or V_m is not enough to explain the diffusion behaviour of low molecular weight molecules. This view has already been shared by several authors, which pointed out the influence of the shape of a molecule on its diffusion mode (Reynier et al. 2001). The higher probability for a long molecule of having many degrees of freedom should facilitate its displacements by crawling, while non-linear molecules are rather supposed to diffuse by jumping. This statement has led to the emergence of an alternative concept according to which the molecular mobility is investigated as a function of a proposed fragmentation of the molecule volume by considering separately the mobility of each part of the molecule. This way, each molecule is considered as an association of linear and flexible chains that can take several conformations making the displacements easy and rigid parts (generally constituted by cycles) for which the conformation is locked. The fractionated volume

of the molecule corresponds to the sum of the different partial volumes of each part; the jump displacements being facilitated by the more or less easy relaxation of the flexible parts of the molecule. Considering the satisfactory correlation between the fractionated volume and the diffusivity, this concept clearly allowed to progress on the understanding of the mechanism of displacement through polymeric matrices. However, as usual size parameter, fractionated volume was assessed on the basis of the most stable conformation of the molecules (or of each part of it). As consequence, this approach did not take into account the variation in shape of the surrogate or, even more so, the energy necessary to induce the modification of the molecule conformation.

3.6 Description of D by a springs-beads model.

With the aim of proposing alternative molecular parameters that could further explain the mobility of diffusing molecules within a polymeric matrix, it can be pointed out that polymers in a rubber-like state exhibit a degree of mobility that can influence the diffusivity of molecules. On this basis, molecules endowed with flexibility should demonstrate a higher ability to diffuse in a moving polymer network. The goal of this approach being not to try to predict diffusivity, but to progress in the description of the diffusion behaviour, new and less generic molecular descriptors have been considered to translate the flexibility of molecules. Considering the studied class of linear and rigid molecules, the flexibility was drawn up by the assessment of their compressibility which was achieved by using the magnitudes issued from the springs-beads consideration of the system (L_{seq} and k_{eq}) and combining them into shape factors. This way, three shape factors were defined: the ratio $\frac{L_{Seq}}{V_m}$, which indicates how similar to a cylinder the molecule can be considered and the ratio $\frac{L_{Seq}}{k_{eq}}$, or linear compressibility of the molecule. The inclusion of the parameter A_{min}, transforms the linear compressibility into $\frac{L_{Seq}}{k_{eq}} \times A_{min}$ or volumetric compressibility, and makes it potentially applicable to molecules other than linear. These compressibility evaluators might indicate how easy a molecule can get through free spaces between the polymeric chains. As well as in the case of M or Vm, the best fit was achieved with a decreasing power law of the kind $D = A\ (F)^{\gamma}$, where F is the studied shape factor, and A and γ are coefficients issued from the fitting (Table 5). The fitting yielded adjusted R^2 coefficients of 0.89, 0.79 and 0.87 respectively (Figure 26); which would, a priori indicate similar, but slightly worse fits than the curves against M or V_m. However, taking a deeper regard at the plots, it can be noticed that the diffusivities of the diphenyl-alkenes and p-terphenyl lay at both sides of the fitted curve and not systematically below it, like it was the case of M or V_m; which means that the diffusivity de-

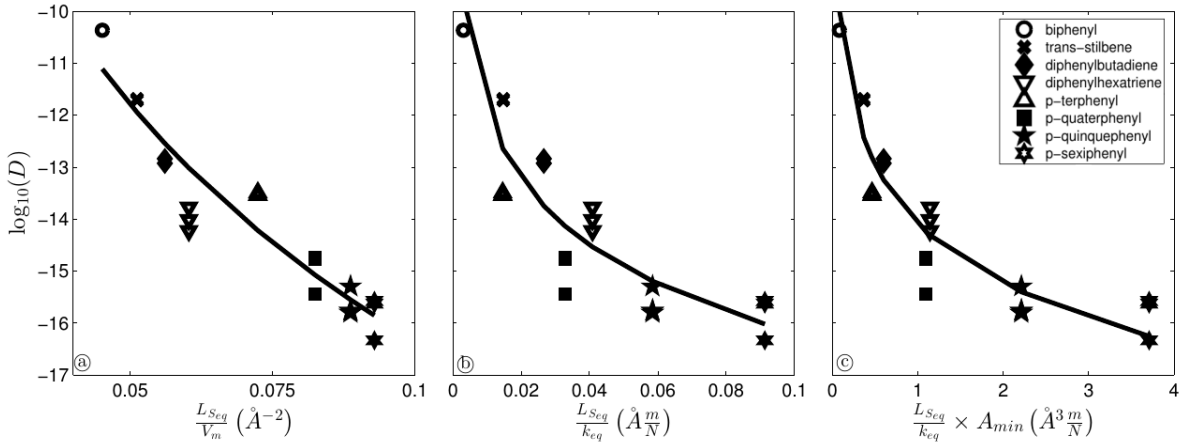

Figure 26: Representation of the log_{10} of experimental diffusivity in function of the shape factors $\frac{L_{Seq}}{V_m}$ (a), $\frac{L_{Seq}}{k_{eq}}$ (b) and $\frac{L_{Seq}}{k_{eq}} \times A_{min}$ (c), issued from the springs-beads model. The black line represents the best fit, of the form $D = A\ F^{\gamma}$, where F corresponds to the shape factor, given by the parameters A and γ on Table 3.

crease on the range between 150 and 230 $g\ mol^{-1}$ becomes milder using these shape factors than using molecular weight or volume alone. While diffusivities found in literature cannot be checked against the values issued from these equations, since the values of L_{seq} and k_{eq} where not calculated for any of them, the experimental values of diffusivity can be plotted against the values predicted by the model and fitted by a straight line forced to pass by 0. Considering that the better the prediction, the closer to 1 the slope of this curve must be, the models yielded slopes of 0.05, 0.11, 0.18, 3.87 and 2.34 for M, V_m, $\frac{L_{Seq}}{V_m}$, $\frac{L_{Seq}}{k_{eq}}$ and $\frac{L_{Seq}}{k_{eq}} \times A_{min}$ respectively. This means that, while yielding greater adjusted R^2 coefficients, M and V_m were actually poor descriptors of the diffusivity trend, which is also confirmed by the width of the confidence intervals of each parameter; and verifies the hypothesis that splitting up generic molecular descriptors into more concrete ones results in an increase of the accuracy; which can be done with simple geometric considerations. Since the polymeric chains have more mobility in the rubbery than in the glassy state, this statements should not be verified in the glassy state. Nevertheless, the calculation of the geometric parameters is pretty straightforward, and the springs-beads concept could lay the foundations of a more general model of diffusion in the rubbery state, or at least in amorphous polystyrene.

General conclusions.

Considering the influence of the physico-chemical characteristics of low molecular weight molecules, results evidenced the influence of the geometry of the molecule on

its diffusion behaviour. Concretely, the classical comparison between molecules of different nature solely based on the molecular weight can induce to big error, especially for little molecules of up to approximately 300 g mol^{-1}. To avoid this, it has been proposed to describe the diffusion behaviour by splitting the most generic molecular descriptors, like M or V_m into more concrete ones, also based in geometric considerations, that describe more accurately the shape of the molecules and their flexibility. This way, new descriptions based on the ratio length/volume, as well as on the linear or volumetric compressibility were proposed. The variables translating the molecular compressibility are based on the inclusion of the elasticity constant issued from the consideration of the molecules as springs-beads systems, according to newtonian mechanics. While still far from a general model to describe diffusion behaviour in the rubbery state, this work shows how a description based on geometric considerations is feasible with simple calculations that do not require an extensive amount of computing power, which is the case of the models based on molecular dynamics; or laying in too abstract concepts which is usually the case of the models based on the free-volume theory. The constants present in the developed equations are *a priori* pertinent on the unique case of amorphous polymers at a rubbery state exhibiting a potential segmental mobility. If the springs-beads model developed in this work was applied to other molecules from literature, the constants issued from the data fitting could be expressed in function of other temperature or polymer dependent parameters (for example, the free-volume fraction) that might lay the foundations of a general model to predict diffusion in polymers at the rubbery state.

Acknowledgments

Authors would like to thank Dr Matthieu Saubanere from Institut Charles Gerhardt (Montpellier, France) for his introduction to the two-body problem and Eddy Petit, from Institut Européen des Membranes for the theoretical spectrum calculations.

Chapter V

This chapter gives new guidelines for a correct application of an empirical equation widely used in industry to overestimate apparent diffusivity, in order to predict worse-scenario migration levels. This chapter fits in the main goal of this dissertation as shown in the following scheme:

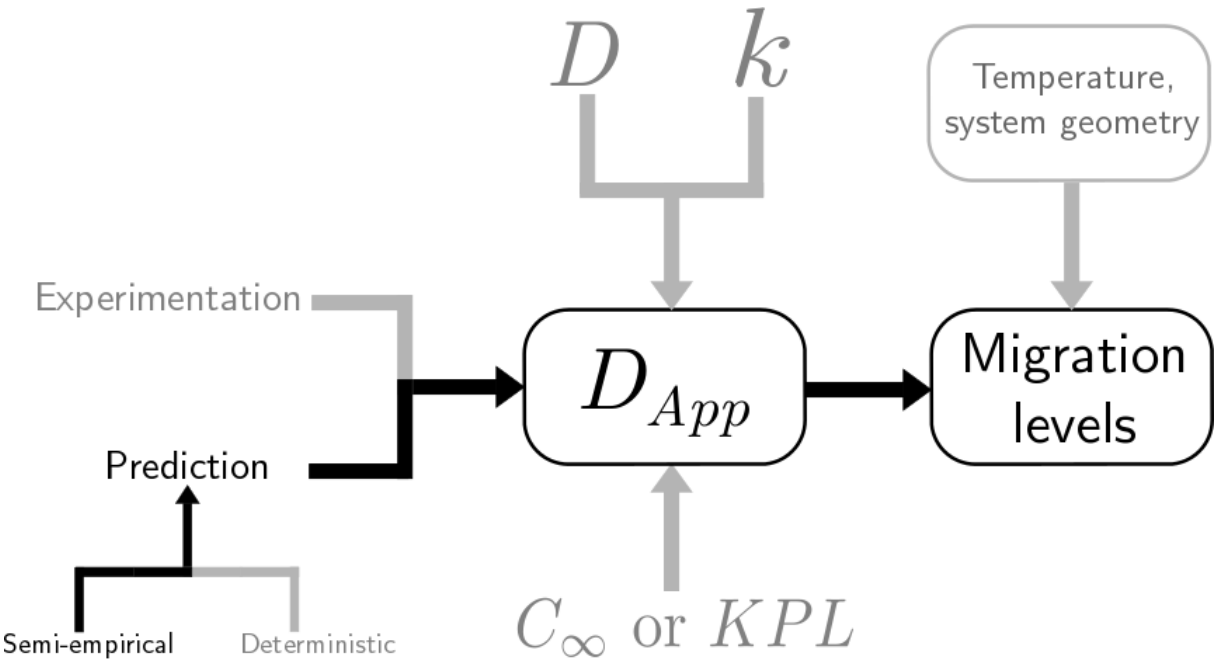

Publication V: Updating the model parameters for worst case prediction of additives migration from polystyrene in contact with food, application to food safety evaluation.

Brais Martínez-López, Stéphane Peyron, Nathalie Gontard

Abstract

A reliable prediction of migration levels of plastic additives in food needs of a robust estimation of diffusivity. Predictive modelling of diffusivity as recommended by the EU commission is carried out by the use of a semi-empirical equation that relies on two polymer-dependent parameters. These parameters were determined for the polymers most used by packaging industry (LLDPE, HDPE, PP, PET, PS, HIPS) from the diffusivity data available at that time. In the specific case of amorphous polystyrene, the diffusivity data published since then, shows that the use of the equation with the original parameters results in systematic underestimation of diffusivity. This study proposes an update of both parameters used for the prediction on amorphous polystyrene, based on diffusivity data available in literature, allowing a reasonable oversestimation of diffusivity that can be used for the prediction of worst-case escenario migration levels.

Keywords: diffusion in polymers, modelling, polystyrene.

In preparation

1 Introduction

Food contact materials (FCMs) must comply with European regulation 1935/2004, which can be summed up in two main requirements: packaging materials shall not transfer their constituents to food in quantities that could (1) endanger the human health and (2) bring about deterioration in organoleptic characteristics. To ensure the safety of consumers, European regulation 10/2011 translates the requirements of regulation 1935/2004 to plastic materials and lays down the procedure for their compliance. In addition to the requirement of intertial for plastic FCMs, regulation 10/2011 provides guidelines on the testing procedure for migration assessment. An important aspect of the regulation is that it allows the use of "general recognized diffusion models based on experimental data [...] under certain conditions" to determine overestimated migration levels and to prevent expensive and time-consuming experiments. This way, the existing models describing migration are based on the Fickian diffusion equation, which involves at least two key parameters: (1) the diffusion coefficient or diffusivity (D), and (2) the partition coefficient (KPL). A commonly accepted approach is the use of a KPL value of 1 if the migrant is soluble in the food or 1000 otherwise (Simoneau 2010). In contrast to KPL, diffusivity must be determined for each polymer/migrant system in defined conditions (temperature, time), because it depends on physical characteristics of both, like molecular mass, volume, polarity of the diffusing molecule, and glassy or rubbery state of the polymer matrix. In addition to experimentation, D can be determined via predictive modelling, which is generally based on empirical or semiempirical relationships that predict diffusivity as a function of the steric hindrance of the diffusing molecule, represented by the molecular weight and as well as generic polymer-related parameters and temperature. One of the most widely used models for worst case prediction of additives migration in the framework of food contact materials safety evaluation, is, the Piringer model (Baner et al. 1996 Piringer 2007), also known as Piringer Interaction model. This equation is recommended by the EU commission for the implementation of diffusion modelling and considered by the Food and Drug Administration as "a semi-empirical method using limited or no migration data" (FDA 2002). Its most used form is given by equation 49

$$D_p = e^{A_p^* - \frac{\tau}{T} - 0.1351 M^{2/3} + 0.003M - \frac{R \cdot 10454}{R \cdot T}} \quad (49)$$

where M is the molecular weight of the diffusing substance and T is the temperature. As seen, this model relies on several constants, valid for any polymer/migrant system, as well as on two polymer-dependent parameters: Ap* and τ. The recommended value

of the parameters Ap* and τ, as well as the range of molecular weight and temperature ranges for their application can be consulted at Simoneau 2010, and are based on the migration data compiled by Begley et al. 2005. Since then, existing diffusivity data has been continuously published on scientific papers for various polymers and diffusing substances (Bernardo 2012, Bernardo 2013, Bernardo et al. 2012, Ogieglo et al. 2013). Polystyrene (PS) is a petrochemical synthetic aromatic polymer made from the monomer styrene that can be rigid or foamed. It is one of the most widely used plastics, the scale of its production being several billion kilograms per year (Maul et al. 2000). Uses include protective packaging (such as packing peanuts), containers (such as "clamshells"), lids, bottles, trays, tumblers, and disposable cutlery. Considering that independant published data on polystyrene diffusivity were scarse when Piringer parameters were established, the goal of this work is to provide updated values for these parameters, based on litterature review, in order to secure reasonably overestimated diffusion coefficients. The Piringer's parameters Ap and τ were checked above and below glass transition temperature, against a large range of experimental data of D and Ea (activation energy) for different substances in polystyrene, which were extracted from litterature. Ap and τ were then adjusted in order to guarantee the requested overestimation of these parameters for purpose of safety evaluation of the use of polystyrene as food contact material. For consolidating the updating of Piringer's parameters, an uncertainty propagation analysis were performed on both parameters in order to calculate the associated 95% confidence intervals of the parameters.

2 Materials and methods

2.1 Diffusivity data

A total of 183 diffusivity values in amorphous general purpose PS (with a glass transition temperature of 105 °C) were collected from literature from 2000 to 2013: Bernardo 2012 homologous series of linear alkanes, gravimetry), Bernardo 2013 (homologous series of linear alcohols, gravimetry), Bernardo et al. 2012 (homologous series of linear carboxylic acids, gravimetry and NMR), Ogieglo et al. 2013 (cyclohexane, spectroscopic ellipsometry), Dole et al. 2006 (toluene, chlorobenzene and phenyl-cyclohexane), Pinte et al. 2010 (homologous series of fluorescent tracers, FRAP), Tseng et al. 2000 (rubrene, FRAP) and Martínez-López et al. 2014 (homologous series of olygophenyls and diphenyl-alkenes, Raman microspectroscopy). Diffusivity of styrene was deducted from migration data found at Begley et al. 2005.

2.2 Values of *Ea*

Values of Ea were calculated by fitting diffusivity data to a linearized version of equation 50 (Arrhenius 1889) with matlab *fit* function (Mathworks, USA).

$$D = D_0 e^{-\frac{Ea}{R \cdot T}} \quad (50)$$

This was only performed to those molecules for which diffusivity was available at, at least three different temperatures after separation on two temperature intervals: below and above the glass transition temperature. After calculation of the 95% confidence intervals with the associated function *confint*, values showing a negative lower confidence bound were discarded. This makes for a total of 27 activation energy values: 13 below and 14 above the glass transition temperature.

2.3 Parameter fitting

Parameters A_p* and τ were calculated by simultaneous regression from diffusivity data to equation 49 by minimizing the sum of the squared residuals between experimental and predicted diffusivity and by using an optimization method (Levenberg-marquardt algorithm, optimization routine predefine from Matlab software). The sum of the squared residuals ($SSQR$) is given by Equation 51 where y_{exp} and y_{pred} are respectively the experimental and predicted diffusivity. 10 independent solvers were used for each identification, in order to ensure that the found minimum was global and not local (*multistart* optimisation routine from Matlab software statistics toolbox).

$$SSQR = (y_{pred} - y_{exp})^2 \quad (51)$$

2.4 Error propagation and impact on parameter determination.

A Monte Carlo sampling was applied to study the error propagation derived from the scatter of diffusivity on the parameter identification. This way, the 95 % confidence intervals associated to each parameter can be determined, and the influence of the experimental error on the range of variation of each of the parameters individually can be studied. The Monte Carlo sampling consists on adding artificial noise to one or more of the variables used in a parameter identification, in this case. One way to do this is to introduce variations on the variable subject of study within a certain interval that imitates the error that can be present in an actual measure. This process is repeated many times, and each of these times the parameter is identified. In this case, the variable subject to measuring error is diffusivity, and the parameters

to identify are A_p* and τ (equation 49)

At the end, a parameter distribution can be built, where the mean of the distribution would be the searched parameter and the confidence interval may be determined as those values that enclose the 95% of the distribution around the mean.

The experimental diffusion coefficients were made variate within the interval ($D/2$, $1.5D$), according to the worse standard deviation found on the experimental values. A Lilliefors test was applied to the parameter distribution to verify the hypothesis of the parameter following a normal distribution. Then, the confidence intervals were calculated by manually discarding the 2.5% of the upper and lower values of the distribution.

3 Results.

Equation 49 is generally applied to widely used groups of plastic relevant for food packaging including polyolefines and polyesters. Only the dimensionless term of Ap* and τ were adjusted to each polymer, regardless diffusing substances. The impact of temperature is described through the parameter τ, which is related to the conventional activation energy according to the following equation 4 (Begley et al. 2005) and it is summarized here. The parameter τ, together with the constant 10454, both with the formal dimension of temperature, supposedly contribute to the activation energy of diffusion, according to equation 52.

$$E_A = (10454 + \tau) \cdot R \quad (52)$$

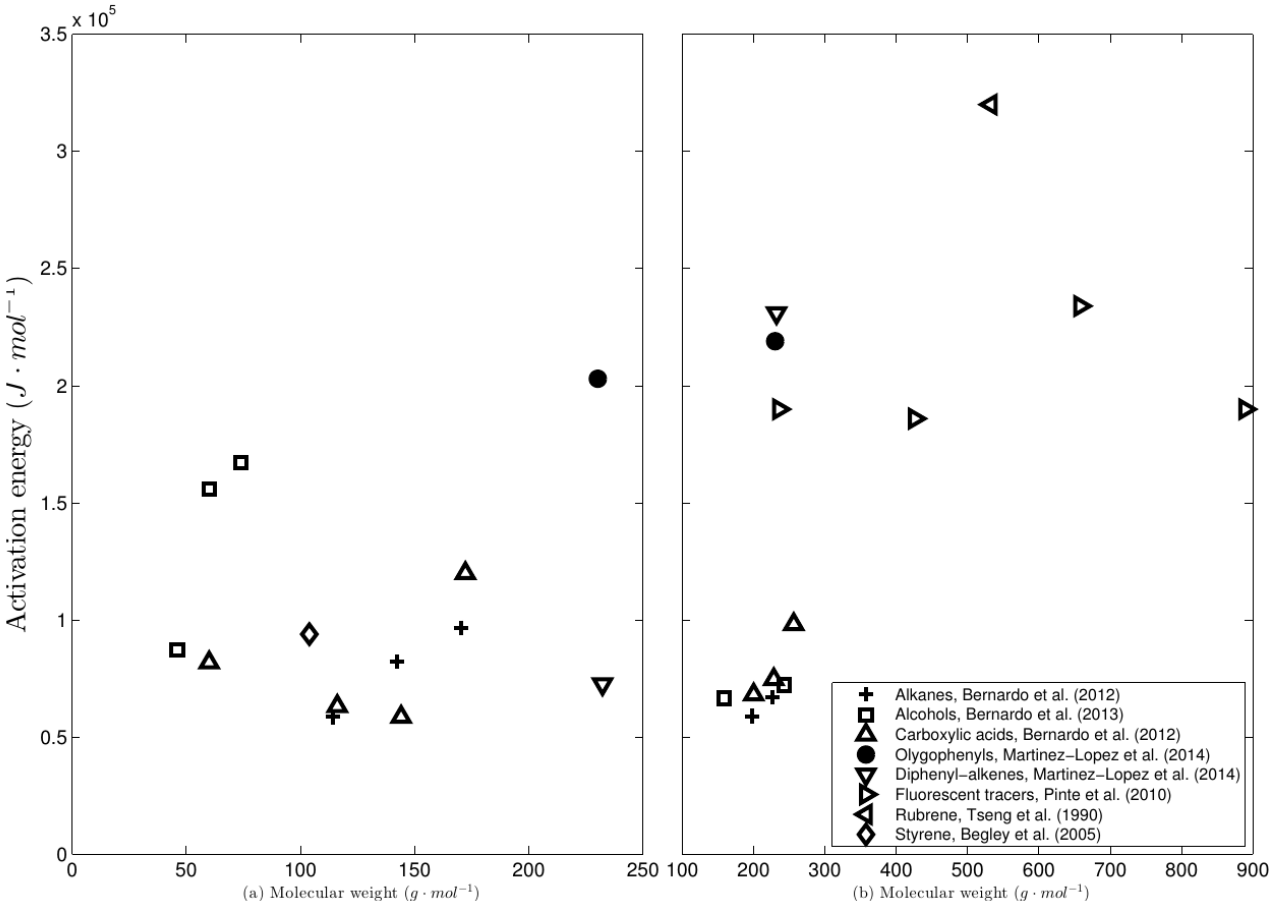

Figure 27: plot of the calculated activation energies in function of the molecular weight of the migrant below (a) and above (b) the glass transition temperature of amorphous PS.

where R=8.3145 $J\ mol^{-1}K^{-1}$ is the gas constant. The authors propose then, two possible values for τ, applicable for all polymers and all substances. They were calculated after analysing activation energy data of a large series of migrants from literature. These two vales are τ=0 K, corresponding to a mean E_A=87 $kJ\ mol^{-1}$ for presumed low-barrier polymers that allow fast diffusion: LDPE, rubber PP, PS, HIPS and PA; while τ=1577 K, corresponding to a mean E_A=100 $kJ\ mol^{-1}$ for presumed high barrier polymers: PET, HDPE, homo and random PP and PEN. aim at simplifying the contribution of activation energy (Mercea 2007). The parameter A_p* is supposedly linked to the polymer and describes the basic diffusion behaviour of the polymer matrix in relation to the migrants. A high value of A_p* reflects high diffusion behaviour and hence high migration, which is the case for polyolefins. In the original publication by Begley et al. 2005, the parameter A_p* was determined for each polymer from diffusivity data available in literature, in the case of LDPE, HDPE and PP; or from diffusivity calculated from migration tests, which was the case of PS, HIPS, PET, PEN and PA. By using equation 49 with the diffusivity of each migrant and the value of τ=0 or τ=1577 depending on the polymer, a value of A_p* for each migrant is obtained. In a next step, the mean $\bar{A}_p^*$ for each polymer is calculated. In order to assure overestimation, an upper bound A_p* is calculated by increasing the mean with the addition of the standard deviation multiplied with the student t-factor for a one (right)-side 95% confidence level. Values of A_p* and τ for each polymer, as well as general guidelines about their molecular weight and temperature range applicability can be found at Simoneau 2010.

In the specific case of amorphous PS, since the original parameters were determined by Begley et al. 2005, new diffusivity data has been published. The comparison between these new data and the prediction issued from equation 49 with the original parameters shows systematic underestimation of diffusivity. This statement led to consider that the scarce knowledge of the diffusion behaviour of this polymeric matrix result in a wrong estimation of the parameters, which might now be considered as obsolete. With the new data, got from the publications detailed in ¶ 2.1, not only new parameters that yields equation 49 useful for the case of amorphous PS can be calculated, but a faster way of finding them just with the need of diffusivity data at several temperatures, without the need of calculating the activation energy of diffusion.

3.1 Activation energy of diffusion.

The glass transition range (around 105 ^oC) of polystyrene can be included in the temperature variation range occurring during life cycle of many packed foods (e.g. microwaves warming of ready to use packed foods). Activation energies of diffusion at each side of the glass transition temperature of PS (105 ^oC) were calculated from diffusivity data got from the publications detailed in ¶ 2.1, as well as the associated

95% confidence intervals. These confidence intervals, calculated were used as criteria to discard those activation energies whose lower confidence bound was negative for considering them too unreliable.

Figure 27 shows a projection of E_A values as a function of molecular weight of migrant. As first approximation, no clear trend relating activation energy and molecular weight was evidenced whatever the temperature range is. Therefore, these results could appear in disagreement with observation of Pennarum et al (2004) and Dole et al. (2006), who report that activation energy of solutes increases with the logarithm of the molecular mass. However, if this trend has been approved for a wide variety of polyolefins (LDPE, HDPE and PP) and for PVC and PET, the lack of data obtained on PS prevents any extrapolation to this polymer. If this statement was not clearly validated in view of the overall results, a dependence of E_A with the molecular weight of the diffusing molecule can be more specifically observed for molecules of the same homologous series.

According to free-volume theory, the activation energy is commonly interpreted as the energy needed for the diffusing molecule to move when a gap is created (Pennarun et al. 2004). As consequence, E_A is known to be related more to the shape of the diffusing molecule than to its molecular weight and additionally depends on the intermolecular forces that may bind it with the polymer (e.g. hydrogen bonding, Van der Waals etc..). This theoretical point of view appears reinforced by these results since, regarding the results within each molecules series (alcohols, carboxylic acids, oly-

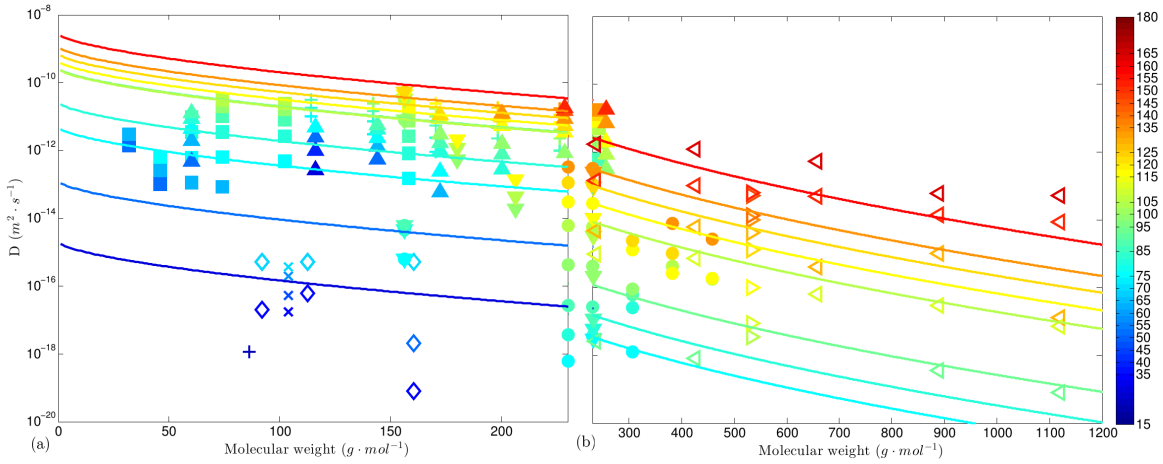

Figure 28: Representation of the experimental diffusivity in function of molecular weight and temperature (symbols), for a molecular weight below (a) and above (b) 230 $gmol^{-1}$. The continuous lines represent the diffusivity predicted by equation 49, using the parameters shown in table 6. The experimental data belongs to + Alkanes, NMR and gravimetry (Bernardo, 2012) and Spectroscopic ellipsometry (Ogieglo et al., 2013), ■ Alcohols, NMR and gravimetry (Bernardo, 2013), ▲Carboxylic acids, NMR and gravimetry (Bernardo et al., 2012), ◊ Toluene, Phenylcyclohexane and Ethylbenzene (Dole et al., 2006), ◄ Homologous series offluorescent tracers, FRAP (Pinte et al., 2010), ►Rubrene, FRAP (Tseng et al., 2000), **X** Styrene (Begley et al. 2005).

olygophenyls, di-phenyl alkenes), the evolution of E_A values seems increase with the length of molecules.

In addition and according to the free-volume theory, the activation energy is expected to increase progressively from rubber to glassy state. Although that the collection of reliable E_A values tabulated in the literature is however insufficient to derive a general law. The results reported in Figure 27 do not confirm this hypothesis since E_A measures individually obtained on each molecule exhibits similar values in the range of 50-150 kJ·mol-1. In the Piringer model, Ap^* and τ are polymer dependent parameters and zero value for τ leads to an apparent activation energy of 87 kJ·mol-1 which corresponds to a median activation energy in polyolefin matrices.

After analysing the activation energy data, and applying equation 52 as it is defined by Begley et al. 2005, it can be concluded that, for amorphous PS, τ=1955 K below the glass transition temperature and τ=7382 K above it. If it is chosen not to make a distinction between the diffusion behaviour at each side of the glass transition temperature, τ=4769 K; which is still far from the value τ=0 K originally proposed that depicts the diffusion behaviour of PS at the same level of LDPE. Since diffusivity

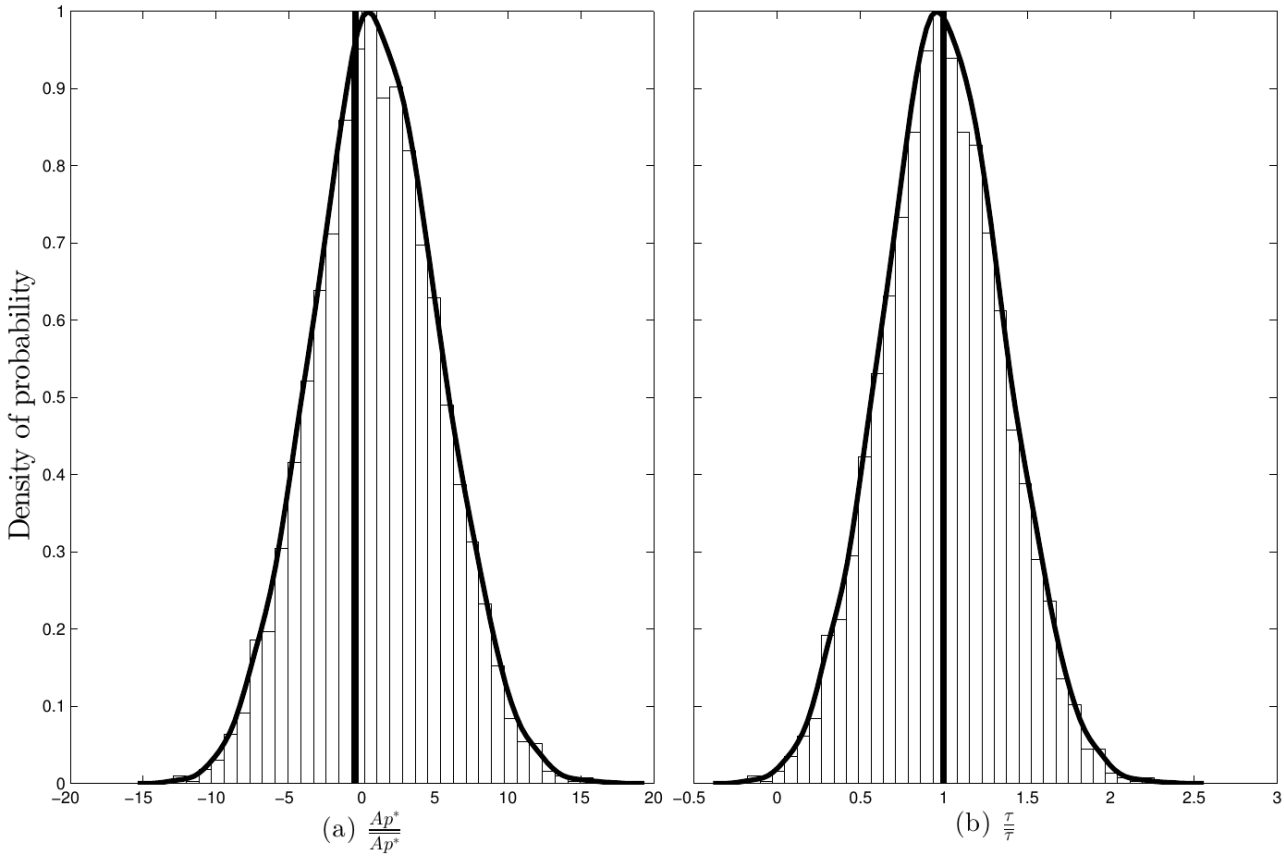

Figure 29: Normal distributions resulting from noise addition within a range of (D/2, 1.5D) to the experimental diffusivity values below 230 gmol^{-1} and above the glass transition temperature of $A_p{}^*$ (a) and τ (b). The x axis has been adimensionalized in relation to the mean of the distribution of each parameter to show the different width of the parameter distribution from the same source of uncertainty.

above T_g seems significantly faster, according to the original reasoning, it should be reflected by a significantly smaller value of E_A, and thus of τ. It can be concluded that the mean of the available activation energies, which are themselves submitted to great error is not a good indicative of the low or high barrier behaviour of PS towards diffusion. Another lecture is that, while τ can be used as a fitting variable for an optimal prediction of D, it has no attached physical meaning.

3.2 Determination of A_p* and τ.

The applied strategy was to regress both parameters simultaneously from the diffusivity data available in literature, which means that the value of A_p* and τ is selected by minimizing the *SSQR* between the experimental and predicted diffusivity. The experimental diffusivity data had previously been multiplied by a 1.3 factor, in order to make for a 30% of overestimation over the measured value. Two ranges of M and T have been considered: from 0 to 230 and 230 to 1200 g·mol^{-1} for molecular weight; and above and below glass transition temperature and to consider the change on the

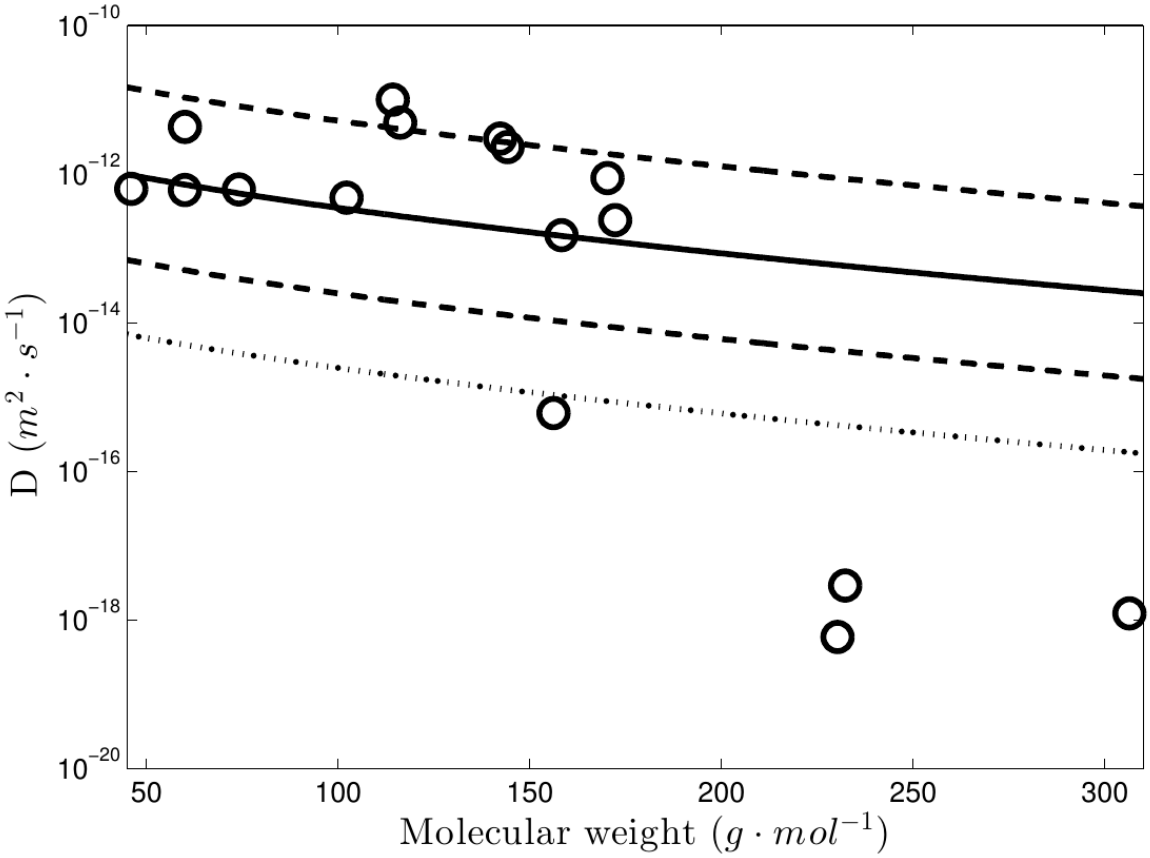

Figure 30: Plot of the experimental diffusivity versus the molecular weight at 75 ^oC (◯). The dashed lines represent the values as calculated with the lower and upper bounds of the confidence intervals. The dotted line represents the values predicted with the original parameters of the equation.

distribution of the free volume holes that may occur on the rubbery state. The results are summarized in Table 6 as well as the number of diffusion coefficients used to regress them. The values obtained this way exhibit large variation according to the temperature with in particular negative values of Ap^* and τ identified for specific conditions of low temperature and low molecular weight ($T<T_g$; M< 230 $g\ mol^{-1}$). The choice was made according to the break on the diffusivity trend that can be observed around 230 g·mol-1; and to consider the change on the distribution of the free volume holes that may occur on the rubbery state. This way, four sets of parameters that will overestimate diffusivity in most of the cases have been determined: M< 230 g·mol^{-1} and $T<T_g$; M< 230 g·mol^{-1} and $T>T_g$; M>230 g·mol^{-1} and $T<T_g$; M>230 g·mol^{-1} and $T<T_g$. They are shown in Table 6 as well as the number of diffusion coefficients used to regress them. Therefore, it must be pointed out that simultaneous regression of two or more parameters is a technique that cannot be applied to every case, since the output (in this case, an overestimated diffusion coefficient result of minimizing the $SSQR$) might be the result of one among many or infinite combinations of parameters that result in a minimal $SSQR$. In other words, even if graphically the fit looks correct in relationship to the experimental data, each identified parameter might be given a value that lays outside of the necessary interval to attach any physical meaning. After analysing the hypothetical physical meaning of the parameter τ, and taking into account that the main application of equation 49 is a fast, direct and rough prediction of diffusion coefficients from just molecular weight and temperature, trying to give the parameters a physical meaning may be considered pointless (Sin et al. 2010), and so may be calculating the value of A_p^* after having previously set the value of τ based on a loose connection with the activation energy. In fact, doing so may force the optimisation algorithm to find a value that, will predict diffusivity worse than it would by the use of two fitting variables. As seen in Table 6, only in one case A_p^* is close to the value originally determined of -1, under the condition that the value of τ is of 2425, far away of the originally proposed value of 0. It can also be noticed that these values, calculated as the best fits to purportedly overestimated experimental diffusivity values change almost in a random fashion from one interval of molecular weight and temperature to another, which is well in agreement with treating them just as fitting parameters of a model without any physical meaning. The fit at both ranges of molecular weight in function of temperature is shown in Figure 28. This projection shows that the new parameters results in a better valuation of the diffusion coefficients with very few underestimated experimental points. The parameters distinctly determined on the both side of the Tg demonstrated similar ability for estimating diffusivity.

	n	τ (K)	τ 95% CI	A_p*	A_p* 95 % C.I.
$T<T_g$, $M < 230$ $g\ mol^{-1}$	67	10459	(10042,10964)	34.2	(32.8, 35.5)
$T>T_g$, M < 230 $g\ mol^{-1}$	43	-2425	(-611.5, -3463)	-1.4	(-4.1, 3.2
$T<T_g$, M > 230 $g\ mol^{-1}$	14	12820	(10732,15036)	31.1	(25.3, 37.2)
$T>T_g$, M > 230 $g\ mol^{-1}$	59	6276	(5683,6867)	16.3	(14.7, 17.6)

Table 6: Values of Ap* and τ calculated from the fit for purpoted overestimation of 30% for each molecular weight and temperature interval. The column n designs the number of diffusivity values used on the determination. Confidence intervals were calculated by introducing random variations on the overestimated diffusivity values within the interval (0.5D, 1.5D).

3.2.1 Uncertainty propagation and impact on the identification of parameters.

A Monte Carlo sampling was applied to obtain the associated 95 % confidence intervals of the parameters $Ap*$ and τ for each molecular weight and temperature range. This is interesting for two reasons: on one hand, the aforementioned 95% confidence intervals can be calculated, on the other hand, the influence of the number of values, as well as of the uncertainty on each of the diffusion coefficients can be studied. In this work, experimental diffusivity was made vary randomly within the interval (D/2, 1.5D). In every case the resulting distribution could be considered normal, according to the Lilliefors test. As well, in every case both parameters vary on a proportion around approximately between (0.8, 1.1) times the mean, except on the case of molecules smaller than 230 $gmol^{-1}$ above the glass transition temperature, which show a variation of (-10, 10) in the case of A_p* and (0, 2) for τ, as it can be seen in Figure 29. The width of the confidence intervals means that these parameters, while calculated for a purported overestimation of 30% may, in the worse case which, understimate diffusivity up to a 50% of the actual value, depending on the reliability of the diffusivity data used on the fit; which is still far better than the systematic underestimation that occurred with the original parameters. As well, it may be noticed that on the cases $T<T_g$, M>230 $gmol^{-1}$ and $T>T_g$, M>230 $gmol^{-1}$ the parameter values resulted from the fit do not lay inside the confidence intervals. Due to the similarities amongst the value of the parameters and the width of the confidence intervals, it could be concluded that above 230 $gmol^{-1}$ the value of the parameters is the same no matter the temperature. Although the prediction of diffusivity using the parameters got from the fit provides overestimation in most cases, there are still be cases of underestimation of diffusivity, due to the scatter of the data. Should be the case, the overestimation can be exaggerated by using as parameters, the upper bound of the confidence interval for A_p* and the lower bound of the confidence interval for τ. As

seen in Figure 30, the original parameters (dotted line) underestimated diffusivity systematically, even compared with the lower bound of the confidence interval.

4 Conclusions.

The determination of the parameters $A_p{}^*$ and τ by simultaneous regression from purportedly overestimated diffusivity on different molecular weight and temperature ranges has been studied. The utilisation of the parameter sets obtained with this strategy proved to yield diffusivity values with a reasonable level of overestimation. This strategy is nevertheless based on the assumption that neither $A_p{}^*$ or τ have attached any physical meaning, and just treats them as fitting variables of the model. . In any case, this results demonstrated the necessity to use available new experimental results issued from up-to-date techniques for refine more precise 'upper-bond' $A_p{}^*$ or τ values.

Originally, $A_p{}^*$ and τ were determined on the basis of a relationship between the latter and the activation energy. The determination of $A_p{}^*$ subjected to a fixed value of τ in combination with the lack of diffusivity data for PS resulted in a set of parameters that depicted the diffusion behaviour of PS towards migrant diffusion at almost the same level as LLDPE, which resulted in systematic underestimation of diffusivity. With the four sets of parameters proposed by this work, it is now possible to use the equation for the safety purpose it was conceived for. As well, it has been shown the great error the activation energies may be subjected to, and the lack of evidence linking them to a high or low barrier behaviour of PS towards diffusion behaviour. As diffusivity data for amorphous PS becomes more common in literature, specially for low temperatures and great molecular weight ranges, the value of the parameters may be refined, or a new unified predictive model of diffusivity from easy to find molecular descriptor, like the molecular weight may be proposed.

Chapter VI : Conclusions

This work has been carried out within the framework of the french Association Nationale de la Recherche project SFPD (acronym for Safe Food Pack Design). This project aims at developing a risk-based approach to address permeation and migration issues during all stages of package conception, which will result on safe-by-design instead of safe-as-stated packaged food products. The contribution of this thesis to the project has been a database of diffusion coefficients and activation energies of diffusion. The creation of this database has been used to set the goals of this thesis.

Goals of this thesis

The bibliographical review (Publication I) confirms that no general methodology exists to determine the diffusion coefficient by either experimentation or predictive modelling. In the case of experimentation, a methodology to characterize phenomenological diffusivity requires choosing (i) the kind of media into contact, (ii) an analytical technique to monitor kinetics and (iii) a mathematical solution to Fick's law of diffusion. The determination of diffusivity via modelling is slightly different, with many existing choices but lacking of a conclusive one. Among the many models that exist today, those based on the microscopic scale demand too much computing power (molecular modelling and Monte Carlo); those based on the free volume theory require extensive and abstract experimental input (Vrentas and Duda); while those based on direct regression from experimental diffusivity data lack of any physical meaning. The need to create a diffusivity and activation energy database fostered the development of a general methodology to determine the diffusion coefficient for any kind of polymer/migrant system at any temperature as part of this thesis. Given the relationship between the other transport properties and the diffusion coefficient, the scope of the methodology might be extended to the mass transfer coefficient and the partition coefficient (or concentration at equilibrium) as well. The diffusivity data that can be gathered with such methodologies, in addition to the prediction of migration levels can be used to develop a predictive model based on the relationship between the molecular geometry and the diffusion behaviour, or to build a model more focused on an industrial application but without any physical meaning. This way, the goals of this thesis can be regarded as: (i) Development of a general methodology allowing to characterize transport properties diffusivity D, mass transfer coefficient k and partition coefficient or concentration at equilibrium C_∞, (ii) Development of a model allowing to predict diffusivity, based on simple concepts with an actual physical meaning and (iii) Development of a semi-empirical model, ready for an industrial application, but without any attached physical meaning. Given the relation-

ship between D, k and the global mass transfer coefficient D_{app}, it is possible to regress D and k from the same kinetics, depending on the conditions under which the data has been gathered. The simultaneous regression of several parameters, is a methodology that might be adapted to many models other than mass transfer, and so a part of this chapter is dedicated to this matter. Amorphous PS, with a glass transition temperature of 105 °C has been throughout this work, except for the development of the methodology to determine D and k, for which a solid-liquid contact is needed. This way, those experiments have been carried out using LLDPE in contact with food simulant miglyol 829.

Determination of transport properties.

As stated, no general methodology exists to characterize the transport properties. The experimental setup (media into contact, analytical technique chosen to monitor kinetics) depends widely on the system under investigation, but literature contains much more information about the determination of diffusivity than about the mass transfer or the partition coefficient, for which, even the conditions under which they can be determined remain obscure.

On the course of this work, three analytical techniques have been extensively used to obtain usable kinetic data for the determination of transport properties: Raman microspectroscopy, Gas chromatography and FTIR. Concretely, FTIR was used to obtain D and k of Uvitex OB in LLDPE in contact with Miglyol 829, Gas chromatography was used to determine diffusivity of p-terphenyl in amorphous PS, while Raman microspectroscopy was used to obtain diffusivity of two homologous families of molecules and the solubility limit (or concentration at equilibrium) C∞ of p-terphenyl in amorphous PS, as well as D and k of Uvitex OB in LLDPE in contact with Miglyol 829. The utilisation of each technique to determine one or other transport property responds to what the technique showed to be more adapted.

FTIR allowed to obtain the average concentration of a molecule in a plastic sample by a fast non-destructive means. It has an outstanding selectivity to distinguish the fingerprint of a molecule. Consequently, a large number of molecules may be analysed with it. However it lacks of sensitivity compared to other analytical methods, making difficult to work on concentrations below 0.1 %wt. This lack of sensitivity made impossible the characterization of diffusivity of any molecule tested on PS. Nevertheless, it was possible to use it to determine D and k of Uvitex OB in LLDPE in contact with Miglyol 829 (Publication III) by the classical sequential method, consisting on measuring the difference between a stirred and an unstirred contact after 24 h.

Gas chromatography, as well as FTIR, permits to obtain the average concentration of a substance in a plastic sample. It also has a remarkable selectivity, allowing even to

work with several migrants simultaneously. Contrary to FTIR, its sensitivity is outstanding, reaching concentrations of ppm or even ppb. The main drawback is its destructive nature, needing to develop a protocol to extract the target molecule from the polymeric matrix. As said, in this work, gas chromatography was used to characterize diffusivity of p-terphenyl in amorphous PS on the glassy state. Two main drawbacks were found in this methodology. First, an extraction protocol from an amorphous polymer necessarily involves dissolution and re-precipitation of the polymer, adding another source of error to the characterization due to the possible re-precipitation of the target molecule along with the polymer. Second, a robust determination of diffusivity by global measuring requires of the concentration in equilibrium, which might be impossible to attain due to the long kinetics characteristic of high-barrier polymers such as amorphous PS in glassy state, which was estimated in more than 600 years according to the diffusivity value obtained with Raman. This way, for the methodology to be successful, it was necessary to find another way to determine C∞ (Ra-man microspectroscopy). It can be concluded that such a methodology may be adapted to rubbery low barrier semi-crystalline polymers, but not is not self-sufficient for amorphous polymers in the glassy state. Though the characterization of diffusivity of p-terphenyl in amorphous PS with a reasonable scatter of the kinetic data was possible after one week of solid-solid contact (Publication II), the author discourages its use for such systems.

FTIR and Gas Chromatography are both global measuring techniques, which means that it is not possible to gather information of the diffusion behaviour inside the polymeric film with any of them, like it is the case of Raman microspectroscopy. This gives two great advantages to the latter over global measuring methods: (i) the concentration at equilibrium can be assesed by taking measures at the interface of a solid-solid contact, and (ii) since the time required to obtain a usable concentration profile is sensibly lower than following kinetics until equilibrium (72h by local measuring versus one week by global measuring with Gas Chromatography), the technique seems specially adapted to slow diffusion behaviour, characteristic of high barrier polymers. As a drawback, it is only applicable to molecules presenting a Raman signal intensity strong enough to be able to distinguish them within the polymer matrix; which means a selectivity clearly inferior compared to FTIR and Gas Chromatography. Raman microspectroscopy probed to be well adapted to the determination of all the three transport properties involving commercial polymer systems. Concretely, the determination of both D and C_∞ was feasible in a high barrier polymer such as amorphous PS in the glassy state (Publication II) and in the rubbery state for two different families of molecules (Publication IV). As well, diffusivity and mass transfer coefficient were determined in LLDPE at the rubbery state, in contact with food simulant Miglyol 829 (Publication III). For both systems (PS solid contact and

LLDPE/Miglyol), the ability of Raman to perform local measures combined with its relatively high sensitivity resulted in robust characterisations that may be exported to other food/packaging/migrant systems. Local measuring is not a feature exclusive of Raman. Other analytical techniques such as FTIR or UV microscopy as well as FRAP allow local measuring. As a consequence, they may replace Raman if the migrant is not detectable with it.

While the main goal of developing a general methodology to measure diffusivity on commercial migrant/polymer systems has not been attained, general guidelines can be deducted from the results of this work. Most importantly, local measuring should be preferred if available, since it reduces considerably the required time to obtain a robust estimation.

The methodology based on local measuring with Raman microspectroscopy (Publication II) was successfully applied to two homologous series of molecules that share the phenyl ring as basic unit: the olygophenyl series, which consists on molecules from 2 to 6 phenyl rings linked in the para- position, and the diphenyl-alkene series, which consists on two phenyl rings linked by conjugated dienes. This allowed to gather enough diffusivity data on amorphous PS in the rubbery state in a short time. This data was used to study the influence of the molecular geometry in the diffusion behaviour.

Influence of molecular geometry in diffusion behaviour on the rubbery state.

It is a common statement to link the diffusion behaviour to the hindrance characteristics of the molecules. Many authors use the molecular weight as representative of this hindrance. In this work, molecular weight has been shown to not to describe accurately the diffusion behaviour of molecules belonging to different families. While a priori representing the hindrance of the molecules more accurately, a description based on molecular volume frequently results on a curve of a similar shape to that of molecular weight. This is caused by molecular weight and volume being related by a linear relationship in most of the cases, which depend on the previous selection of the molecules of the study. Consequently, it can be stated that the description of the diffusion behaviour solely based on one parameter yields poor correlation, no matter the geometrical meaning of the parameter. With the goal of finding new parameters that allow a correct description of the diffusion behaviour without the need of huge computing power, abstract conceptions or extensive experimental input; a new mechanical model based on the two body problem was developed. The model presents the molecules as springs-beads systems, representing each phenyl group as a bead, and the bond between them as a spring, with an equivalent elasticity constant calculated ac-

cording to Hooke's law of Newtonian mechanics. Then, this elasticity constant was combined with other structural parameters, like the length or the volume of the molecule, in order to create linear and volumetric compressibility shape factors. This model allowed a correct description of the diffusivity trend in the rubbery state of both homologous series of molecules (Publication IV) by using mere trigonometrical relationships. All geometrical parameters used by the model are easily retrieved on database with the exception of the aforementioned elasticity constant, that is calculated from the raman vibration frequency, found by reconstructing the theoretical spectrum with a molecular modelling software package.

As well as in the case of the general methodology to characterize diffusivity, the goal of developing a general model to predict diffusivity has not been achieved due to the molecule population used on its development being too small for a general conclusion. However, the model being based on mechanical concepts makes it understandable to a wide audience, without the needs of abstract thermodynamical considerations. As well, the model remains potentially applicable to any other diffusivity data available in literature on the same amorphous PS. Further research in the same direction, might allow to express the constants issued from the data fitting in function of other temperature or polymer dependent parameters (for example, the free-volume fraction) that might lay the foundations of a general model to predict diffusion in polymers in the rubbery state.

The next section also deals with methodologies to determine transport properties and it could have been covered in the first section of this chapter, it has been chosen not to do so, because it discusses the limitations of the analytical technique from a more theoretical point of view, dealing with mathematical treatment of the experimental data and sensitivity of the involved analytical techniques.

Simultaneous determination of diffusivity and mass transfer coefficient.

Migration can be described as a combination of diffusion and desorption. As such, a complete description may include not only the diffusion coefficient, but also the mass transfer coefficient, which is systematically neglected, based on its supposed irrelevance compared to diffusivity. The partition coefficient is also essential, but its retrieval can be considered as a part on the determination of diffusivity. The neglect of the mass transfer coefficient results in a substantial simplification of the integration procedure of the differential equation. Such a simplification may have had sense when resolution of differential equations was done by hand, and the data fitting had to be performed by using pre-made plots of the output of the model, such as those found in Crank 1980. With the availability of mathematical tools that allow data fitting with

relatively easy to implement calculation routines, along with the decrease on the prize of computing power, such simplifications may not be necessary today. Consequently, in order to take into account the effect of desorption, it is enough to solve Fick's law with the imposition of the appropriate boundary condition. This results in a numerical equation including both diffusivity and mass transfer coefficient, that can be used to regress them simultaneously. However, this practice may be performed carefully, since there might be several or infinite combinations of parameter values producing the same model output; or in other words, there might be more than one combination of values for D and k that yield the same concentration value. In order to avoid an erroneous determination, it is necessary to check the presence of collinearity between D and k. The concept of collinearity refers to an exact or approximate linear relationship between two theoretically independent variables that define the system. If such a relationship between both variables exist, the minimization algorithm will reach the same result by randomly changing the value of the other coefficient, producing combinations of parameters that may lack of actual physical meaning. This way, a practical identifiability analysis, based on searching the ranges of Fo and Bi that display the lowest collinearity, allowed to know the conditions under which both coefficients can be simultaneously regressed (Publication III). As expected, for a reliable simultaneous determination of both coefficients, measures must be taken at early stages of the kinetics (low Fo number) when desorption is the limiting stage of the transfer, while a high ratio of the external over the internal transfer (high Bi number). As well, it demonstrated that decreasing the spacing between measures increases the likelihood of the determination. The validity of this theory was checked against two experimental methodologies: one based on global measuring with FTIR and another one based on local measuring with Raman microspectroscopy. As predicted by the practical identifiability analysis, the spacing between the global measures taken with FTIR was not small enough to reach the low collinearity required for a simultaneous determination of both transport properties, which was attainable by local measuring with Raman microspectroscopy. This result is the combination of, on the one hand, the lack of sensitivity of FTIR and, on the other hand the fact that local measuring provides information about the spatial distribution of the points besides the time information also present in global measuring. This way, one concentration profile taken at a low Fo number contains many data points compared to the single point obtained from a single global measure.

Besides the contribution of the calculated mass transfer coefficients to the scarce literature available about it for food packaging systems, this work permitted to set the foundations of a general methodology that will allow to determine both diffusivity and mass transfer coefficient in function of the minimum measuring spacing attain-

able, according to the sensitivity of the analytical technique used to monitor the transfer.

The next section deals with simultaneous regression of parameters of any model, provided that they lack of any actual physical meaning. The diffusivity data used to retrieve the parameters was got from the results of Publication IV, as well as other data on similar amorphous PS found in literature.

Simultaneous regression of several parameters of a semi-empirical model.

Mass transfer is not the only physical magnitude that is described by a model requiring more than one parameter. As a part of this work (Publication V), the Piringer overestimating equation was analysed, in order to propose an update to the values of the two parameters Ap^* and τ needed to predict diffusivity. Four sets of parameters were proposed, for different ranges of molecular weights and temperatures (below and above the glass transition temperature), found by simultaneous regression. Ap^* and τ are supposed to have an attached physical meaning related to the conductance of the polymeric matrix and the activation energy of diffusion respectively. This means that, theoretically, the same identifiability analysis as performed in Publication III would have had to be performed, in order to assure that their values are kept within reasonable orders of magnitude. Instead, the claimed physical meaning of the parameters was checked by calculating the value of τ according to its supposed relationship with the activation energy of diffusion, which states that τ may have a value of 1577 in the case of a high barrier polymer (PET, HDPE, homo and random PP and PEN), and 0 in the case of low barrier polymers (LDPE, PS, HIPS and PA). The value of τ were of 1955 below the glass transition temperature and of 7382 above it. If τ was really representative of the high or low barrier behaviour of the polymer towards diffusion, τ should be significantly above the glass transition temperature to take into account the freedom of movement of the polymeric chains in the rubbery state. This was taken as a proof of its lack of physical meaning, thus justifying the retrieval of the parameters by simultaneous regression.

The diffusivity data gathered in Publication IV by the use of the methodology developed in Publication II was used, along with other data available in literature for amorphous PS in order to update the parameters of the equation recommended by the EU commission for the implementation of diffusion model. The new sets of parameters render the equation ready for a direct engineering application of diffusivity overestimation to ensure worse-scenario migration levels for amorphous PS.

Perspectives

Some scientific questions remain unanswered, and should be subject of further research. For example, the application of Raman microspectroscopy has been probed successful for LLDPE and PS, in the glassy and in the rubber state for a robust characterization of all three transport properties: D, k and C_∞. Its applicability to other polymers widely used by packaging industry, like PP or PET has not been tested.

The practical identifiability analysis permitted to identify the conditions under which diffusivity and mass transfer coefficients can be simultaneously determined. Further research might allow to develop a general methodology allowing to determine both diffusivity and mass transfer coefficient in function of the minimum measuring spacing attainable according to the sensitivity of the analytical technique used to monitor the transfer.

By increasing the molecule population to which the springs-beads model has been applied, the ultimate goal of providing a model to predict diffusivity based on molecular structure, without requiring a huge computing power, (models based on molecular modelling) or based on abstract parameters (models based on the free volume theory) might be fulfilled. Until then, or until other alternative appears, the characterisation of diffusivity will rely mainly on experimentation or in empirical correlations.

A general semi-empirical model to predict diffusivity in amorphous PS has not been developed. Instead, the diffusivity data as a result of this work was used to update the parameters of an existing semi-empirical model to predict diffusivity in commercial packaging for the specific case of amorphous PS with safety purposes.

Bibliography

Amsden, B. 1999. An Obstruction-Scaling Model for Diffusion in Homogeneous Hydrogels. *Macromolecules* 32, 874-879.

Anandan, C. Basu, B. Rajam, K. 2004a. Study of the diffusion of pyrene in silicone polymer coatings by steady state fluorescence technique: effects of pyrene concentration. *European Polymer Journal* 40, 1833-1840.

Anandan, C. Basu, B. J. Rajam, K. 2004b. Investigations of the effect of viscosity of resin on the diffusion of pyrene in silicone polymer coatings using steady state fluorescence technique. *European Polymer Journal* 40, 335 - 342.

Antonietti, M. Sillescu, H. 1985. Self-diffusion of polystyrene chains in networks. *Macromolecules* 18, 1162-1166.

Arrhenius, S. 1889. Ober die reacktionsgeschwindigkeit bei der inversion von rohrzucker durch sauren.. *Zeitschrift für Physikalische Chemie* 4, 226–248.

Axelrod, D. Koppel, D. Schlessinger, J. Elson, E. Webb, W. 1976. Mobility measurement by analysis of fluorescence photobleaching recovery kinetics. *Biophysical Journal* 16, 1055 - 1069.

Baner, A. Brandsch, J. Franz, R. Piringer, O. 1996. The application of a predictive migration model for evaluating the compliance of plastic materials with European food regulations†. *Food Additives & Contaminants* 13, 587-601.

Begley, T. Biles, J. Cunningham, C. Piringer, O. 2004. Migration of a UV stabilizer from polyethylene terephthalate (PET) into food simulants. *FOOD ADDITIVES AND CONTAMINANTS* 21, 1007-1014.

Begley, T. Castle, L. Feigenbaum, A. Franz, R. Hinrichs, K. Lickly, T. et al. 2005. Evaluation of migration models that might be used in support of regulations for food-contact plastics. *Food Additives & Contaminants* 22, 73-90.

Begley, T. H. Hsu, W. Noonan, G. Diachenko, G. 2008. Migration of fluorochemical paper additives from food-contact paper into foods and food simulants. *FOOD ADDITIVES AND CONTAMINANTS* 25, 384-390.

Bernardo, G. 2012. Diffusivity of alkanes in polystyrene. *Journal of Polymer Research* 19, 1-9.

Bernardo, G. 2013. Diffusivity of alcohols in amorphous polystyrene. *Journal of Applied Polymer Science* 127, 1803-1811.

Bernardo, G. Choudhury, R. P. Beckham, H. W. 2012. Diffusivity of small molecules in polymers: Carboxylic acids in polystyrene. *Polymer* 53, 976 - 983.

Bower, D. I. Maddams, W. F. 1989. In *The vibrational spectroscopy of polymers*

/ D.L. Bower and W.F. Maddams, Cambridge [Cambridgeshire] ; New York : Cambridge University Press .
Brown, R. 1827. A Brief Account of microscopical observations (original manuscript). *Not published* --, -.
Brun, R. Kühni, M. Siegrist, H. Gujer, W. Reichert, P. 2002. Practical identifiability of ASM2d} parameters—systematic selection and tuning of parameter subsets . *Water Research* 36, 4113 - 4127.
Brun, R. Reichert, P. Künsch, H. R. 2001. Practical identifiability analysis of large environmental simulation models. *Water Resources Research* 37, 1015-1030.
Calvert, P. D. Billingham, N. C. 1979. Loss of additives from polymers: A theoretical model. *Journal of Applied Polymer Science* 24, 357-370.
Carr, G. 1999. High-resolution microspectroscopy and sub-nanosecond time-resolved spectroscopy with the synchrotron infrared source. *Vibrational Spectroscopy* 19, 53 - 60.
Cava, D. Catala, R. Gavara, R. Lagaron, J. 2005. Testing limonene diffusion through food contact polyethylene by FT-IR spectroscopy: Film thickness, permeant concentration and outer medium effects. *Polymer Testing* 24, 483-489.
Cava, D. Lagaron, J. Lopez-Rubio, A. Catala, R. Gavara, R. 2004. On the applicability of FT-IR spectroscopy to test aroma transport properties in polymer films. *Polymer Testing* 23, 551 - 557.
Cohen, M. H. Turnbull, D. 1959. Molecular Transport in Liquids and Glasses. *The Journal of Chemical Physics* 31, 1164-1169.
Crank, J. 1980. In *The Mathematics of Diffusion,* Press, C. Oxford University Press.
Cruz, J. Silva, A. S. Garcia, R. S. Franz, R. Losada, P. P. 2008. Studies of mass transport of model chemicals from packaging into and within cheeses. *Journal of Food Engineering* 87, 107 - 115.
Cukier, R. I. 1984. Diffusion of Brownian spheres in semidilute polymer solutions. *Macromolecules* 17, 252-255.
Darken, L. S. 1948. Diffusion, Mobility And Their Interrelation Through Free Energy In Binary Metallic Systems. *Transactions of AIME* 175.1, 184-194.
Dole, P. Feigenbaum, A. De la Cruz, C. Pastorelli, S. Paseiro, P. Hankemeier, T. et al. 2006. Typical diffusion behaviour in packaging polymers - application to functional barriers. *Food Additives & Contaminants* 23, 202-211.
Dong, W. Gijsman, P. 2010. The diffusion and solubility of Irganox® 1098 in polyamide 6. *Polym. Degrad. Stab.Polymer Degradation & Stability* 95, 955 - 959.
Doppers, L.-M. Breen, C. Sammon, C. 2004. Diffusion of water and acetone into poly(vinyl alcohol)–clay nanocomposites using ATR-FTIR. *Vibrational Spectroscopy* 35, 27 - 32.
Duda, J. Romdhane, I. H. Danner, R. P. 1994. Diffusion in glassy polymers — relaxation and antiplasticization. *Journal of Non-Crystalline Solids* 172–174, Part 2, 715 - 720.

Durand, M. Meyer, H. Benzerara, O. Baschnagel, J. Vitrac, O. 2010. Molecular dynamics simulations of the chain dynamics in monodisperse oligomer melts and of the oligomer tracer diffusion in an entangled polymer matrix. *The Journal of Chemical Physics* 132, 194902.
Einstein, A. 1905. The motion of elements suspended in static liquids as claimed in the molecular kinetic theory of heat. *Annalen der Physik* 17, 549-560.
Ewender, J. Welle, F. 2013. Determination of the activation energies of diffusion of organic molecules in poly(ethylene terephthalate). *Journal of Applied Polymer Science* 128, 3885-3892.
Fang, X. Domenek, S. Ducruet, V. Refregiers, M. Vitrac, O. 2013. Diffusion of Aromatic Solutes in Aliphatic Polymers above Glass Transition Temperature. *Macromolecules* 46, 874-888.
Fankhauser-Noti, A. Grob, K. 2006. Migration of plasticizers from PVC} gaskets of lids for glass jars into oily foods: Amount of gasket material in food contact, proportion of plasticizer migrating into food and compliance testing by simulation . *Trends in Food Science & Technology* 17, 105 - 112.
FDA 2002. Guidance for Industry-Preparation of Premarket Notifications for Food Contact Substances: Chemistry Recommendation. *FDA*
Ferrara, G. Bertoldo, M. Scoponi, M. Ciardelli, F. 2001. Diffusion coefficient and activation energy of Irganox 1010 in poly(propylene-co-ethylene) copolymers. *Polym. Degrad. Stab.Polymer Degradation & Stability* 73, 411 - 416.
Fick, A. 1855. Ueber Diffusion. *Annalen der Physik* 170, 59-86.
Fieldson, G. Barbari, T. 1993. The use of FTIR-ATR spectroscopy to characterize penetrant diffusion in polymers. *Polymer* 34, 1146 - 1153.
Fieldson, G. T. Barbari, T. A. 1995. Analysis of diffusion in polymers using evanescent field spectroscopy. *AIChE Journal* 41, 795-804.
Franz, R. Brandsch, R. 2013. Migration of Acrylic Monomers from Methacrylate Polymers - Establishing
Parameters for Migration Modelling. *PACKAGING TECHNOLOGY AND SCIENCE* 26, 435-451.
Franz, R. Welle, F. 2008. Migration measurement and modelling from poly(ethylene terephthalate) (PET) into soft drinks and fruit juices in comparison with food simulants. *Food Additives & Contaminants Part A: Chemistry Analysis Control* 25, 1033-1046.
Fricke, H. 1924. A Mathematical Treatment of the Electric Conductivity and Capacity of Disperse Systems I. The Electric Conductivity of a Suspension of Homogeneous Spheroids. *Physical Review* 24, 575-587.
Fu, Y. Lim, L.-T. 2012. Investigation of multiple-component diffusion through LLDPE film using an FTIR-ATR technique. *Polymer Testing* 31, 56 - 67.
Fujita, H. 1961. In *Diffusion in polymer-diluent systems,* 1-47, by Springer Berlin / Heidelberg.

Gall, T. P. Kramer, E. J. 1991. Diffusion of deuterated toluene in polystyrene . *Polymer* 32, 265 - 271.
Gandek, T. P. Hatton, T. A. Reid, R. C. 1989a. Batch extraction with reaction: phenolic antioxidant migration from polyolefins to water. 1. Theory. *Industrial & Engineering Chemistry Research* 28, 1030-1036.
Gandek, T. P. Hatton, T. A. Reid, R. C. 1989b. Batch extraction with reaction: phenolic antioxidant migration from polyolefins to water. 2. Experimental results and discussion. *Industrial & Engineering Chemistry Research* 28, 1036-1045.
de Gennes, P. G. 1971. Reptation of a Polymer Chain in the Presence of Fixed Obstacles. *The Journal of Chemical Physics* 55, 572-579.
Grinsted, R. A. Clark, L. Koenig, J. L. 1992. Study of cyclic sorption-desorption into poly(methyl methacrylate) rods using NMR imaging. *Macromolecules* 25, 1235-1241.
Gubbins, K. E. Moore, J. D. 2010. Molecular Modeling of Matter: Impact and Prospects in Engineering. *Industrial & Engineering Chemistry Research* 49, 3026-3046.
Hahn, K. Karger, J. Kukla, V. 1996. Single-File Diffusion Observation. *Phys. Rev. Lett.* 76, 2762-2765.
Hanwell, M. Curtis, D. Lonie, D. Vandermeersch, T. Zurek, E. Hutchison, G. 2012. Avogadro: an advanced semantic chemical editor, visualization, and analysis platform. *Journal of Cheminformatics* 4, 17.
Helmroth, I. Dekker, M. Hankemeier, T. 2003. Additive diffusion from LDPE slabs into contacting solvents as a function of solvent absorption. *Journal of Applied Polymer Science* 90, 1609-1617.
Hong, S. 1995. Prediction of polymer-solvent diffusion behaviour using free-volume theory. *Industrial & Engineering Chemistry Research* 34, 2536-2544.
Jackson, P. L. Huglin, M. B. 1995. Use of inverse gas chromatography to measure diffusion coefficients in crosslinked polymers at different temperatures. *European Polymer Journal* 31, 63 - 65.
Jeschke, G. Sajid, M. Schulte, M. Ramezanian, N. Volkov, A. Zimmermann, H. et al. 2010. Flexibility of Shape-Persistent Molecular Building Blocks Composed of p-Phenylene and Ethynylene Units. *Journal of the American Chemical Society* 132, 10107-10117.
Johansson, L. Elvingson, C. Loefroth, J. E. 1991a. Diffusion and interaction in gels and solutions. 3. Theoretical results on the obstruction effect. *Macromolecules* 24, 6024-6029.
Johansson, L. Loefroth, J.-E. 1991. Diffusion and interaction in gels and solutions: 1. Method. *J. Colloid Interface Sci.Journal of Colloid & Interface Science* 142, 116 - 120.
Johansson, L. Skantze, U. Loefroth, J. E. 1991b. Diffusion and interaction in gels and solutions. 2. Experimental results on the obstruction effect. *Macromolecules*

24, 6019-6023.
Karbowiak, T. Gougeon, R. D. Rigolet, S. Delmotte, L. Debeaufort, F. Voilley, A. 2008. Diffusion of small molecules in edible films: Effect of water and interactions between diffusant and biopolymer. *Food Chemistry* 106, 1340 - 1349.
Krüger, K.-M. Sadowski, G. 2005. Fickian and Non-Fickian Sorption Kinetics of Toluene in Glassy Polystyrene. *Macromolecules* 38, 8408-8417.
Kulkarni, S. S. Stern, S. A. 1983. The diffusion of CO2, CH4, C2H4, and C3H8 in polyethylene at elevated pressures. *Journal of Polymer Science: Polymer Physics Edition* 21, 441-465.
Lagaron, J. Cava, D. Gimenez, E. Hernandez-Munoz, P. Catala, R. Gavara, R. 2004. On the use of vibrational spectroscopy to characterize the structure and aroma barrier of food packaging polymers. *Macromolecular Symposia* 205, 225-237.
Langevin, D. Rondelez, F. 1978. Sedimentation of large colloidal particles through semidilute polymer solutions. *Polymer* 19, 875 - 882.
Lazare, L. 2000. Physical properties of additives in poly(ester-block-ether)s. University of Sussex.
Lazare, L. Billingham, N. 2001. Diffusion of a UV-absorbing stabiliser in some poly(ester-block-ether) copolymers. *Polymer* 42, 9461 - 9467.
Leger, L. Hervet, H. Rondelez, F. 1981. Reptation in entangled polymer solutions by forced Rayleigh light scattering. *Macromolecules* 14, 1732-1738.
Lodge, T. P. 1999. Reconciliation of the Molecular Weight Dependence of Diffusion and Viscosity in Entangled Polymers. *Physical Review Letters* 83, 3218-3221.
Loren, N. Nyden, M. Hermansson, A.-M. 2009. Determination of local diffusion properties in heterogeneous biomaterials. *Adv. Colloid Interface Sci.Advances in Colloid & Interface Science* 150, 5 - 15.
Mackie, J. S. Meares, P. 1955. The Sorption of Electrolytes by a Cation-Exchange Resin Membrane. *Proceedings of the Royal Society of London. Series A. Mathematical and Physical Sciences* 232, 485-498.
Martinez-Lopez, B. Chalier, P. Guillard, V. Gontard, N. Peyron, S. 2014. Determination of mass transport properties in food/packaging systems by local measurement with Raman microspectroscopy. *Journal of Applied Polymer Science* 131, 40958.
Masaro, L. Zhu, X. 1999. Physical models of diffusion for polymer solutions, gels and solids. *Progress in Polymer Science* 24, 731 - 775.
Matsukawa, S. Yasunaga, H. Zhao, C. Kuroki, S. Kurosu, H. Ando, I. 1999. Diffusion processes in polymer gels as studied by pulsed field-gradient spin-echo NMR spectroscopy. *Progress in Polymer Science* 24, 995 - 1044.
Maul, J. Frushour, B. G. Kontoff, J. R. Eichenauer, H. Ott, K.-H. Schade, C. 2000. In *Polystyrene and Styrene Copolymers,* Wiley-VCH Verlag GmbH

& Co. KGaA. http://dx.doi.org/10.1002/14356007.a21_615.pub2
Mauricio-Iglesias, M. 2009. Impact of high pressure thermal treatments on food/packaging interactions. Université Montpellier 2.
Mauricio-Iglesias, M. Guillard, V. Gontard, N. Peyron, S. 2009. Application of FTIR and Raman microspectroscopy to the study of food/packaging interactions. *Food Additives & Contaminants Part A: Chemistry Analysis Control* 26, 1515-1523.
Mauricio-Iglesias, M. Guillard, V. Gontard, N. Peyron, S. 2011. Raman depth-profiling characterization of a migrant diffusion in a polymer. *Journal of Membrane Science* 375, 165 - 171.
Mauricio-Iglesias, M. Jansana, S. Peyron, S. Gontard, N. Guillard, V. 2010. Effect of high-pressure/temperature (HP/T) treatments of in-package food on additive migration from conventional and bio-sourced materials. *Food Additives & Contaminants Part A: Chemistry Analysis Control* 27, 118-127.
Maxwell, J. C. 1873. In *A treatise on electricity and magnetism,* 500, by of California Libraries, U. Clarendon Press: Oxford, U.K..
Mercea, P. 2007. In *Appendix I,* 479-530, by Wiley-VCH Verlag GmbH. http://dx.doi.org/10.1002/9783527613281.app1
Metropolis, N. Rosenbluth, A. W. Rosenbluth, M. N. Teller, A. H. Teller, E. 1953. Equation of State Calculations by Fast Computing Machines. *The Journal of Chemical Physics* 21, 1087-1092.
Miltz, J. 1986. Inverse gas chromatographic studies of styrene diffusion in polystyrene and monomer/polymer interaction . *Polymer* 27, 105 - 108.
Moisan, J. 1980. Diffusion des additifs du polyethylene: Influence de la nature du diffusant. *European Polymer Journal* 16, 979 - 987.
Molyneux, P. 2001. "Transition-site" model for the permeation of gases and vapors through compact films of polymers. *Journal of Applied Polymer Science* 79, 981-1024.
Mueller, F. Krueger, K.-M. Sadowski, G. 2012. Non-Fickian Diffusion of Toluene in Polystyrene in the Vicinity of the Glass-Transition Temperature. *Macromolecules* 45, 926-932.
Neyertz, S. Brown, D. 2008. Molecular Dynamics Simulations of Oxygen Transport through a Fully Atomistic Polyimide Membrane. *Macromolecules* 41, 2711-2721.
Neyertz, S. Brown, D. 2009. Oxygen Sorption in Glassy Polymers Studied at the Molecular Level. *Macromolecules* 42, 8521-8533.
Neyertz, S. Brown, D. 2013. Molecular Dynamics Study of Carbon Dioxide Sorption and Plasticization at the Interface of a Glassy Polymer Membrane. *Macromolecules* 46, 2433-2449.
Neyertz, S. Brown, D. Pandiyan, S. van der Vegt, N. F. A. 2010. Carbon Dioxide Diffusion and Plasticization in Fluorinated Polyimides. *Macromolecules* 43, 7813-7827.

Neyertz, S. Gopalan, P. Brachet, P. Kristiansen, A. Männle, F. Brown, D. 2014. Oxygen Transport in Amino-Functionalized Polyhedral Oligomeric Silsesquioxanes (POSS). *Soft Materials* 12, 113-123.
Nilsson, F. Gedde, U. Hedenqvist, M. 2009. Penetrant diffusion in polyethylene spherulites assessed by a novel off-lattice Monte-Carlo technique. *European Polymer Journal* 45, 3409-3417.
Nishikida, K. Coates, J. 2003. In *Handbook of Plastics Analysis,* 201-340, by Lobo, H.and Bonilla, J. Marcel Dekker.
Ogieglo, W. Wormeester, H. Wessling, M. Benes, N. E. 2013. Temperature-induced transition of the diffusion mechanism of n-hexane in ultra-thin polystyrene films, resolved by in-situ Spectroscopic Ellipsometry. *Polymer* 54, 341 - 348.
Ogston, A. G. Preston, B. N. Wells, J. D. 1973. On the Transport of Compact Particles Through Solutions of Chain-Polymers. *Proceedings of the Royal Society of London. A. Mathematical and Physical Sciences* 333, 297-316.
Okino, T. 2013. Ending of Darken Equation and Intrinsic Diffusion Concept. *Journal of Modern Physics* 4, 1495-1498.
Pawlisch, C. A. Bric, J. R. Laurence, R. L. 1988. Solute diffusion in polymers. 2. Fourier estimation of capillary column inverse gas chromatography data. *Macromolecules* 21, 1685-1698.
Pawlisch, C. A. Macris, A. Laurence, R. L. 1987. Solute diffusion in polymers. 1. The use of capillary column inverse gas chromatography. *Macromolecules* 20, 1564-1578.
Penicaud, C. Peyron, S. Bohuon, P. Gontard, N. Guillard, V. 2010. Ascorbic acid in food: Development of a rapid analysis technique and application to diffusivity determination . *Food Research International* 43, 838 - 847.
Pennarun, P. Dole, P. Feigenbaum, A. 2004a. Functional barriers in PET recycled bottles. Part I. Determination of diffusion coefficients in bioriented PET with and without contact with food simulants. *Journal of Applied Polymer Science* 92, 2845-2858.
Pennarun, P. Y. Ngono, Y. Dole, P. Feigenbaum, A. 2004b. Functional barriers in PET recycled bottles. Part II. Diffusion of pollutants during processing. *Journal of Applied Polymer Science* 92, 2859-2870.
Percus, J. K. 1974. Anomalous self-diffusion for one-dimensional hard cores. *Phys. Rev. A* 9, 557-559.
Phillies, G. D. J. 1986. Universal scaling equation for self-diffusion by macromolecules in solution. *Macromolecules* 19, 2367-2376.
Phillies, G. D. J. 1987. Dynamics of polymers in concentrated solutions: the universal scaling equation derived. *Macromolecules* 20, 558-564.
Phillies, G. D. J. 1989. The hydrodynamic scaling model for polymer self-diffusion. *The Journal of Physical Chemistry* 93, 5029-5039.

Pickup, S. Blum, F. D. 1989. Self-diffusion of toluene in polystyrene solutions. *Macromolecules* 22, 3961-3968.
Pinte, J. Joly, C. Dole, P. Feigenbaum, A. 2010. Diffusion of homologous model migrants in rubbery polystyrene: molar mass dependence and activation energy of diffusion. *Food Additives & Contaminants Part A: Chemistry Analysis Control* 27, 557-566.
Pinte, J. Joly, C. Ple, K. Dole, P. Feigenbaum, A. 2008. Proposal of a Set of Model polymer additives designed for confocal FRAP diffusion experiments. *J. Agric. Food Chem.Journal of Agricultural & Food Chemistry* 56, 10003-10011.
Piringer, O. 2007. In *Prediction of diffusion coefficients in gases, liquids, amorphous solids and plastic materials using an uniform model,* 159-181, by Wiley-VCH Verlag GmbH. http://dx.doi.org/10.1002/9783527613281.ch06
Piringer, O. 2008. Prediction of Diffusion Coefficients in Plastic Materials. *Chemistry Magazine* 11, 1186-1189.
Piringer, O. Baner, A. 2008. In *Plastic Packaging: Interactions with Food and Pharmaceuticals, 2nd, Completely Revised Edition,* 163-191, by Otto G. Piringer, A. B. Wiley.
Poças, M. F. Oliveira, J. C. Brandsch, R. Hogg, T. 2012. Analysis of Mathematical Models to describe the migration of additives from packaging plastics to foods. *Journal of Food Process Engineering* 35, 657-676.
Reynier, A. Dole, P. Feigenbaum, A. 2001a. Additive diffusion coefficients in polyolefins. II. Effect of swelling and temperature on the D = f(M) correlation. *Journal of Applied Polymer Science* 82, 2434-2443.
Reynier, A. Dole, P. Feigenbaum, A. 2002. Integrated approach of migration prediction using numerical modelling associated to experimental determination of key parameters. *Food Additives & Contaminants* 19, 42-55.
Reynier, A. Dole, P. Feigenbaum, A. Feigenbaum, A. 1999. Prediction of worst case migration: presentation of a rigorous methodology. *Food Additives & Contaminants* 16, 137-152.
Reynier, A. Dole, P. Humbel, S. Feigenbaum, A. 2001b. Diffusion coefficients of additives in polymers. I. Correlation with geometric parameters. *Journal of Applied Polymer Science* 82, 2422-2433.
Riquet, A. Wolff, N. Laoubi, S. Vergnaud, J. Feigenbaum, A. 1998. Food and packaging interactions: determination of the kinetic parameters of olive oil diffusion in polypropylene using concentration profiles. *Food Additives & Contaminants* 15, 690-700.
Rosca, D. Kouali, M. E. Vergnaud, J. 2001. Testing of a simple method for measuring the diffusivity of a chemical through polymers. *Polymer Testing* 20, 563 - 568.
Rouse, P. 1998. A theory of the linear viscoelastic properties of dilute solutions of coiling polymers. II. A first-order mechanical thermodynamic property. *Journal of*

Chemical Physics 108, 4628-4633.
Rouse, P. E. 1953. A Theory of the Linear Viscoelastic Properties of Dilute Solutions of Coiling Polymers. *Journal of Chemical Physics* 21, 1272-1280.
Rouvray, D. Kumazaki, H. 1991. Prediction of molecular flexibility in halogenated alkanes via fractal dimensionality. *Journal of Mathematical Chemistry* 7, 169-185.
Sakakibara, Y. Takatori, H. Yamada, I. Hiraoka, S. 1990. Concentration Dependence of Diffusivity for the Styrene–Polystyrene and Ethylbenzene–Polystyrene Systems. *Journal of Chemical Engineering of Japan* 23, 247-249.
Sammon, C. Yarwood, J. Everall, N. 2000. A FTIR–ATR study of liquid diffusion processes in PET films: comparison of water with simple alcohols. *Polymer* 41, 2521 - 2534.
Sanches Silva, A. Cruz Freire, J. M. Sendon Garcia, R. Franz, R. Paseiro Losada, P. 2007. Time-temperature study of the kinetics of migration of DPBD from plastics into chocolate, chocolate spread and margarine. *Food Research International* 40, 679-686.
Sanches Silva, A. Garcia, R. S. Cooper, I. Franz, R. Losada, P. P. 2006. Compilation of analytical methods and guidelines for the determination of selected model migrants from plastic packaging. *Trends in Food Science & Technology* 17, 535 - 546.
Schulz, B. Karatchentsev, A. Schulz, M. Dieterich, W. 2006. Ion diffusion in a polymer network: Monte Carlo studies and the dynamic percolation approach. *Journal of Non-Crystalline Solids* 352, 5136-5140.
Simoneau, C. 2010. Applicability of generally recognised diffusion models for the estimation of specific migration in support of EU Directive 2002/72/EC. *Publications Office of the European Union* Publications repository, -.
Sin, G. Meyer, A. S. Gernaey, K. 2010. Assessing Reliability of Cellulose Hydrolysis Models to Support Biofuel Process Design – Identifiability and Uncertainty Analysis. *Computers & Chemical Engineering* 34, 1385-1392.
Sok, R. M. 1994. Permeation of Small Molecules across a Polymer Membrane: a Computer Simulation Study. Rijksuniversiteit Groningen.
Sommer, A. J. Katon, J. E. 1991. Diffraction-Induced Stray Light in Infrared Microspectroscopy and Its Effect on Spatial Resolution. *Applied Spectroscopy* 45, 1633-1640.
Stern, S. A. Sampat, S. R. Kulkarni, S. S. 1986. Tests of a free-volume model of gas permeation through polymer membranes. II. Pure Ar, SF6, CF4, and C2H2F2 in polyethylene. *Journal of Polymer Science Part B: Polymer Physics* 24, 2149-2166.
Tomba, J. P. Arzondo, L. M. Pastor, J. M. 2007. Depth Profiling by Confocal Raman Microspectroscopy: Semi-empirical Modeling of the Raman Response. *Applied Spectroscopy* 61, 177-185.

Tseng, K. Turro, N. Durning, C. 2000. Tracer diffusion in thin polystyrene films . *Polymer* 41, 4751 - 4755.
Vergnaud, J. 1995. General survey on the mass transfers taking place between a polymer and a liquid. *Journal of Polymer Engineering* 15, 57-78.
Vitrac, O. Hayert, M. 2006. Identification of diffusion transport properties from desorption/sorption kinetics: An analysis based on a new approximation of fick equation during solid-liquid contact. *Industrial & Engineering Chemistry Research* 45, 7941-7956.
Vitrac, O. Lezervant, J. Feigenbaum, A. 2006. Decision trees as applied to the robust estimation of diffusion coefficients in polyolefins. *Journal of Applied Polymer Science* 101, 2167-2186.
Vitrac, O. Mougharbel, A. Feigenbaum, A. 2007. Interfacial mass transport properties which control the migration of packaging constituents into foodstuffs . *Journal of Food Engineering* 79, 1048 - 1064.
Von Meerwall, E. D. Amis, E. J. Ferry, J. D. 1985. Self-diffusion in solutions of polystyrene in tetrahydrofuran: comparison of concentration dependences of the diffusion coefficients of polymer, solvent, and a ternary probe component. *Macromolecules* 18, 260-266.
Vrentas, J. Duda, J. 1977a. Diffusion in polymer-solvent systems.1. Re-examination of Free-volume theory. *Journal of Polymer science part B-Polymer physics* 15, 403-416.
Vrentas, J. Duda, J. 1977b. Diffusion in polymer- solvent systems .2. Predictive theory for dependence of diffusion coefficients on temperature, concentration and molecular-weight. *Journal of polymer science part B-polymer physics* 15, 417-439.
Vrentas, J. Duda, J. 1977c. Diffusion in polymer-solvent systems .3. Construction of Deborah number diagrams. *Journal of polymer science part B-polymer physics* 15, 441-453.
Vrentas, J. Duda, J. 1977d. Solvent and temperature effects on diffusion in polymer-solvent systems. *Journal of Applied Polymer Science* 21, 1715-1728.
Vrentas, J. Vrentas, C. 1998. Predictive methods for self-diffusion and mutual diffusion coefficients in polymer–solvent systems . *European Polymer Journal* 34, 797 - 803.
Vrentas, J. S. Vrentas, C. M. 1994. Solvent Self-Diffusion in Rubbery Polymer-Solvent Systems. *Macromolecules* 27, 4684-4690.
Vrentas, J. S. Vrentas, C. M. 1995. Determination of Free-Volume Parameters for Solvent Self-Diffusion in Polymer-Solvent Systems. *Macromolecules* 28, 4740-4741.
Vrentas, J. S. Vrentas, C. M. Faridi, N. 1996. Effect of Solvent Size on Solvent Self-Diffusion in Polymer−Solvent Systems. *Macromolecules* 29, 3272-3276.
Waggoner, R. A. Blum, F. D. MacElroy, J. M. D. 1993. Dependence of the solvent diffusion coefficient on concentration in polymer solutions. *Macromolecules* 26, 6841-6848.

Waharte, F. Steenkeste, K. Briandet, R. Fontaine-Aupart, M.-P. 2010. Diffusion Measurements inside Biofilms by Image-Based Fluorescence Recovery after Photobleaching (FRAP) Analysis with a Commercial Confocal Laser Scanning Microscope. *Applied Environmental Microbioly* 76, 5860-5869.
Wei, Q. Yimin, S. Lun, F. 1993. NMR Imaging of Acetone Diffusion Process in Polycarbonate. *Chinese Journal of Polymer Science* 11, 358-363.
Weibull, W. 1951. A Statistical Distribution Function of Wide Applicability. *Journal of Applied Mechanics* 18, 293 - 297.
Welle, F. 2012. Simulation of the Decontamination Efficiency of PET Recycling Processes based on Solid-state Polycondensation. *Packaging Technology and Science* Published online, n/a-n/a.
Welle, F. 2013. A new method for the prediction of diffusion coefficients in PET. *Journal of Applied Polymer Science* 129, 1845-1851.
Welle, F. Franz, R. 2012. Diffusion coefficients and activation energies of diffusion of low molecular weight migrants in Poly(ethylene terephthalate) bottles. *Polymer Testing* 31, 93 - 101.
Whitley, D. 1998. Van der Waals surface graphs and molecular shape. *Journal of Mathematical Chemistry* 23, 377-397.
Williams, M. L. Landel, R. F. Ferry, J. D. 1955. The Temperature Dependence of Relaxation Mechanisms in Amorphous Polymers and Other Glass-forming Liquids. *Journal of the American Chemical Society* 77, 3701-3707.
Wind, M. Lenderink, H. 1996. A capacitance study of pseudo-fickian diffusion in glassy polymer coatings. *Progress in Organic Coatings* 28, 239 - 250.
Xu, T. Fu, R. 2004. Determination of effective diffusion coefficient and interfacial mass transfer coefficient of bovine serum albumin (BSA) adsorption into porous polyethylene membrane by microscope FTIR-mapping study. *Chemical Engineering Science* 59, 4569 - 4574.
Yang, L. Qi, C. Wu, G. Liao, R. Wang, Q. Gong, C. et al. 2013. Molecular dynamics simulation of diffusion behaviour of gas molecules within oil–paper insulation system. *Molecular Simulation* 39, 988-999.
Young, D. C. 2002a. In *Ab Initio Methods,* 19-31, by John Wiley & Sons, Inc.. http://dx.doi.org/10.1002/0471220655.ch3
Young, D. C. 2002b. In *Semiempirical Methods,* 32-41, by John Wiley & Sons, Inc.. http://dx.doi.org/10.1002/0471220655.ch4

Development of new characterization methodologies and modelling of transport properties on plastic materials: application to homologous series of tracers.

Abstract. Food contact materials must comply with the inertia criteria defined by European regulation, which establishes migration limits for substances that may be transferred into food. Traditionally, migration levels were determined experimentally by performing money and time-consuming migration tests. Recently, modelling tools have been approved to predict migration levels of additives from plastics. However, these models need of certain parameters: the diffusion coefficient or diffusivity, the mass transfer coefficient and the partition coefficient. These coefficients, particularly diffusivity, may be determined experimentally or by predictive modelling

Raman microspectroscopy was used to develop a methodology for the characterisation of diffusivity, using amorphous polystyrene as model polymeric matrix. This methodology was applied to two families (homologous series) of molecules presenting the benzenic ring as fundamental unit, with the goal of establishing relationships between diffusivity in the polymeric matrix and geometrical characteristics of the molecules (volume, length, compressibility), describing molecular mobility in function of their hindrance.

This method has also been adapted to LLDPE, with the goal of establishing the operating conditions allowing to simultaneously determine both diffusivity and mass transfer coefficient.

This work has also permitted to lay the foundations of a diffusivity prediction model, based on geometrical and dynamical characteristics of molecules, without the need of a huge computing power compared to other models present in literature. As well, this work permitted to study the sensitivity of the mathematical models regarding simultaneous regression of several variables used in the description of mass transfer.

Keywords: Diffusion in polymers, Raman microspectroscopy, mass transfer modelling, packaging.

Développement de nouvelles méthodes de caractérisation et de modélisation des propriétés de transport des matériaux d'emballage plastiques: application aux séries homologues de traceurs.

Résumé. Les matériaux placés au contact avec des aliments doivent répondre aux critères d'inertie définie par la réglementation Européenne, qui fixe les limites de migration des substances qui peuvent être transférés aux aliments. Traditionnellement, ces niveaux de migration étaient déterminés expérimentalement par la mise en oeuvre de tests de migration impliquant des moyens analytiques et des délais de temps importants. Récemment et par une évolution de la réglementation, les outils de modélisation ont été validés en tant que moyens d'estimation du niveau de migration des additifs dans les matériaux d'emballage plastiques. Néanmoins, les modèles appliqués nécessitent certains paramètres tels que le coefficient de diffusion (ou diffusivité), le coefficient de transfert de matière et le coefficient de partage. Ces coefficients, en particulier la diffusivité, peuvent être déterminés expérimentalement, ou par la voie de la modélisation prédictive.

La microspectroscopie Raman a été utilisée pour développer une méthode de caractérisation du coefficient de diffusion, en utilisant comme matrice polymérique modèle le polystyrène amorphe. Cette méthode a été appliquée à deux familles (série homologue) de molécules qui présentent comme unité fondamentale un noyau benzénique, ceci dans le but de pouvoir établir des relation entre les variations des valeurs de diffusivité dans la matrice polymérique et les caractéristiques géométriques des molécules (volume, longueur, compressibilité) qui décrivent la mobilité des molécules en fonction de leur encombrement.

Cette méthode a, par ailleurs, été adaptée de manière à être appliqué au polyéthylène basse densité dans le but d'établir les conditions opératoires qui permettent de caractériser simultanément la diffusivité et le coefficient de transfert de matière.

Ce travail a ainsi permis de poser les bases d'un modèle de prédiction de la diffusivité qui repose sur des caractéristiques géométriques et dynamiques des molécules, sans imposer une puissance de calcul importante par rapport aux autres modèles proposés dans la littérature. En outre, ce travail a permis d'étudier la sensibilité des modèles mathématiques par rapport à la régression simultanée de plusieurs variables descriptifs des transferts de matière.

Mots clés: Diffusion dans des polymères, microspectroscopie Raman, modélisation des transferts de matière, emballage.